Standardizing the CRISPR-Cas9 System in Oat to Understand Beta-glucan Regulation

Thomas Donoso

Department of Plant Science, Macdonald Campus, McGill University

Montréal, Québec, Canada

December 2021

A thesis submitted to McGill University in partial fulfillment of the requirements of the degree of a Master's in Science

Abstract

The common oat (*Avena sativa L.*) is a cereal grown worldwide for animal and human consumption. This cereal has grown in popularity because of its many health benefits. Namely, oats contain a significant amount of dietary fibre, beta-(1,3;1,4)-glucan, which has been well documented to reduce the incidence of cardiovascular disease. Despite the plethora of data exploring the health benefits, little is known about the role, regulation, and synthesis of beta-glucan within cereals themselves. Recently, our laboratory discovered that *Thaumatin-like protein 8* (*TLP8*) expression in germinating barley seeds was inversely correlated with the beta-glucan content. This finding sparked our interest in inquiring about this relationship within the common oat. Using the newly released oat genome (variety OT3098), the orthologs of *TLP8* in barley were found in the oat variety park (*AsTLP8-A*, *-C*, and *-D*). Interestingly, the A and C subgenomes homoeologs of *TLP8* demonstrate mutations in the previously described sugar-binding motif. Each homoeolog contained conserved residues found in TLPs showing the beta-glucanase activity, further hinting that *AsTLP8* homoeologs may be involved in beta-glucan regulation. To demonstrate this, we report a standardized analysis of *AsTLP8* homoeolog expression through qRT-PCR in different oat varieties. Further studies involving measuring the relative expression of germinating seeds are required to demonstrate the same relationship observed in barley. Three CRISPR/Cas9-based gene editing constructs were designed to target each homoeolog. The *AsTLP8-A*, *-C*, and *-D* targeting constructs demonstrated a 5.23, 0.47, and 2.86% transformation frequency, respectively. The confirmed transformed T0 was brought to the T1 generation and analyzed through Sanger sequencing. This study reports the first-ever successful CRISPR/Cas9 mediated mutagenesis of the common oat. Further studies are required to determine whether *AsTLP8* knockout mutants directly affect the beta-glucan content of oat.

Résumé

L'avoine commune (*Avena sativa* L.) est une céréale cultivée autour du monde pour la consommation animale et humaine. Cette céréale a augmenté en popularité en raison de ses nombreux bienfaits pour la santé. Plus précisément, l'avoine contient une quantité importante de fibres alimentaires, le bêta-(1,3;1,4) -glucane, qui a été bien documenté de pouvoirs réduire l'incidence des maladies cardio-vasculaires. Malgré la pléthore de données explorant les bienfaits pour la santé, on sait peu sur le rôle, la régulation et la synthèse du bêta-glucane dans les céréales elles-mêmes. Récemment, notre laboratoire a découvert que l'expression de la *protéine similaire à la Thaumatine 8* (*Thaumatin-like protein 8, TLP8*) dans les graines d'orge en germination était inversement corrélée à la teneur en bêta-glucane. Cette découverte a suscité notre intérêt à explorer cette relation au sein de l'avoine commune. En utilisant le génome de l'avoine nouvellement publié (variété OT3098), les orthologues de *TLP8* dans l'orge ont été trouvés dans la variété Park d'avoine (*AsTLP8-A*, *-C* et *-D*). Fait intéressant, les homéologues des sous-génomes A et C de *TLP8* présentent des mutations dans le motif de liaison au sucre décrit précédemment. Chaque homéologue contenait des résidus conservés trouvés dans les TLP montrant l'activité bêta-glucanase, suggérant en outre que les homéologues *AsTLP8* peuvent être impliqués dans la régulation du bêta-glucane. Pour le démontrer, nous rapportons une analyse standardisée de l'expression des homéologues *AsTLP8* par qRT-PCR dans différentes variétés d'avoine. D'autres études impliquant la mesure de l'expression relative des graines en germination sont nécessaires pour démontrer la même relation observée chez l'orge. Trois constructions d'édition de gènes basées sur CRISPR/Cas9 ont été conçues pour génétiquement bloquées chaque homéologue. Les constructions de génétiquement bloquées *AsTLP8-A*, *-C* et *-D* ont démontré une fréquence de transformation de 5,23, 0,47 et 2,86 %, respectivement. La T0 transformée confirmée a été amenée à la génération T1 et analysée par séquençage de Sanger. Cette étude rapporte la première

mutagenèse réussie de l'avoine commune par CRISPR/Cas9. D'autres études sont nécessaires pour déterminer si les mutants génétiquement bloquées *AsTLP8* affectent directement la teneur en bêta-glucane de l'avoine.

Table of Contents

Abstract 2
Résumé 3
List of Abbreviations 8
Acknowledgements 12
Preface 13
Contribution of authors 13
Chapter I: Introduction 14
1.1 General hypotheses 14
1.2 General objectives 15
Chapter II: Literature Review 16
2.1 Feeding a growing population 16
2.2 The common oat (*Avena sativa*) 17
2.3 Genetics of oats 17
2.4 Beta-glucan 20
2.5 Health benefits of beta-glucan 23
2.6 Improving the beta-glucan content of crops 24
2.7 Gene editing techniques 27
2.8 CRISPR/Cas9 28
2.9 Development of the CRISPR/Cas9 gene-editing system 33
2.10 Construct delivery systems 34
2.11 Tissue culture 36
2.11.1 Selection markers 36
2.11.2 Plant regeneration 37
Connecting statement 38
Chapter III: 39
3.1 Abstract 39
3.3 Introduction 40
3.3 Materials and Methods 41
3.3.1 Plant growth 41
3.3.2 Determining *HvTLP8* orthologs in *Avena sativa* 41
3.3.3 Guide RNA design 42

3.3.4 Construct design 42
3.3.5 Digestion of Construct 43
3.3.6 Formation of undifferentiated cells 43
3.3.7 Microprojectile bombardment 44
3.3.8 Selection of transgenic plants 46
3.3.9 Regeneration of shoots/roots 46
3.3.10 Genomic DNA extraction 46
3.3.11 Analysis of transgenic plants 47
3.3.12 Primer design 47
3.3.13 RNA extraction 49
3.3.14 DNase treatment of RNA samples 50
3.3.15 cDNA synthesis 50
3.3.16 qRT-PCR analysis 50
3.4 Results 51
3.4.1 Discovery of *HvTLP8* orthologs in oat 51
3.4.2 Analyzing the TLP8 homologs in oat 52
3.4.3 Standardizing qRT-PCR-Based Analysis of *AsTLP8* homoeologs 54
3.4.4 Designing CRISPR/Cas9 gene-editing constructs 55
3.4.5 Transformation of oats using the *AsTLP8* gene-editing constructs 59
3.4.6 Analyzing the CRISPR/Cas9 efficiency in transgenic lines 62
3.5 Discussion 66
3.6 Future studies 72
Chapter IV General Conclusion 74
Appendices 76
References 84

List of Figures

Chapter II

Figure 2. 1: The proposed two-phase mechanism of beta-glucan synthesis. 23
Figure 2. 2: Summary of the CRISPR/Cas9 system as a form of adaptive immunity 31
Figure 2. 3: Summary of homologous non-homologous end joining (NHEJ) and homologous directed repair (HR) 32

Chapter III

Figure 3. 1: PCR-amplification of AsTLP8 homoeologs in oat. 51
Figure 3. 2: Sugar-binding motif variations between *TLP8* amino acid sequences in barley and oat. 53
Figure 3. 3: All *TLP8* homoeologs and orthologs contain conserved amino acids in fungal beta-1,3-glucanases.. 54
Figure 3. 4: Transcript abundance of *AsTLP8* homoeologs in the mature seed of different varieties. 55
Figure 3. 5: Gene-editing constructs targeting each *AsTLP8* homoeolog.. 58
Figure 3. 6: Digestion of *AsTLP8* targeting CRISPR/Cas9 constructs with SacI. 59
Figure 3. 7: PCR-based analysis of putative pTAN transformed plants.. 60
Figure 3. 8: PCR-based analysis of putative pTCN transformed plants.. 61
Figure 3. 9: PCR-based analysis of putative pTDN transformed plants.. 61
Figure 3. 10: Screening for CRISPR/Cas9 induced deletion within the *AsTLP8-A* gene of T1 transgenic lines 63
Figure 3. 11: Screening for CRISPR/Cas9 induced deletion within the *AsTLP8-C* gene of T1 transgenic lines 63
Figure 3. 12: Screening for CRISPR/Cas9 induced deletion within the *AsTLP8-D* gene of T1 transgenic lines 64
Figure 3. 13: Mutations detected through sanger sequencing of gene-edited T1 plants 65

Appendices

Appendix A 1: Shuttle vector carrying the first sgRNA.. 76
Appendix A 2: Shuttle vector carrying the second sgRNA.. 77
Appendix A 3: Shuttle vector carrying the third sgRNA 78
Appendix A 4: Destination vector of the CRISPR/Cas9 gene editing constructs.. 79
Appendix A 5: Sequences of *HvTLP8* orthologs in *Avena sativa* variety Park 80
Appendix A 6: Sequences of *HvTLP8* orthologs in *Avena sativa* variety OT3098 81
Appendix A 7: Sequences of *HvTLP8* orthologs in *Avena byzantina* (red oat) 82
Appendix A 8: Beta-glucan content by dry weight (d.w.) of various *Avena sativa* varieties. 83

List of Tables

Chapter III

Table 3. 1: Components of regeneration and rooting media 44
Table 3. 2: Primers used in PCR-based analysis of putative gene-edited plants. 48
Table 3. 3: Percent Identity between *AsTLP8* homoeologs in OT3098 and Park 52
Table 3. 4: Single-guide RNA designed for gene-editing *AsTLP8* homoeologs 57
Table 3. 5: Regeneration frequency of gene-editing constructs. 60
Table 3. 6: Transformation frequency of gene-editing constructs 62
Table 3. 7: Mutation frequency in *AsTLP8-D* of CRISPR/Cas9 by guide RNA. 66

List of Abbreviations

ANOVA - Analysis of variance

BAP: 6 - benzylaminopurine

BLAST - Basic Local Alignment Search Tool

bp - Base pair (nucleotide)

Cas - CRISPR Associated protein

Cas9 - CRISPR associated protein 9

cDNA - Complementary DNA

CDS - Coding sequence

CRISPR - Clustered Regularly Interspaced Short Palindromic Repeats

crRNA - CRISPR-RNA

Csl - Cellulose synthase-like

CslA - Cellulose synthase-like A

CslF - Cellulose synthase-like F

CslF6 - Cellulose synthase-like F6

CslH - Cellulose synthase-like H

CVD - Cardiovascular disease

DNA - Deoxyribonucleic acid

DP3 - cellotriosyl

DP4 - cellotetraosyl

DSB - Double-stranded break

EDTA - Ethylenediaminetetraacetic acid

d.w. - Dry weight

FISH - Fluorescent in situ hybridization

FSH_2O - Filter sterile water

Gb - Giga-base pairs (nucleotides)

gRNA - Guide RNA

GWAS - Genome-wide association studies

HDR - Homologous-directed repair

Hpt - Hygromycin phosphotransferase

IAA - indole-3-acetic acid

IBA - indole-3-butyric acid

Ma - Million years

MS - Murashige & Skoog Basal Salt

MSP - Monocot-specific promoter

NAA -Naphthaleneacetic acid

NHEJ - Non-homologous end joining

PAM - Protospacer adjacent motif

Pol III - RNA polymerase III

PR - Pathogenesis-related protein

pre-crRNA - pre-CRISPR-RNA

PCR - Polymerase Chain Reaction

qRT-PCR - Real-Time Quantitative Reverse Transcription PCR

QTL - Quantitative trait loci

RNA - Ribonucleic acid

RNAi - Ribonucleic acid interference

sgRNA - Single-guide RNA

snRNA - Small nuclear RNA

TALEN - Transcription activator-like effector nuclease

TE buffer - Tris/EDTA buffer

TLP - Thaumatin-like protein

TLP8 - Thaumatin-like protein 8

tracrRNA - Trans-activating CRISPR RNA (tracrRNA)

USDA - United States Department of Agriculture

USE - Upstream sequence element

v. - Variety

w/w - Wet weight

ZFN - Zinc-finger nuclease

2,4-D - 2,4-dichlorophenoxyacetic acid

Acknowledgements

The completion of this project could not have been completed without the support of those around me—my gratitude to Dr. Jaswinder Singh for this great opportunity, his guidance, and advice. I am grateful for Dr. Rajvinder Kaur and her knowledgeful instruction and recommendations over the years that led to my success. I appreciate Dr. Valerio Hoyos-Villegas for his insights and feedback as my committee member. Thank you to Dr. Rajiv Kumar Tripathi for his guidance and his direct contribution to my work. I would like to thank my lab mates, Wei-Yuan Chen, Sukhjiwan Kaur Kadoll, Dr. Zhou Zhou, Purnima Kandpal, and Mehtab Singh, for providing a lovely environment to work in and for your interesting conversation. I would like to thank Irfan Iqbal for your friendship and the memories made.

I am forever grateful for my family and friends. I am incredibly thankful to my parents for their love and care. Finally, thank you to my girlfriend, Maygan Godin, for keeping me grounded and encouraging me throughout my studies.

This work is funded by the Prairie Oat Growers of Canada (POGA), Natural Sciences and Engineering Research Council (NSERC), Genome Editing for Food Security and Environmental Sustainability (GEFSES), and the Fonds de Recherche du Quebec – Nature et Technologies (FRQNT). Thank you for your support.

Preface

The entirety of this thesis is original work. The third chapter is formatted in the style of a manuscript, of which the contributing authors are as follows.

Contribution of authors

The experiments in chapter III were planned and designed by Thomas Donoso and Jaswinder Singh. Chapters 1-IV were written by Thomas Donoso. Rajiv Kumar Tripathi performed quantitative Real Time Reverse Transcription PCR (qRT-PCR), and Thomas Donoso and Rajiv Kumar Tripathi analyzed the data.

Chapter I: Introduction

The common oat (*Avena sativa*) is a cereal grown around the globe. Oat production reached 23.33 million metric tons worldwide in 2019/2020 (USDA 2021). This cereal demonstrates economic importance in Canada, as it is the leading exporter and second-leading producer of oats (USDA 2021). The economic value of *Avena sativa* is further compounded by its recent gain in popularity due to its plethora of health benefits. Specifically, oats contain a significant amount of (1,3;1,4)-beta-glucan, a dietary fibre. This dietary fibre has demonstrated the ability to reduce dietary intake (Lumaga et al. 2012), lower the occurrence of bacterial and viral infections (Daou and Zhang 2012), and reduce the incidence of cardiovascular heart disease (Whitehead et al. 2014). Despite these fascinating features, relatively little is known about the mechanism and regulation behind beta-glucan production. Excitingly, Singh et al. (2017) demonstrated a reverse correlation between the expression of *Thaumatin-like protein 8* (*TLP8*) and the beta-glucan content in barley (*Hordeum vulgare*). This study also highlighted that *TLP8* contained a sugar-binding motif (CQTGDCC), suggesting that this protein may interact with beta-glucan. Considering this evidence, our lab was interested in investigating this gene within *Avena sativa*. The recent availability of the sequenced oat genome and precise gene-editing capabilities of the CRISPR/Cas9 system opened the door to uncovering the potential role of *TLP8* in beta-glucan regulation.

1.1 General hypotheses

1. *Avena sativa* contains three orthologs to the *HvTLP8* gene in barley.
2. *TLP8* expression corresponds to beta-glucan content in oat
3. *Avena sativa* v. Park will be amenable to microprojectile bombardment transformation and CRISPR/Cas9 gene-editing
4. CRISPR/Cas9 constructs could generate knockouts in *AsTLP8* homoeologs

The first and second hypotheses are based on the hexaploid state of *Avena sativa*, and that barley and oat are closely related species in terms of synteny (Maughan et al. 2019). These hypotheses will be fulfilled by determining the *AsTLP8* homoeologous sequences through sequencing and determining the expression of these genes in varieties with differing beta-glucan content.

The third hypothesis stems from the knowledge that microprojectile bombardment has historically demonstrated success in oats (Cho et al. 1999; Ismagul et al. 2018; Mahmoud 2019) and demonstrated capabilities in CRISPR/Cas9-based gene editing (Zhang et al. 2016). The final hypothesis derives from the efficiency of CRISPR/Cas9 in other cereals (Galli et al. 2021; Shan et al. 2014; Wang et al. 2014c). These hypotheses will be fulfilled by analyzing microprojectile bombarded plantlets through PCR-based methods and sequencing.

1.2 General objectives

In this thesis, the main research goals were to:

1) Determine if *TLP8* orthologs were present in *Avena sativa* and whether the same correlation with beta-glucan exists.
2) Knockout the *TLP8* orthologs in oat v. Park using CRISPR/Cas9 gene-editing to ascertain if this Thaumatin-Like Protein is associated with the beta-glucan content.

Chapter II: Literature Review

2.1 Feeding a growing population

The challenge of meeting the increasing food demands of our growing population proves difficult considering current agricultural practices. The population is expected to grow to over 9 billion by 2050 (Godfray et al. 2010). Consequently, an agricultural output increase of 100-110% will be needed to sustain this rising population (Tilman et al. 2011). Traditional breeding methods have led to substantial crop improvement in the past (Alston et al. 2009; Tester and Langridge 2010; Zerai et al. 2010). Despite their success, these techniques prove to be slow, inefficient and laborious. In addition, these practices often reduce genetic diversity and, in turn, lead to disease susceptibility (Babiker et al. 2015; Keneni et al. 2012). The need for faster crop improvement has sparked an interest in genetic engineering. The theory behind gene modification is simple. As DNA acts as the blueprint for the cell, altercations within its instructions can lead to a different outcome. Harnessing the powerful ability of gene editing will allow for endless applications of crop improvement. Consider the imminent threat of climate change; Through the ability to alter the genetic makeup of plants, one can increase the tolerance of plants to extreme temperatures, decrease their susceptibility to drought or floods, or improve the traits that are beneficial to providing a healthier diet. While the green revolution focused on providing enough calories to a starving world at any cost, the gene-editing frontier aims to develop nutritional-focused agricultural practices. In other words, there is a call for functional foods. Recently, the beta-glucan found in oat (1→3, 1→4) has been shown to have significant health benefits, including lowering blood cholesterol (Pereira et al. 2004; Whitehead et al. 2014), strengthening the immune system (Daou and Zhang 2012), and lowering food intake (Lumaga et al. 2012).

2.2 The common oat (*Avena sativa*)

The common oat (*Avena sativa*) is a cereal grown worldwide mainly for its grain. After Russia, Canada is the second-largest oat producer, with 4 million metric tons produced in 2019/2020 (FAO 2019). To add, Canada is the largest exporter of oat worldwide, with 1.8 million metric tons. As this figure accounts for about half of all production, oat has evident economic importance in Canada (USDA 2019). Although most oat production is for livestock feed, this cereal has garnered interest in nutrition as a health food (Kaur and Singh 2017). This interest stems from the many components of oat that contribute to its health benefits. For example, *Avena sativa* contains potent antioxidants known as avenanthramides. This powerful molecule has been shown to reduce DNA damage, inflammation and reactive oxygen species (Hastings and Kenealey 2017; Kang et al. 2018). Other components that add to their whole food status include tocols (Vitamin E), phenolic acids, vitamin B_1, fibre, magnesium, and iron (Chen et al. 2004; Gutierrez-Gonzalez et al. 2013; Kemppainen et al. 2010). Most importantly, the high amount of beta-glucan found within the grain of the common oat contributes significantly to its health benefits.

2.3 Genetics of oats

The common oat is a member of the Poaceae family, an agronomically important group. Colloquially known as cereals, the Poaceae family includes three subfamilies: Oryzoideae (rice), Panicoideae (maize, sorghum), and Pooidea (wheat, rye, barley, and oat). The Pooidea subfamily is further split into 14 tribes, including Brachypodieae, Poeae (syn Aveneae), and Triticeae (barley, wheat, and rye) (Maughan et al. 2019). The tribe Triticeae demonstrates the largest synteny with the tribe Poeae, which includes the common oat. These two tribes are estimated to have diverged around 49 Ma (Schubert et al. 2019). The *Avena* genus is a large group with thirty families, spanning various ploidy levels, including diploids, tetraploids, and hexaploids (Baum and Baum 1977; Ladizinsky 1998). Due to the variety of ploidy levels, the *Avena* genus has a wide range of

genome sizes between 4.1 and 12.8 Gb (Yan et al. 2016b). A variety of genome subtypes and combinations have been characterized within the *Avena* genus, including AsAs, AdAd, ApAp, AcAc, AlAl, CvCv, and CpCp diploids, AABB, and AACC tetraploids, and an AACCDD hexaploid (Jellen et al. 1994). The A genome, specifically the subgenome AsAs, demonstrates a large amount of synteny with the barley (*Hordeum vulgare*) genome, while the C genome demonstrates a relatively large amount of chromosomal rearrangement. It has been suggested that this chromosomal rearrangement indicates genomic instability in C-genome diploid species (Maughan et al. 2019). The common oat is a hexaploid species, meaning it has more than two homologous chromosomes. In total, *Avena sativa* has 42 chromosomes (6x = 42) and three different ancestral genomes (AACCDD) (Leggett and Thomas 1995). The A, C, and D genomes are concluded to have been acquired through the crossing of a tetraploid and diploid *Avena* species (Loskutov 2008). It is suspected, due to a high similarity evidenced in the morphology (Baum et al. 1973), fluorescent in situ hybridization (FISH) (Linares et al. 1998), and isoenzyme variation (Craig et al. 1974), that the D genome diverged from the A genome in a recent diploid ancestor (Yan et al. 2016a).

In contrast, the C genome has highly diverged from the A genome. This divergence has been supported through a more pronounced C-banding of the C genome (Fominaya et al. 1988; Jellen and Gill 1996) and through FISH (Hayasaki et al. 2000; Linares et al. 1998). It has been generally proposed that the hexaploidy of oat occurred from the crossing of a tetraploid with an AACC genome and a diploid with the DD genome. The reason for this inference is that there are several current tetraploid species with an A+C genome (Loskutov 2008; Thomas 1992). Interestingly, evidence also challenges the presumption that the A+C configuration merged with the D genome. According to molecular evidence (Oliver et al. 2011a), FISH (Linares et al. 1998), and meiotic

chromosome pairing (Ladizinsky 1998), it is possible that these known tetraploids contain the D genome, rather than the A genome. In other words, the hexaploid oat was likely obtained through a tetraploid with the CCDD genome and a diploid with the AA genome (Yan et al. 2016a). So, a hexaploid AACCDD genome is formed when the A genome is acquired.

The appearance of acquired genomes in *A. sativa* means it is an allopolyploid. In other words, their polyploidy is caused by the crossing of multiple different species (Leggett and Thomas 1995). The polyploidy state has several advantages. For example, an extra set of chromosomes reduces the chance of deleterious effects caused by mutations (Comai 2005). Polyploid crops are more resistant to these deleterious mutations because they have extra copies of each gene. So, if a gene essential for a plant's survival is mutated, there is still another copy to provide that vital trait. This buffer also allows for diversification. As extra copies are redundant, a polyploid can mutate redundant sequences and produce genes with a new function (Adams and Wendel 2005; Prince and Pickett 2002). However, this polyploidy creates difficulty in the field of genomics. When undergoing SNP discovery, more complex analysis is required to differentiate true SNPs from pseudo-SNPs, which occur from the misalignment of homoeologous sequences found within other acquired genomes (Oliver et al. 2011b). In other words, it is difficult to tell whether these detected SNPs are occurring because of variation between different individual plants or because there is variation between the homologous genome sequences within the same individual. The hexaploid oat's highly redundant genome has led to a challenge in sequencing and characterizing it. The accessibility of the functionally characterized gene sequences, of course, is the groundwork for the gene-editing field.

2.4 Beta-glucan

β-glucan is a polymer of glucose, characterized by the β-glycosidic bonds linking the monomers together. In its simplest structure, the monomers of beta-glucan bind in the form of (1,3)-beta-glucan, which are unbranched, linear, and typically found within prokaryotes (Zeković et al. 2005). However, more complex forms of beta-glucan occur in nature. For example, fungal species often incorporate the branched form of beta-glucan, (1→3, 1→6)-beta-glucan, within their cell walls at varying branching frequencies (Chen and Seviour 2007). The complexity of beta-glucans is not limited to the branching of the monomers, though. The presence of a variety of linkages can also change the physiochemical properties of beta-glucan. A unique beta-glucan exists for the family Gramineae, composed of grasses and commercial cereals. This molecule consists of both (1→3) and (1→4) beta-glycosidic bonds binding the glucose monomers together. Depending on the ratio of the two linkages, the physiochemical properties of this beta-glucan are altered (Burton and Fincher 2009). Despite the variance in properties, (1→3,1→4)-beta-D-glucan is typically viscous. In fact, a high concentration of this form of beta-glucan in barley has been shown to present problems throughout the brewing process (Edney and Mather 2004; Vis and Lorenz 1998). Within cereals, (1→3,1→4)-beta-D-glucan is approximately 20% of the starchy endosperm's dry weight (Nemeth et al. 2010). In addition, for both oat and barley, beta-glucan is also found within the aleurone and subaleurone of the endosperm-coating bran (Butardo and Sreenivasulu 2016; Miller and Fulcher 2011). There is also a biochemical link between the synthetic pathways of both starch and beta-glucan. Increasing the expression of starch and other grain components leads to an alternative method of influencing beta-glucan content (Marcotuli et al. 2016). Although the function of beta-glucan is not entirely proven, it seems that this dietary fibre acts as alternative storage for metabolizable glucose. The metabolizable glucose role is exemplified in the fact that the beta-glucan content reaches 10% w/w while exposed to a natural light day cycle but reaches

near zero when placed in the dark (Roulin et al. 2002). Furthermore, the expression of (1,3;1,4)-beta-D-glucan hydrolase increased 2- to 4-fold when dark-incubated, indicating that beta-glucan acts as glucose storage when light levels are low (Roulin et al. 2002). In addition, it has been theorized that beta-glucan is synthesized as a much more accessible source of glucose than starch. The reason for this is that the biosynthesis of beta-glucan is relatively simple compared to the complex synthesis of starch (Burton and Fincher 2012). Beta-glucan synthesis is maintained through the Cellulose synthase-like (*Csl*) gene family. The *Csl* family is generally involved in synthesizing various non-starch polysaccharides, and not every member of this gene family has been assigned a biological function. For example, the *CslA* gene group was shown to encode for the *mannan synthase* gene when expressed in insect cells (Liepman et al. 2005). This gene family has two subgroups, dubbed *CslF* and *CslH*, attributed to beta-glucan synthesis. As beta-glucan is not found within the cell walls of *Arabidopsis*, both of these genes were introduced to determine whether they would induce the synthesis of (1,3;1,4)-beta-glucan. Interestingly, the introduction of both *CslF* and *CslH* led to the production of beta-glucan in *Arabidopsis*, demonstrating that both of these genes are involved in synthesizing this soluble fibre (Burton et al. 2006; Doblin et al. 2009). It has been hypothesized that the production of beta-glucan through CslH and CslF happens independently from each other (Doblin et al. 2009). In other words, the expression of *CslF* genes are not altered by the expression of the *CslF* gene and vice versa. As both the *CslF* and *CslH* families do not seem to be close on the phylogenetic tree, it is likely that these two gene families arose independently of one another (Fincher 2009; Kaur et al. 2017). Despite the knowledge surrounding beta-glucan synthesis, it is still unclear where the soluble fibre is produced. Using immunocytochemistry to detect adjacent (1,3)- and (1,4)-beta-glycosyl residues in barley tissues, detection of (1,3;1,4)-beta-glucan in the cell walls was demonstrated, but not within the

cells themselves (Meikle et al. 1994). Interestingly, it was also found that the enzymes known to be involved in the beta-glucan synthesis, such as CslH, were detected within the Golgi and the endoplasmic reticulum (Doblin et al. 2009). This result spawned a new question: Why were the enzymes synthesizing beta-glucan found within the cell, but not beta-glucan itself? It has been theorized that, within the Golgi and ER, (1,4)-beta-linkages are first synthesized and that (1,3) branches are then connected either within the plasma membrane or the periplasmic space, as seen in Figure 2.1 (Burton et al. 2010; Doblin et al. 2009). The structure of (1,3;1,4)-beta-D-glucan lends a hand to the solubility of this dietary fibre. Approximately 90% of the beta-glucan chain is comprised of cellotriosyl (DP3) and cellotetraosyl (DP4) separated by one (1,3)-beta-linkage (Figure 2.2) (Woodward et al. 1983). In other words, there are two (DP3) or three (DP4) (1,4)-beta-linkages in a chain before another (1,3)-beta-linkage occurs. The other 10% consists of ten or more (1,4)-beta-linkages in a chain (Woodward et al. 1983). The random distribution of cellotriosyl and cellotetraosyl groups makes it nearly impossible for the (1,3;1,4)-beta-D-glucan chains to align with one another. For this reason, these chains are partly soluble in water (Fincher and Stone 2004). The solubility is often related to the DP3:DP4 ratio. A higher DP3:DP4 ratio is met with low solubility. Meanwhile, a low ratio leads to high solubility. Grains in which (1,3;1,4)-beta-D-glucan concentration is high, such as in oat and barley, the ratio between DP3:DP4 is typically low, meaning they are highly soluble (Trafford and Fincher 2014).

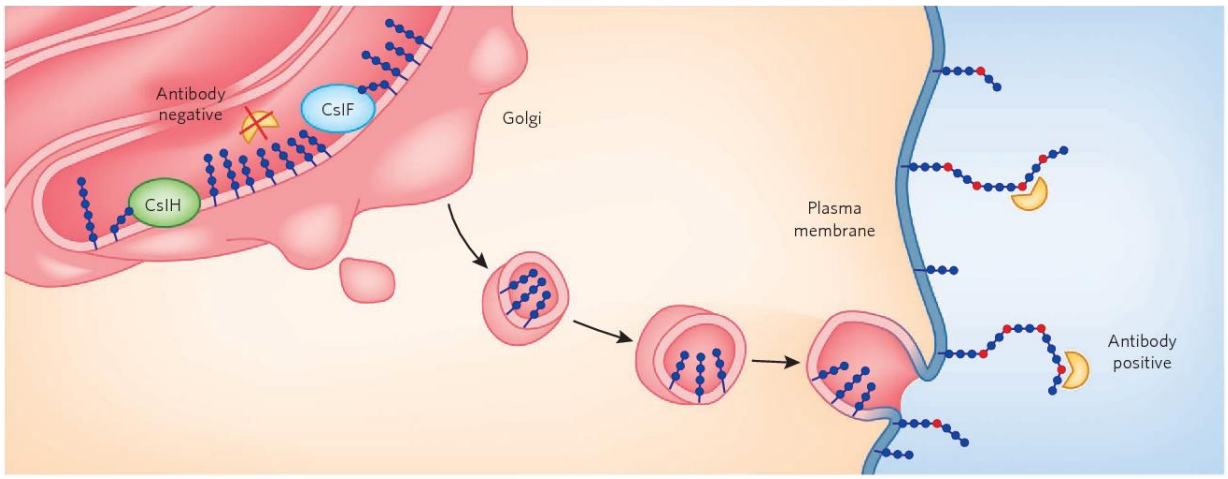

Figure 2. 1: The proposed two-phase mechanism of beta-glucan synthesis. The blue circles demonstrate (1,4)-beta-linkages. The red circles represent (1,3)-beta-linkages. In the absence of both (1,4)- and (1,3)-beta-linkages, the antibody would test negative in the Golgi but positive on the plasma membrane (Derived from Burton et al. (2010)).

2.5 Health benefits of beta-glucan

As hull-less groats are the most commonly consumed product of oat, the presence of beta-glucan within the groats plays a vital role in the dietary benefits of beta-glucan. Beta-glucan is a dietary fibre, meaning it is a carbohydrate polymer with ten or more monomers that cannot be hydrolyzed by the endogenous enzymes found within the small intestine of humans. However, dietary fibre does undergo partial or complete fermentation within the large intestine (Phillips and Cui 2011). Dietary fibre has been shown, in many aspects, to be an essential aspect in reducing calorie intake. To begin, dietary fibre in the morning was demonstrated to reduce food consumption for the rest of the day (Lumaga et al. 2012). So, when consuming beta-glucan, one can prevent overeating. Furthermore, the beta-glucan of cereals has been shown to have immune system stimulatory effects. Therefore, this soluble fibre helps reduce the incidence of bacterial and viral infections (Daou and Zhang 2012). Beyond all of these health components, the strongest proponent of the health benefits is oat beta-glucan's ability to combat cardiovascular heart disease by lowering blood cholesterol (Pereira et al. 2004; Theuwissen and Mensink 2008; Whitehead et al. 2014). This

characteristic of oat beta-glucan consumption is theorized to promote cholesterol and lipid lysis in the blood (Grundy et al. 2017). In particular, cholesterol lysis is thought to be because highly soluble beta-glucans lead to greater production of bile acids. Highly soluble dietary fibres tend to bind the bile acids and not allow them to be reabsorbed by the intestine (Eastwood and Hamilton 1968; Kritchevsky and Story 1974). So, more bile acid synthesis is required, and because bile acid production requires the breakdown of cholesterol, the blood cholesterol concentration is lowered (Theuwissen and Mensink 2008). Andersson et al. further exemplified this theory by demonstrating that consumption of oat bran stimulated bile acid synthesis (Andersson et al. 2002). Considering all of the research, many governmental agencies, including the UK, Sweden, Finland, Netherlands, and the USA, support the health claims of beta-glucan in oat (Tiwari and Cummins 2009). Despite the improvements in health care and education, heart disease remains the leading cause of mortality worldwide (Mozaffarian et al. 2016). Considering the potency of beta-glucan in lowering the incidence of heart disease, increasing the concentration of soluble fibre in the grain of oat will play an essential role in combatting this public health crisis.

2.6 Improving the beta-glucan content of crops

Considering the ample evidence that dietary fibre is beneficial for health, increasing the amount of beta-glucan in the diet is important. According to various meta-analyses of randomized controlled trials, the consensus is that one should consume more than 3g a day of oat beta-glucan (Tiwari and Cummins 2011; Whitehead et al. 2014). However, this amount of fibre is difficult to consume. The reason for this difficulty is that oat bran is highly satiating (Lumaga et al. 2012). An argument could be made that extracted beta-glucan could be a source of the needed daily 3 grams instead of consuming whole oats. However, it has been shown that extracted beta-glucan does not as effectively lower glycosylated hemoglobin, fasting glucose, and fasting insulin when compared to beta-glucan acquired from consuming oats (He et al. 2016). There is a clear genetic component

598 to the beta-glucan content, as shown by Ajithkumar et al. (2005). This study showed that beta-
599 glucan was more of a heritable trait rather than being associated with environmental conditions.
600 Knowing this, efforts have been made to increase the beta-glucan content through traditional
601 breeding methods. In barley, Transit and CDC Alamo varieties demonstrate a beta-glucan content
602 as high as 97 g kg^{-1} (Obert et al. 2011). To add, many quantitative trait loci (QTL) have been
603 associated with a high concentration of beta-glucan through the use of QTL mapping (Gutiérrez et
604 al. 2011; Islamovic et al. 2013; Kim et al. 2011). QTL mapping involves crossing two
605 phenotypically distinct cultivars to understand the genomic loci associated with the variation in
606 phenotypes. For example, in the case of beta-glucan, one could cross a cultivar with high beta-
607 glucan content with a cultivar with a low concentration. Through the further crossbreeding of
608 successive generations, one can map the genomic loci associated with the production of beta-
609 glucan. In barley, the 1H, 2H, 3H, 4H, 5H, and 7H chromosomes have been shown to contain
610 genes potentially involved in beta-glucan regulation or synthesis (Han et al. 1995; Igartua et al.
611 2002; Islamovic et al. 2013; Li et al. 2008; Molina-Cano et al. 2007; Singh et al. 2012). In oat,
612 genome-wide association studies (GWAS) and QTL mapping studies have been conducted to
613 determine the genomic regions involved in beta-glucan concentration. Genome-wide association
614 studies differ from QTL mapping in that they do not require the crossing of phenotypically distinct
615 parental lines. Instead, GWAS uses the slight variations between a large population of the same
616 cultivar to map genomic loci associated with the trait of interest. QTLs were identified in oat
617 through the crossing of Kanota x Ogle (Orr and Molnar 2008) and Terra x Marion (De Koeyer et
618 al. 2004). Through GWAS, many QTLs have been discovered, indicating that beta-glucan is a
619 complex trait with many genomic components (Asoro et al. 2013; Newell et al. 2012).
620 Interestingly, Newell et al. (2012) discovered a QTL that contained genes with sequence homology

621 to the *CslF* gene family in rice. These QTL regions prove especially useful in breeding programs.
622 This is because breeders can select for QTL variations positively associated with a trait of interest.
623 As a production of breeding, one of the leading barley varieties in beta-glucan content is HiFi,
624 which boasts a concentration of 4.5-5.0% (McMullen et al. 2005). However, considering the
625 downsides to traditional breeding methods, such as loss of genetic diversity and disease
626 susceptibility (Babiker et al. 2015; Keneni et al. 2012), it is clear that gene editing methods are
627 required to improve the beta-glucan content of cereals. For this reason, it is important to
628 functionally understand the genes involved within a QTL. After their discovery in QTL mapping,
629 genes involved in the synthesis of beta-glucan have previously been used to improve the beta-
630 glucan in barley through overexpression. Burton et al. (2011) overexpressed the *CslF6* gene and
631 found an increase of up to 80% in total beta-glucan content. Of the known genes within the *CslF*
632 family, there is evidence supporting *CslF6* as being the most influential with respect to the beta-
633 glucan content. This evidence is based on the transcript abundance during endosperm development
634 (Burton et al. 2008), in the complete removal of (1,3;1,4)-beta-D-glucan synthesis through the
635 mutation of *HvCslF6* (Taketa et al. 2012), and RNAi leading to lower concentrations of (1,3;1,4)-
636 beta-D-glucan in wheat (Nemeth et al. 2010). Unfortunately, although the *CslF6* overexpression
637 construct led to a substantial improvement in the trait of beta-glucan, it was often lethal (Burton et
638 al. 2011). Additional complications of *CslF6* overexpression included an elongated aleurone layer
639 and changes to the endosperm transfer cell. These altercations lead to a squeezed starch layer and
640 a reduced ability to uptake sucrose (Lim et al. 2019). Recently, the expression of Thaumatin-Like
641 Protein 8 has been demonstrated to be associated with the beta-glucan content in barley (Singh et
642 al. 2017). Thaumatin-Like Proteins (TLPs), also known as pathogenesis-related (PR) proteins, are
643 a family of proteins that have a function in host-defence and a wide range of developmental

processes (Liu et al. 2010). *TLP8* has been shown to potentially be implicated in the regulation of beta-glucan. In malting varieties, which are varieties with low beta-glucan content, the expression of *TLP8* is relatively high. In contrast, the feed varieties with high beta-glucan content have low expression of *TLP8* (Singh et al. 2017). Although association does not necessarily imply causation, the same study demonstrated that *TLP8* contained a carbohydrate-binding motif, suggesting it could bind to beta-glucan. Considering that this form of beta-glucan is found in a high concentration in cereals, it is likely that TLP8 plays a regulatory role in beta-glucan content. Overall, beta-glucan remains a complex genetic trait, and it is of interest to study the regulatory role of TLP8 to identify a putative new target for gene editing. However, to implement gene-editing techniques in oat, it is important to understand the challenges involved within the genetics of the species.

2.7 Gene editing techniques

Since discovering the central dogma of biology, in that DNA produces RNA, which produces proteins, the manipulation of DNA sequences has been of interest. Within the past few decades, a plethora of techniques have been developed to perform the task of gene-editing. Some of the initial promising gene-editing practices involved the nuclease domain of the FokI restriction enzyme. This FokI was sequence-independent and could be used in precise genome editing when coupled with other components, such as zinc-finger mediated DNA binding. Zinc-fingers are transcription factors that bind to DNA. They typically bind to approximately three to six nucleotides in triplets (Pavletich and Pabo 1991). Interestingly, the zinc-fingers can be designed to appear in tandem, binding to an extended sequence of nucleotides. For example, three zinc fingers could bind a sequence of DNA nine base pairs long, further increasing the specificity of the designed zinc fingers. By engineering these zinc fingers to interact with a single sequence of DNA, one can harness both the DNA interaction of the zinc fingers alongside the nuclease activity of FokI to

incorporate double-stranded cuts at a site of interest (Hartung and Schiemann 2014). The creation of a double-stranded break (DSB) can lead to an insertion or deletion, disrupting the proper expression of a protein. FokI, however, requires dimerization for the nuclease activity to work. Therefore, two adjacent zinc fingers need to be designed to allow dimerization. In other words, one zinc finger needs to be designed upstream of the target site, and another needs to be designed downstream. Altogether, the engineering of the zinc-finger nuclease (ZFN) system is complicated. As an alternative to this complexity, transcription activator-like effector nucleases (TALENs) take advantage of TALE proteins' one-to-one code (Gao et al. 2012). That is, each TALE protein binds to a specific nucleotide, allowing for the ability to string a combination of TALE proteins that bind to a sequence of interest. Like the ZFN, TALEN takes advantage of the catalytic domain of the FokI nuclease to induce DSBs (Maeder and Gersbach 2016). However, the large size of these TALE proteins makes this system complicated, and the cost of designing a TALEN system hinders this technology (Khan 2019).

2.8 CRISPR/Cas9

Over 30 years ago, a research group in Japan discovered repeated, palindromic sequences of about 30 bp, separated by a 36 bp spacer region in *Escherichia coli* (Ishino et al. 1987). Then, Mojica et al. (1995) discovered this same pattern in Archaea. Considering the vast phylogenetic differences between Bacteria and Archaea, the appearance of these same patterns in both domains demonstrated that these repeats played an important functional role. The name clustered regularly interspaced short palindromic repeats (CRISPR) was then coined, followed by the discovery of CRISPR-related genes, such as the *cas* (CRISPR-associated) genes (Jansen et al. 2002). Despite these findings, the function of this system remained unclear. This mystery began to unravel when Mojica et al. (2009) searched for sequences similar to the spacer sequences found between the repeats. This group found that these spacers were homologous to bacteriophages, plasmids,

transposons, and chromosomal sequences. From this information, the question arose: Why would it be so important to store the genetic information of these transposable elements? The answer came from developing bacteriophage-resistant strains in the fermentation process of yogurt. While studying resistant strains and comparing them to susceptible strains, it was found that resistance was acquired by incorporating the bacteriophage DNA into the spacer regions (Barrangou et al. 2007). In other words, these CRISPR regions were acting as an acquired immune system for the bacteria. The findings did not end there, as it was also found that the short palindromic repeats and spacers were not the only required component for the acquisition of immunity. When the *cas* genes were removed, bacteria lost their ability to resist bacteriophages, demonstrating that these CRISPR-associated genes played an essential role in the acquired immunity of bacteria (Barrangou et al. 2007). It was then discovered that the CRISPR and spacer regions would encode for small RNA sequences. Cas proteins processed these small sequences and then guided other cas proteins to the target DNA (Brouns et al. 2008). These small RNAs were dubbed pre-crRNA (pre-CRISPR-RNA) before processing, and crRNA after processing. Then, Mojica et al. (2009) discovered that these crRNA spacer regions contained a conserved protospacer adjacent motif (PAM). This discovery suggests that the incorporated sequence is chosen based on the presence of this motif. Strikingly, it was then found that the CRISPR-associated protein *Cas9* created double-stranded breaks three nucleotides upstream of the PAM sequence in the CRISPR type II system (Garneau et al. 2010). In short, the spacer region is taken from the bacteriophage-based on the presence of a PAM sequence, as it dictates where the double-stranded break occurs. Bringing it all together, Deltcheva et al. (2011) discovered a *trans*-encoded small RNA (tracrRNA), which is a necessity for the processing of pre-crRNA through the RNA-specific ribonuclease RNase III in the presence of Cas9. Interestingly, this discovery demonstrates the utility of the type II system over other

CRISPR systems. While other systems require specialized processing *cas* proteins, the type II system uses the already available RNase III. So, tracrRNA acts as both a signal for the processing of pre-crRNA and activation of Cas9 activity (Jinek et al. 2012). In summary, the CRISPR-Cas9 system is a form of adaptive immunity in bacteria. The bacteria will incorporate foreign DNA containing a PAM sequence between palindromic repeats. When infected by the same foreign DNA, the pre-crRNA and Cas9 will be expressed. Pre-crRNA is processed into crRNA with the help of *cas* proteins and tracrRNA. The processed crRNA and tracrRNA, becoming a guide for the Cas9 enzyme, brings the nuclease to its intended target. Once it reaches the foreign DNA, Cas9 deactivates it through the formation of double-stranded breaks (DSBs). Overall, the CRISPR-Cas9 system acts as an effective protection against repeat infections.

The interest in CRISPR-Cas9 has grown in the past decade due to its ability to precisely target and cleave sequences of DNA. After the characterization of the adaptive bacterial immunity, the CRISPR-Cas9 system showed potential to revolutionize the genome-editing field. Yet, the system was still far from demonstrating its efficacy. Progress began when Gasiunas et al. (2012) demonstrated that the crRNA could be efficiently used at a length of 20 nucleotides. Additionally, this group showed that the crRNA could be replaced with any sequence and still cleave the intended target. The idea of harnessing the nuclease ability for gene editing was then further popularized by Jinek et al. (2012) by studying the CRISPR type II system in *Streptococcus pyogenes*. This group demonstrated that the Cas9 nuclease could be led to its target through a single guide RNA (gRNA). The gRNA consisted of a combination of the tracrRNA and the crRNA. In other words, instead of individual expression of these two critical components of the CRISPR-Cas9 system, the tracrRNA and crRNA could be fused and retain their function. The valuable aspect of the CRISPR-Cas9 system in this form is that one only needed to attach the target

to the overall sequence to create DSBs at any point in the genome. However, the improvement of the system is meaningless without the demonstration of its functionality as a tool in gene editing.

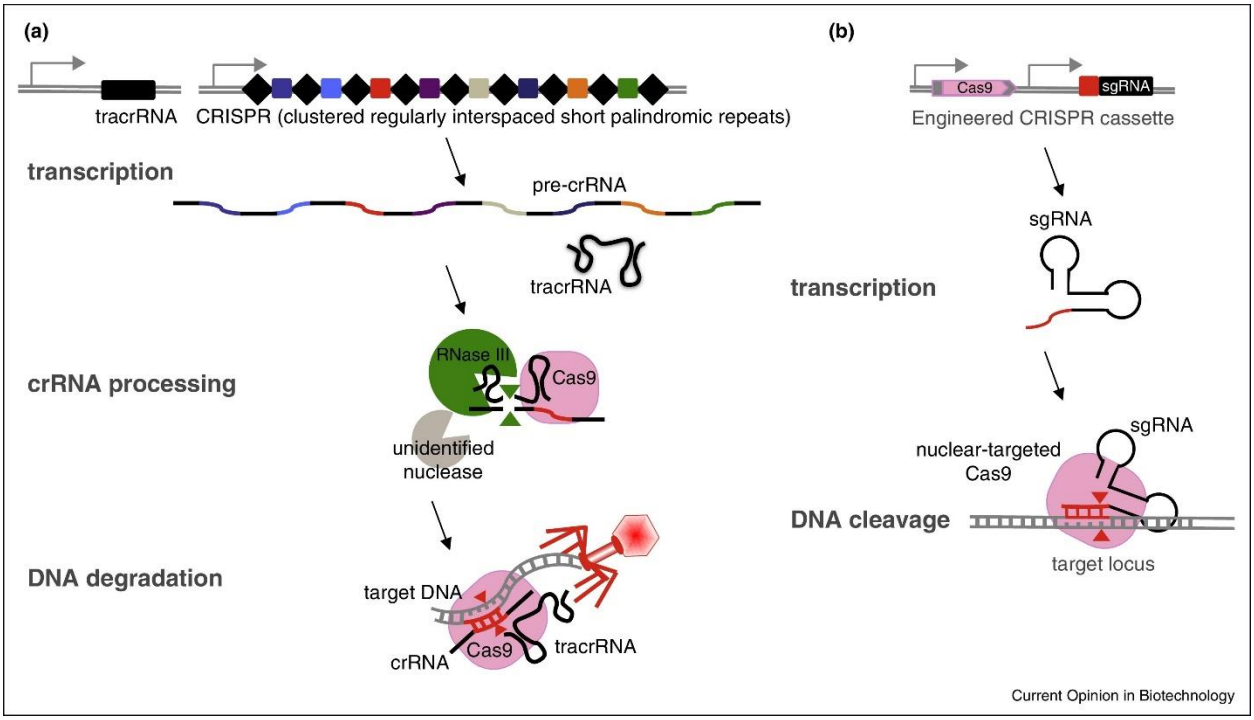

Figure 2. 2: Summary of the CRISPR/Cas9 system as a form of adaptive immunity **(a)** and as a gene-editing tool **(b)**. (*Derived from Belhaj et al. (2015)*)

The CRISPR-Cas9 system was first used for gene editing in mice and humans. In a particular study, it was shown that not only can the CRISPR-Cas9 system be used to perform precise genetic modification, but it can also be used for multiplex genome engineering (Cong et al. 2013). Simply put, this technique can be used to edit multiple loci of the genome simultaneously. In the case of other gene-editing methods, only one mutation was possible at a time, making the process laborious. Depending on the goal, the CRISPR-Cas9 system can use several DNA double-stranded break (DSB) repair mechanisms. The most common DBS repairing mechanism used is the non-homologous end joining (NHEJ). The popularity behind this mechanism is that it is the most common to occur. The NHEJ repair mechanism joins the ends of a DSB. However, this form of

repair is not perfect and often leads to insertions or deletions (Figure 2.3). The insertion/deletion causes a frameshift, thereby inactivating the protein that the sequence is expressing (Bortesi and Fischer 2015). The NHEJ repair mechanism can also be used to insert foreign DNA. This process is done by introducing segments with the same overhangs as the nuclease creates when it cleaves its target (Cristea et al. 2013). The second mechanism is homologous-directed repair (HR). This mechanism uses a template to repair the DSB to provide a mistake-free fix (Figure 2.3) (Iliakis et al. 2004). Usually, the HDR will use the sister chromatin as the repair template. However, if a gene of interest is introduced with homologous ends, one can use this system to produce an error-free insertion. So, if exogenous DNA with compatible homologous ends is presented with the CRISPR-Cas9 system, one can insert any sequence into the genome at a specific location. The HDR, however, is not as common as the NHEJ repair. For this reason, the efficiency of DNA insertion using the HDR is low (Puchta 2004).

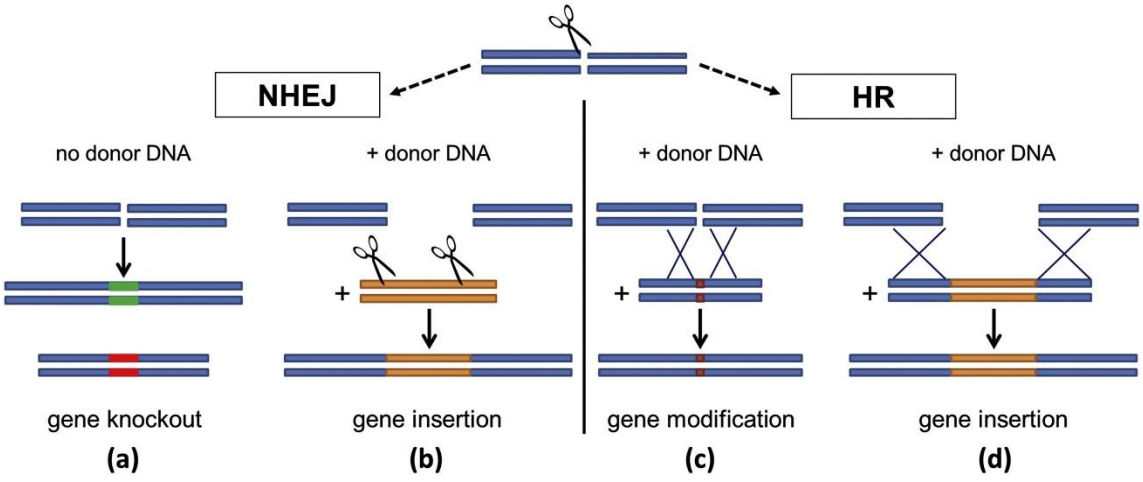

Figure 2. 3: Summary of homologous non-homologous end joining (NHEJ) and homologous directed repair (HR) (*Derived from Bortesi and Fischer (2015)*)

Precise gene editing is a potent tool for the improvement of modern-day crops. Yet, these tools are limited by incomplete genome sequences, difficulty in delivery systems due to the presence of the cell wall, and the lack of functional characterization of the known sequences. Despite these

obstacles, progress in the gene-editing of plants has occurred. Improvements in the resistance of biotic stress using the CRISPR/Cas9 system have been demonstrated in *A. thaliana* (Ji et al. 2015), rice (Wang et al. 2016; Zhou et al. 2015), and wheat (Wang et al. 2014b). In terms of abiotic stress, improvements have been made in maize (Shi et al. 2017), tomato (Wang et al. 2017a), and rice (Shan et al. 2014; Xie and Yang 2013). Lastly, the improvement of nutritional traits has been explored in soybean (Du et al. 2016), maize (Liang et al. 2014), and tomato (Ito et al. 2015).

2.9 Development of the CRISPR/Cas9 gene-editing system

An essential aspect of introducing the CRISPR-Cas9 system into the genome of any species is the selection of a promoter. An appropriate promoter should allow for the expression of both the Cas9 nuclease and the gRNA at a high level. Kumar et al. (2018) demonstrated the efficacity of the *HvU3* promoter for the expression of the CRISPR/Cas9 system in barley. This sequence is a *U3* snRNA promoter, an RNA polymerase III (Pol III) specific promoter. *U3* snRNA promoters have successfully been used in rice (Miao et al. 2013), wheat (Belhaj et al. 2013), and maize (Feng et al. 2016). Kumar et al. (2018) considered three characteristics of the promoter sequence when searching for an appropriate *U3* promoter. These characteristics include a TATA box, an upstream sequence element (USE), and a monocot-specific promoter (MSP). An upstream sequence element (USE) acts as a cis-regulating segment of DNA. In other words, it is a sequence that increases neighbouring genes' expression (Bachhawat et al. 1995). However, the TATA box and USE are not enough to promote gene expression, as the MSP also plays an important role. MSPs are found upstream of the USE and are essential for binding RNA polymerase III (Pol III) (Connelly et al. 1994). Altogether, these three elements play an important role in the success of this type of promoter in tandem with the CRISPR/Cas9 system and are all found within the *HvU3* promoter. Under this promoter, only 40% of all calli bombarded did not have a mutation at the target sequence (Kumar et al. 2018). Simply put, this promoter is highly efficient for gene editing.

However, the expression of the genes is not solely enough to efficiently perform genomic alteration.

The efficiency of the CRISPR/Cas9 system is highly dependent on the development of the sgRNA. Single guide RNA design has been experimentally optimized based on specificity and on-target efficiency. In terms of specificity, a study conducted by Hsu et al. (2013) analyzed the parameters that would allow a sgRNA to tolerate binding to a non-identical off-target. This study found that the further the nucleotide position was to the PAM sequence, the more likely the sgRNA was to tolerate a mismatch. However, it was also found that off-target binding could tolerate a maximum of 2 mismatches within the seed region (2-8 nucleotides from the PAM) of the sgRNA (Cho et al. 2014). Hsu et al. (2013) also discovered that the CRISPR/Cas9 system tolerated a PAM sequence of NAG instead of NGG, but at a much lower cleaving efficiency. An important aspect to consider is the abundance of the Cas9 enzyme and the sgRNA transcripts, as off-target effects with low cleaving efficiency are more likely to occur at high concentrations (Young et al. 2019). On-target efficiency is another crucial component of gRNA design. Doench et al. (2014) looked at sequence features that improved the on-target efficiency of different sgRNA. In terms of the PAM sequence, CGGT demonstrated the highest efficiency level, while a PAM of TGGG demonstrated the lowest. Interestingly, a high or low GC content is detrimental to the productivity of the gRNA (Wang et al. 2014a). Lastly, gRNA targeting the untranscribed strand was more effective than those targeting the transcribed strand (Wang et al. 2014a). Despite the ability to develop an efficient CRISPR/Cas9 system in oat, these findings are meaningless without delivering the construct to the plant cells.

2.10 Construct delivery systems

Many delivery systems for the insertion of exogenous DNA into a plant's genetic makeup have been developed. The transformation of plant cells entails two significant components—first, the

introduction of foreign DNA into the plant cell. Then, the integration of the foreign DNA into the genome (Altpeter et al. 2016). The first case of introducing a novel foreign gene into a plant was achieved in tobacco (*Nicotiana* tabacum) using a Polyethylene Glycol technique (Paszkowski et al. 1984). Since then, many transformation systems have been applied in plants, including electroporation, microprojectile, ultraviolet laser microbeam, viral vector-mediated transformation, agrobacterium-mediated transformation, and microprojectile bombardment (Keshavareddy et al. 2018). Of those mentioned above, agrobacterial-mediated and microprojectile bombardment are the most extensively used for plant transformation.

Agrobacterium tumefaciens has proven to be an effective delivery technique in many species, as it can deliver a discrete segment of DNA to its host. This trait has been exploited to transform a wide range of hosts, including cereals (Repellin et al. 2001). While Agrobacterium-mediated transformation can involve callus induction and regeneration, several methods have been adapted to allow for transformation *in planta*, such as the floral drop, agroinfiltration, spraying, and sonification (Ratanasut et al. 2017). This method has been demonstrated in cereals, including wheat (Cheng et al. 1997), barley (Tingay et al. 1997), and rice (Supartana et al. 2005). However, despite demonstrating potential, agrobacterial-mediate transformation remains inefficient in *Avena sativa*. This low efficiency is likely a result of oats not having an optimized train of *A. tumefaciens* (Gasparis et al. 2008). Fortunately, particle bombardment has been shown to have a higher transformation frequency in oats (Shrawat and Lörz 2006).

Microprojectile bombardment involves directly introducing DNA into the plant cell through its adhesion to gold particles (Sanford 1988). These DNA-covered gold particles are delivered to the plant cells at high velocity, penetrating the plant cell wall. In turn, these introduced sequences can be expressed transiently or stably expressed through their integration into the genome (Baltes et

al. 2017). This method has many advantages, including its high frequency and wide compatible species range (Altpeter et al. 2016; Cho et al. 1999; Mahmoud 2019). As a delivery system, it is also helpful for insertion using modern techniques. For example, the biolistic method can prove more effective than agrobacterial gene transfer when introducing a foreign sequence using the HDR repair pathway and CRISPR/Cas9. This is because the biolistic method provides many copies of the introduced sequences of DNA and will therefore provide a higher number of repair templates (Svitashev et al. 2015). Nonetheless, these benefits can also act as a crutch in some cases. To begin, the integration of the introduced sequence is random. So, the insertion can interrupt essential genes. To add, multiple insertions are common during transformation using biolistics (Cho et al. 1998; Cho et al. 1999; Ismagul et al. 2018). Despite these hindrances, the biolistic method remains a favourable delivery system due to its ability to transform a wide range of species, co-bombard multiple genes at once, and the flexibility of incorporating modern gene-editing techniques such as the CRISPR/Cas9 system.

2.11 Tissue culture

2.11.1 Selection markers

The ability to deliver foreign DNA into a cell is an essential aspect of gene editing. Without this crucial step, it is impossible to manipulate the phenotypes of various crops. However, post-edit, an effective method to differentiate between transgenic and wild-type, and the ability to regenerate transgenic plants is required to analyze the DNA changes. For this reason, it is crucial to have a protocol developed to have a practical selection and high regenerability. Hygromycin phosphotransferase (*hpt*) has been shown to be an effective selectable marker with few escapes due to hygromycin's aggressive killing of non-transgenic calli (Olhoft et al. 2003; Tian et al. 2009; Van Den Elzen et al. 1985; Yu et al. 1999).

2.11.2 Plant regeneration

Alongside hygromycin, the media will be supplemented with 2,4-dichlorophenoxyacetic acid (2,4-D), 6-benzylaminopurine (BAP), and high cupric sulfate. The 2,4-D and BAP both increase the regeneration potential of calli post-transformation by up to 4.4-fold (Cho et al. 1999). In combination, these two chemicals increase green shoot formation. BAP and copper together produce shinier, more compact and brownish calli. These calli are also meristem-like in their ability to produce shoots (Cho et al. 1998). In a comparison of DBC2 and DBC3 media (DBC2 = 2mg/L BAP, 0.1 µM $CuSO_4$, DBC3 = 1mg/L BAP 0.5µM $CuSO_4$), regenerated plants had improved shoot formation and higher fertility in DBC3 (Cho et al. 1998; Choi et al. 2000). These results imply that DBC3 concentrations are optimal for oat growth. Altogether, the supplements BAP, $CuSO_4$, and 2,4-D are used to maintain calli that have a high potential to regenerate. With this goal achieved, the possibility of losing transgenic calli to lack of regenerability lessens.

Supplementation using the compounds mentioned above (BAP, $CuSO_4$, 2,4-D) works extraordinarily for the production of shoots but poorly induces root formation. As a result, the use of the auxin hormones indole-3-acetic acid (IAA), indole-3-butyric acid (IBA), and 1-Naphthaleneacetic acid (NAA) are important for root production. The plant hormones IAA and IBA both can induce lateral root growth (Woodward and Bartel 2005; Zolman et al. 2000). These auxins also share the ability to promote the adventitious formation of roots (King and Stimart 1998; Woodward and Bartel 2005). That is, they increase the likelihood of root cells forming in anatomically incorrect positions. This trait proves helpful when producing plants from undifferentiated cells and when producing roots in any position is valuable, such as in the case of putative transgenic plants. While IAA and IBA share root-promoting traits, they also share an inhibition of root elongation (Woodward and Bartel 2005). However, the inhibition by IBA is

much less than that of IAA. Therefore, IBA can be used at a much higher effective concentration without detrimental inhibition of root elongation. Lastly, NAA has also been shown to promote lateral root formation (Woodward and Bartel 2005). Therefore, this chemical proves helpful in overall lateral root formation without inhibition. Altogether, IAA, IBA, and NAA aid in the root growth of plants from tissue culture.

Connecting statement

Until recently, the lack of genomic resources in *Avena sativa* has held back the ability to employ precise gene-editing techniques such as CRISPR/Cas9. The setbacks were two-fold: A lack of a sequenced genome inhibited the ability to perform effective off-target analysis, and the ability to discover orthologous genes from other species. However, the sequenced genome of oat variety OT3098 v1 (https://wheat.pw.usda.gov/GG3/graingenes_downloads/oat-ot3098-pepsico) has newly been released, opening the floodgates for the implementation of precise gene-editing techniques. Considering the lacking information surrounding the mechanism of beta-glucan regulation and synthesis, we endeavoured to add to this body of knowledge. Recently, our lab discovered that Thaumatin-like protein 8 (TLP8) was negatively correlated with the beta-glucan content in barley. In the following study, we aimed to explore this relationship in the common oat using the published genome and the CRISPR/Cas9 system. The following chapter is formatted as a manuscript. The co-authors are listed as follows: Thomas Donoso, Rajiv K. Tripathi, Jaswinder Singh. The contribution of each author is fully described in the preface.

Chapter III

3.1 Abstract

Dietary fiber has gained interest due to the growing evidence that it lowers the incidence of cardiovascular disease (CVD), the second leading cause of mortality in Canada. Despite this attention, few genes have been identified to be involved in the regulation of dietary fibers, such as beta-glucan. Recently, our lab identified that the expression of *Thaumatin-Like Protein 8* (*TLP8*) has a negative correlation with beta-glucan content in barley (*Hordeum vulgare* L.). This result prompted the investigation of the relationship between TLP8 and beta-glucan in the common oat (*Avena sativa* L.) using the precise gene-editing tool CRISPR/Cas9. The orthologous *TLP8* sequences in oat were then sequenced for all three subgenomes (A, C, and D). Each homoeolog was determined to contain our previously reported sugar-binding motif and conserved residues in TLPs demonstrating beta-glucanase activity. Using this data, measuring relative gene expression of six different oat varieties was standardized using qRT-PCR analysis and homoeolog-specific primers. To further investigate the relationship between beta-glucan and *AsTLP8*, three CRISPR/Cas9-based constructs were designed to target each homoeolog specifically. All constructs were transformed in the oat variety Park, using hygromycin as a selection marker. The A, C, and D targeting constructs demonstrated a transformation frequency of 5.23%, 0.47% and 2.86%, respectively. Transgenic lines (T0) were moved to the T1 generation and sequenced through Sanger sequencing. All but one transgenic plant demonstrated a CRISPR/Cas9-induced mutation within the *AsTLP8-D* sequence. Further studies will involve analysis of *AsTLP8* knockout lines for modifications in the beta-glucan content.

3.3 Introduction

The ever-growing population and limited arable land have developed the challenge of balancing sustainability and agricultural production. In other words, not only does the output of the agricultural industry need to increase, but so does the quality of the crops. These improvements must consider the health needs of the population, rather than just the caloric requirements. The common oat is an essential crop in Canada, as they are the largest exporter of this grain and second-largest producer (USDA 2019). Oats are also growing in popularity due to their myriad of health benefits, including boosting the immune system, promoting skin health, and reducing the risk of cardiovascular heart disease (CDV) (Daou and Zhang 2012; Du et al. 2014; Whitehead et al. 2014). The reduction in heart disease is of particular interest as CVD is the second leading cause of mortality in Canada, claiming the lives of over fifty-thousand Canadians in 2018 (Canada 2019). Despite acknowledging the effectiveness of dietary fibre in preventing heart disease, there is little known about the genetics involved in the synthesis and regulation of beta-glucan in cereals. Intriguingly, Thaumatin-like Protein 8 (TLP8) has been associated with a reduced beta-glucan content in barley (Singh et al. 2017). In other words, varieties with a higher amount of *TLP8* expression, have a lower beta-glucan content. In this study, we aimed to uncover the nature of this relationship within the oats.

The common oat (*Avena sativa*) is a hexaploid (AACCDD) species derived from alloploidy of ancestral diploid and tetraploid oat species (Leggett and Thomas 1995; Maughan et al. 2019). The complexity of oat genetics has led to difficulties in producing the sequenced genome. Fortunately, the sequence of oat variety OT3098 has been recently released. This data allows us to determine the orthologs of *HvTLP8* in oats and measure the relationship between their expression and the beta-glucan content.

The CRISPR/Cas9 system presents the opportunity to precisely gene-edit the oat genome. This genetic modification tool has been implemented in many cereals, including wheat (Liang et al. 2017; Sánchez-León et al. 2018), barley (Kapusi et al. 2017; Kumar et al. 2018), maize (Char et al. 2017; Shi et al. 2017) and rice (Dong et al. 2020; Wang et al. 2020). Surprisingly, this revolutionary tool has never been implemented in oats. Using the newly released oat genome, and the CRISPR/Cas9 system, our goal is to implement and standardize precise gene-editing techniques in *Avena sativa* for the first time. We will explore the association between AsTLP8 expression and the beta-glucan content using this protocol.

3.3 Materials and Methods

3.3.1 Plant growth

Oat seeds from a variety, Park were planted and grown in the Macdonald campus growth chambers at McGill University. A 16:8 photoperiod was used, with a day temperature of 22^{o}C and a night temperature of 15^{o}C. A fertilizer containing 20:20:20 (nitrogen: phosphorus: potassium) was added after sowing and when seeds began to form and promote tiller growth.

3.3.2 Determining *HvTLP8* orthologs in *Avena sativa*

Using the known TLP8 sequence in barley, a BLAST (https://blast.ncbi.nlm.nih.gov/Blast.cgi) was performed on the red oat (*Avena byzantina*) sequences provided by Dr. Tim Langdon of Aberystwyth University. Primers were designed using the upstream and downstream sequences of the predicted CDS of each BLAST hit (Table 3.1). Each copy was amplified by its respective primers. Amplicons are ligated into the pGem-T Easy Vector (Promega), and then plasmid extractions were done using the QIAGEN Plasmid Midiprep Kits using provided protocols. The extracted plasmids are then sent for Sanger sequencing using the primers M13F and M13R (Table 3.1). Genome Quebec performed sequencing. The sequences in Park were then used to perform a

BLAST using the Geneious Prime software version 2022.0.1 against the PepsiCo OT3098 genome v1. The subgenomes of each Park sequence were determined by comparing the percent identity to the homoeologs of the OT3098 genome.

3.3.3 Guide RNA design

The guide RNA design was conducted through the software Geneious, as it allows the creation of a local database for off-target analysis. The *Avena sativa* variety OT3098 genome (Pepsico v1, https://wheat.pw.usda.gov/GG3/graingenes_downloads/oat-ot3098-pepsico) was used as a database. Three guide RNAs were chosen for each subgenome's copy of *AsTLP8*. The guide RNA was determined based on position, off-target score (Hsu et al. 2013), and efficiency score (Doench et al. 2014). The positions of the gRNA were chosen with an approximately 100bp gap between the first and last, potentially leading to a deletion large enough to be visible when run on an agarose gel.

3.3.4 Construct design

The construct design will be based on the previously designed shuttle and recipient vectors. (Kumar et al. 2018). All shuttle and recipient vectors were provided by Dr. Johannes Stuttmann of the Martin Luther University Halle-Wittenberg. Oligos designed for each sgRNA (Table 3.4) were mixed with their respective oligo at a concentration of 10µM. The mixture was incubated at 98 ^{o}C for 5 minutes. The mixture is then allowed to cool/hybridize at room temperature for several minutes. The hybridized oligos are then diluted to a concentration of 100 fmol/µl. These oligos were placed in three separate shuttle vectors (Appendix A1-3) using the described cut/ligation reaction (Kumar et al. 2018). This cut/ligation reaction used a Thermocycler program of 30 cycles of 37 ^{o}C for 2 minutes and 16 ^{o}C for 5 minutes, 50 ^{o}C for 10 minutes, and then 80 ^{o}C for 10 minutes. Ligated shuttle vectors were then transformed into competent DH5α cells and grown on selective

media (Lysogeny broth (LB) supplemented with 100mg/L Ampicillin). Colonies are picked, and plasmid extraction is performed using the QIAGEN Plasmid Midiprep Kits using provided protocols. The shuttle vectors are then combined with the destination vector (Appendix A4), and a previously described cut/ligation reaction is done through Golden Gate Cloning to produce the final gene-editing plasmid (Engler and Marillonnet 2014; Kumar et al. 2018). The same aforementioned thermocycler program is used. Ligated final vectors were then transformed into competent DH5α cells and grown on selective media (Lysogeny broth (LB) supplemented with 100mg/L Streptomycin). A final plasmid extraction is performed using the same extraction kit.

3.3.5 Digestion of Construct

The insertion of the gRNA and *U3* promoters into the destination vector was confirmed through digestion using High Fidelity SacI (SacI-HF) from New England Biolabs. The produced *AsTLP8*-targeting gene-editing constructs were all digested at 37^{o}C for three hours. The construct without the insert was also digested as a control. The constructs with an insert contain three cut sites within the *HvU3* promoters, leading to two segments 777bp in size, and a backbone of 16,580bp. The digested products were run on a 0.8% agarose gel.

3.3.6 Formation of undifferentiated cells

Mature seeds of the oat spring variety GAF/Park-1 were used for their past success in microprojectile bombardment (Cho et al. 1999). Seeds were surface sterilized for 10 minutes in a 1.5% bleach solution. Then, seeds were placed on Regeneration media (Table 3.1), covered with aluminum foil, and allowed to germinate. Once germinated, the germinated embryo is separated, and any formed roots/shoots are removed. The trimmed embryo is placed on C' media (Table 3.1). To maintain undifferentiated cells, any formed shoots and roots are removed from the calli every two weeks.

Table 3. 1: Components of regeneration and rooting media

Media	Regeneration	Rooting	C’
MS salts (g/L)	4.4	4.4	4.4
Maltose (g/L)	--	--	30
Sucrose (g/L)	30	30	--
Casein hydrolysate (g/L)	--	--	1
Proline (g/L)	--	--	0.69
Myo-inositol (g/L)	--	--	0.25
Thiamine HCl (mg/L)	1	1	1
Pyridoxine HCl (mg/L)	0.5	0.5	--
Nicotinic acid (mg/L)	0.5	0.5	--
$CuSO_4$	0.16 mg/L	0.16 mg/L	5 µM
2,4-D (mg/L)			2
BAP (mg/L)	1	--	0.5
IAA (mg/L)	1	1	--
IBA (mg/L)	--	1	--
NAA (mg/L)	--	1	--
pH	5.8	5.8	5.8

3.3.7 Microprojectile bombardment

The transformations were all done in the oat variety Park. To prepare for microprojectile bombardment, a circle of undifferentiated cells (calli) about 3 cm in diameter is first placed on osmotic media for three hours (c’ supplemented with 0.*2 M* mannitol and 0.2 *M* sorbitol). Approximately 35 calli are bombarded per plate. For each bombarded plate, 6µl of suspended gold-stock solution (60mg of 0.6 µm gold particles in 1ml of 100% ethanol). The following protocol is for a total of 36 µl of gold stock. The suspension is centrifuged at 13,000 rpm for 1 minute and the supernatant is discarded. To the pellet, 200-300 µl of filtre sterile water (FSH_2O)

is added, and the mixture is centrifuged at 13,000 rpm for 1 minute. The supernatant is discarded. To the pellet, 6 µg of plasmid DNA is added, and the tube is gently tapped. To this mixture, up to 250 µl of FSH_2O from the volume added in DNA), 250 µl of calcium chloride ($CaCl_2$) and 50 µl of spermidine are added. This concoction is vortexed briefly to mix and incubated on ice for 30 minutes, occasionally tapping to remix. After incubation, the mixture is centrifuged at 13,000 rpm for 1-2 minutes. The supernatant is removed, and 200 µl of ethanol is added. The sample is centrifuged again at 13,000 rpm and the supernatant removed. To the pellet, 36 µl of ethanol is added, and the plasmids are now ready for bombardment.

The microprojectile bombardment was accomplished using the BioRad PDS-1000/He system. All removable pieces are autoclaved to ensure sterility. The laminar hood and inside of the PDS-1000 device are cleaned using 70% ethanol. For each plate, 6 µl of the above prepared mixture is loaded onto a macrocarrier. The ethanol is allowed to evaporate. The macrocarrier is then placed onto a macrocarrier holder. The system is turned on in the order of helium tank, vacuum, and then the PDS-1000 device. A rupture disc (pressure retention of 1100psi) is placed in its retaining cap and screwed tightly to the gas acceleration tube. A stopping screen is placed on the microcarrier launch assembly. The macrocarrier in the macrocarrier holder is placed above the stopping screen, with the dried plasmid mixture facing down. The macrocarrier cover lid is screwed onto the assembly to ensure it stays fixed. The prepared calli on osmotic media are uncovered and placed on the target plate shelf. With the door closed, the vacuum is brought to a value of 25-30 Hg, and the button is switched to hold to maintain the vacuum. Then, the fire button is pressed until the gauge hits a value of 1100 psi and then released. The plate is removed and covered. The stopping screen, rupture disc, and the macrocarrier are discarded. Then, the inside of the PDS-1000 device is

cleaned and the process repeated for each plate. Subsequently, the bombarded calli are left on osmotic media overnight before being transferred to callus induction media (C', Table 3.1).

3.3.8 Selection of transgenic plants

Following bombardment, calli were exposed to DBC3 media supplemented with 10 mg/L of Hygromycin. Each selection round lasted 2-3 weeks before healthy calli were sub-cultured on fresh media containing the same concentration of Hygromycin. In total, two rounds of selection were used.

3.3.9 Regeneration of shoots/roots

Selected calli undergo shoot/root formation on regeneration and rooting media (Table 3.1). The regenerating plants are left on each media until shoot or root formation is substantial. This process takes approximately 1.5-2.5 weeks on each medium.

3.3.10 Genomic DNA extraction

Genomic DNA extraction was done using leaf samples of the variety Park. A one-inch leaf sample is placed into an Eppendorf tube containing small metal beads and immediately frozen in liquid nitrogen. The tissue is then lysed using a QIAGEN TissueLyser II at 30 oscillations/second for 3 minutes until made into a fine powder. Then, 500 µl of urea buffer (Chen and Dellaporta 1994) is added to each sample and is immediately vortexed for 2-3 seconds. To this mixture, 500 µl of the bottom layer of 1:1 phenol:chloroform is added. Samples are mixed on a tabletop shaker for 1hr. The mixture is centrifuge at 13,000 rpm for 6 minutes and the top layer pipetted into a clean Eppendorf tube. To this tube, 400 µl of Isopropanol and 40 µl of ammonium acetate are added. The samples are then mixed by inversion and centrifuged for two minutes. The supernatant is discarded, 400 µl of 70% ethanol is added, and the mixture is centrifuged at 13,000 rpm for 2 minutes. The supernatant is discarded carefully so as not to lose the pellet of DNA and allowed to

dry for 15 minutes. Once dry, 40 µl of TE buffer is added. Genomic DNA samples are then stored at -20^{o}C.

3.3.11 Analysis of transgenic plants

A thermocycler and Promega Green Master Mix (PCR) will amplify the inserted construct. The thermocycler conditions for PCR-based analysis were 95^{o}C for 2 minutes, 30 cycles of the combined primer melting temperature for 30 seconds and 72^{o}C for 45 seconds, and 72^{o}C for 5 minutes. The combined temperature is calculated by taking the forward and reverse primers' average melting temperature. Each construct will be amplified by its respective inserted gRNA (Table 3.2). The amplified genes were run on a 0.8% agarose gel with the wild type (v. Park) and water as a negative control and the construct as a positive control. The subsequent generation of transgenic plants containing the insert (T1) was screened for deletions caused by the gRNA. Subgenome-specific primers were designed for each copy of *AsTLP8* (Table 3.2). PCR amplicons were then run on a 2% agarose gel to compare against the wild type (v. Park). Any shift indicates a possible deletion by the designed gRNA.

3.3.12 Primer design

All primers used for analysis are displayed in Table 3.2. Primers were ordered from Integrated DNA Technologies (IDT). Primers used for PCR-based screening (Columns 1-14, 21-26) were designed using the Geneious prime primer design tool. Primers designed for qRT-PCR analysis (Columns 15-20, 27-30) were designed using the IDT RealTime qPCR Assay design tool (www.idtdna.com/scitools/Applications/RealTimePCR).

1099 Table 3. 2: Primers used in PCR-based analysis of putative gene-edited plants.

#	Primers	Orientation	Sequence	Notes	Amplicon Size (bp)
1	TLP8 Oat1 gF	F	TAGTCTCGTGTCTTGCTACCT	Amplifying C-Genome *TLP8* for sequencing	1015
2	TLP8 Oat1 gR	R	GAATACATCCATTGCCAGCTTTAC		
3	TLP8 Oat2 pF	F	GGAGTCCAGCTACCTCGT	Amplifying D-Genome *TLP8* for sequencing	1027
4	TLP8 Oat2 pR	R	AGAGAAGATTTCTCTCCATGAAAGAG		
5	TLP8 Oat3 bF	F	TCCACGTTACGCAGCAATATAA	Amplifying A-Genome *TLP8* for sequencing	1349
6	TLP8 Oat3 bR	R	CCCTAATTCCAGATGAGGTGATG		
7	M13F	F	GTTTTCCCAGTCACGAC	Sequencing pGem-T Easy Vector (Promega)	N/A
8	M13R	R	CAGGAACAGCTATGACCAT		
9	ASG1O1	F	AGCAGCAACAGTGGAAGGTCGAGG	Screening for Transgenic Plants (A-Genome)	804
10	ASG3O2	R	AAACGTACGAAGGCCAGGACTTCA		
11	CSG2O1	F	AGCATGGAACATCAACGTGCCGGC	Screening for Transgenic Plants (C-Genome)	784
12	CSG1O2	R	AAACGCAGGAAGTTCATGGGCACG		
13	DSG1O1	F	AGCATGGAACATCAACGTGCCTGC	Screening for Transgenic Plants (D-Genome)	784
14	DSG2O2	R	AAACTGGCCGAGTTCGGGCTCAAC		
15	qPCR-TLP8A-1F	F	GACTTCATCGACATCTCCGTC	qPCR for A-Genome	139
16	qPCR-TLP8A-1R	R	CCTTGAGCTCGTTCGGG		
17	qPCR-TLP8C-2F	F	AACGTGCCCATGAACTTCC	qPCR for C-Genome	153
18	qPCR-TLP8C-2R	R	CTTGTCCTGCTTGAACACC		
19	qPCR-TLP8D-2F	F	CAATGTGCCCATGAACTTCC	qPCR for D-Genome	155
20	qPCR-TLP8D-1R	R	ACTTGTCCTGCTTGAACACC		
21	AsTLP8A-In2F	F	ACCAACAAGTGCCAGTTCA	Screening for CRISPR/Cas9 Induced Deletions	605
22	AsTLP8A-In3R	R	GGCAGAAGATGACCTGATAGTT		

23	AsTLP8C-In2F	F	CTCTCCACCTCTTCCATGTTG	Screening for CRISPR/Cas9 Induced Deletions	531
24	AsTLP8C-In2R	R	GCAGTACTTGTCCTGCTTGA		
25	AsTLP8D-In2F	F	GTCACCAACAAGTGCCAGTA	Screening for CRISPR/Cas9 Induced Deletions	603
26	AsTLP8D-In1R	R	CAGAAGATGACCTGGTAGTTGG		
27	qRT_AsEIF4A_F	F	TCTCGCAGGATACGGATGTCG	Housekeeping Gene (Yang et al. 2020)	88
28	qRT_AsEIF4A_R	R	TCCATCGCATTGGTCGCTCT		
29	qRT_AsEF1A_F	F	GTGAAGATGATTCCCACCAAGC	Housekeeping Gene (Yang et al. 2020)	87
30	qRT_AsEF1A_R	R	CCTCATGTCACGCACAGCAAA		

3.3.13 RNA extraction

The RNA extractions were done using the Sigma-Aldrich Spectrum Plant Total RNA Kit with a modified protocol. Two replicates were done of six oat cultivars, including AC Morgan, CDC Morrison, Marion, Park, Terra, and Goslin. Starting with 2-3 seeds, the samples are frozen in liquid nitrogen and ground with a mortar and pestle until homogenized. The lysis solution (700µl lysis solution + 7 µl 2-Mercaptoethanol) is added to the crushed sample and vortexed immediately. The mixture is incubated for 5 minutes at room temperature, followed by centrifugation at 13,000 rpm for 3 minutes. The lysate is pipetted (supernatant) and put into the centre of the filtration column in a clean Eppendorf tube. The column is centrifuged at 13,000 rpm for 3 minutes. To the flowthrough, a 700µl binding buffer is added and mixed by pipetting. The mixture is then loaded into the centre of a binding column in a clean Eppendorf tube. The column is centrifuged at 9000 rpm for 1 minute. The flowthrough is discarded, and the rest of the filtrate from the filtration column step is loaded into the binding column. The column is centrifuged again at 9000 rpm. To the column, 500 µl of the Washing Solution I is added and centrifuged at 9000 rpm for 1 minute. The filtrate is discarded. To the column, 500 µl of the Washing Solution II is added and centrifuged

at 9000 rpm for 1 minute. After pouring the filtrate, this washing step (Washing Solution II) is repeated. Again, the filtrate is poured, and dry spun at 13,000 rpm for 1 min is performed. The binding column is placed in a new Eppendorf tube. To the centre of the column, 30 µl of the elution buffer is added and centrifuged at 13,000 rpm for 1 minute. The flowthrough is then stored at -80^{o}C.

3.3.14 DNase treatment of RNA samples

DNase treatment was done by initially taking a total of 1000ng of RNA. Each sample was then brought to a total volume of 8 µl with nuclease-free water. To this mixture, 1 µl of DNase I enzyme and 1 µl of RQ1 DNase reaction 10x buffer are added (Invitrogen) to bring the final volume to 10 µl. Then, the samples are incubated at 37^{o}C for 40 minutes. After incubation, 1µl of EDTA (25mM) is added. The mixture is incubated at 65^{o}C for 10 minutes and stored at 4^{o}C prior to cDNA synthesis.

3.3.15 cDNA synthesis

The synthesis of cDNA was accomplished with 1000ng of DNAse treated RNA in each sample. The Agilent Technologies cDNA synthesis kit was used with the conditions of 42 ^{o}C for 5 minutes, 55 ^{o}C for 15 minutes, and 95 ^{o}C for 5 minutes.

3.3.16 qRT-PCR analysis

Quantitative PCR analysis will be done using the synthesized cDNA and the primers designed for each subgenome homoeolog (Table 3.2). The housekeeping gene used was the *Eukaryotic translation elongation factor* (*EF1A*) (Table 3.2) used in previous studies (Yang et al. 2020). In the qRT-PCR process, SYBR Green qPCR Master Mix from Wisent and the Stratagene Mx3005P qPCR System was used. Each variety had two biological and two technical replicates. The qPCR conditions used were 95^{o}C for 2 minutes, 40 cycles of 95^{o}C for 5 seconds, and 60^{o}C for 30 seconds.

The relative gene expression of each sample was analyzed using the $2^{-\Delta\Delta Cq}$ method (Livak and Schmittgen 2001).

3.4 Results

3.4.1 Discovery of *HvTLP8* orthologs in oat

A Basic Local Alignment Search Tool (BLAST) was used to find highly similar sequences in red oat to the *TLP8* sequence in barley. Three sequences were found within the genome of *Avena byzantina* (Appendix A5-7). Primers were designed using the upstream and downstream sequences of the BLAST hits (Table 3.2). The primers were used to amplify the three homoeologs in oat variety Park (Figure 3.1). Amplified sequences were then ligated into a pGEM-T vector and sent for Sanger sequencing using the primers M13-F and M13-R (Appendix A5-7).

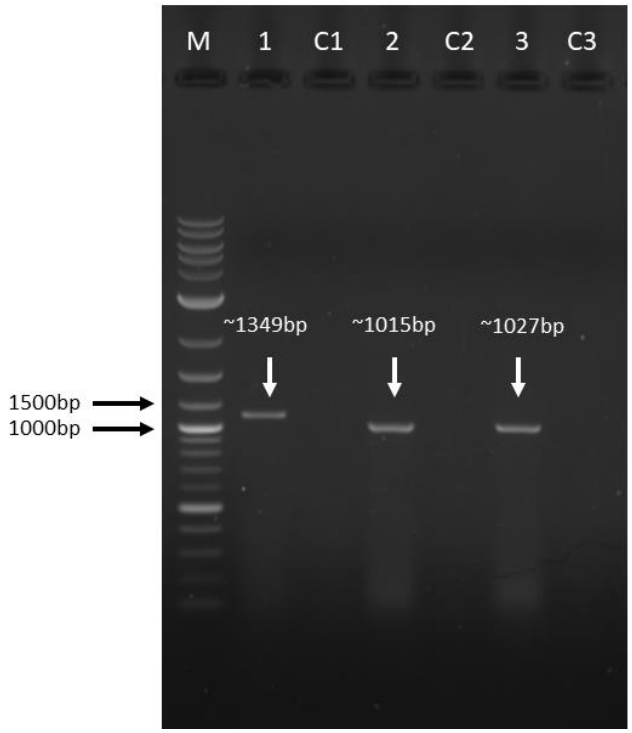

Figure 3. 1: PCR-amplification of AsTLP8 homoeologs in oat. The well M has a 1kb plus ladder (NEB). Lane 1 contains the PCR amplification of *AsTLP8-A* in oat variety Park at the size of 1349bp. C1 has a water control. Samples 1 and C1 were PCR amplified using the primers TLP8-Oat3-bF and TLP8-Oat3-bR (Table 3.2).Well 2 contains a PCR amplification of *AsTLP8-C* in

oat variety Park at the size of 1015bp. Well C2 has a water control. The samples in well 2 and C2 were PCR amplified using the primers TLP8-Oat1-gF and TLP8-Oat1-gR (Table 3.2). Well 3 contains the PCR amplification of *AsTLP8-D* in oat variety Park at a size of 1027bp. Well C3 includes a water control. The samples in well 3 and C3 were PCR amplified using the primers TLP8-Oat2-pF and TLP8-Oat2-pR (Table 3.2).

The subgenome of each copy and the sequence of each AsTLP8 homoeolog in OT3098 were determined through a BLAST against the PepsiCo v1 oat genome (https://wheat.pw.usda.gov/GG3/graingenes_downloads/oat-ot3098-pepsico,) and by comparing the hits by percent identity. In each case, only one v. Park homoeolog had the highest percent identity with the corresponding OT3098 homoeologs (Table 3.3). The *AsTLP8-A*, and *-C* in Park demonstrated a high percent identity with their respective homoeolog in OT3098 (97.126 and 99.713%, respectively). However, the Park *AsTLP8-D* showed a relatively low percent identity (76.101%) due to the deletion within this homoeolog in OT3098 (Table 3.3).

Table 3. 3: Percent Identity between *AsTLP8* homoeologs in OT3098 and Park. The percent identity was measured by taking the percent of bases that are identical in the Geneious alignment tool.

Homoeolog	*AsTLP8-A* (OT3098)	*AsTLP8-C* (OT3098)	*AsTLP8-D* (OT3098)
AsTLP8-A (Park)	97.126%	86.063%	69.969%
AsTLP8-C (Park)	86.063%	99.713%	74.057%
AsTLP8-D (Park)	85.057	96.695%	76.101%

3.4.2 Analyzing the TLP8 homologs in oat

The amino acid sequences of *TLP8* in oat varieties were compared to the *HvTLP8* sequence in barley (Figure 3.2). The A genome in both varieties (OT3098 and Park) demonstrated an amino change in the second residue of the previously described sugar-binding motif of CQTGDCGG

(Singh et al. 2017). Glutamine was changed to glutamic acid (Q (E) in both cases. In the case of the C genome homoeolog in the variety Park, this same residue was changed to arginine (Q →R). Interestingly, a 20 amino acid deletion was observed in the D genome of OT3098, a variety with high beta-glucan content (Appendix BG). Certain thaumatin-like proteins have been reported to break down polymeric beta-1,3-glucans(Grenier et al. 1999). Some conserved residues have been observed among these TLPs and fungal beta-1,3-glucanases (Grenier et al. 2000). Every homoeolog in both varieties OT3098 and Park contain these conversed amino acids (Figure 3.3).

```
OT3098-AsTLP8-A WGAAVP-GGGQKLDPGQQWKVEVPAGTTSGRVWARTGCNFDGSGNGKCETGDCGGKLQCT   96
Park-AsTLP8-A   WGAAVP-GGGQQLDPGQQWKVEVAAGTTSGRVWARTGCNFDGSGNGKCETGDCGGKLQCT   96
HvTLP8          WAAAVPAGGGQKLDAGQTWSINVPAGTTSGRVWARTGCSFDGAGNGRCQTGDCGGKLRCT  120
OT3098-AsTLP8-D WAAAVPAGGGRKLDPGQSWNINVPAGTTGGRVWARTGCNFDGSG----------------   80
Park-AsTLP8-D   WAAAVPAGGGRKLDPGQSWNINVPAGTTGGRVWARTGCNFDGSGNGRCQTGDCGGKLQCT   96
Park-AsTLP8-C   WAAAVPVGGGRKLDPGQTWNINVPAGTTSGRVGARTGCNFDGSGNGRCRTGDCGGKLQCT   96
OT3098-AsTLP8-C WAAAVPVGGGRKLDPGQTWNINVPAGTTSGRVWARTGCNFDGSGNGRCQTGDCGGKLQCT   96

OT3098-AsTLP8-A QYGQAPNTLAEFGLNQYEGQDFIDISVIDGFNVPMDFLPADGTTGCPKGGPRCDADITAQ  156
Park-AsTLP8-A   *YGQAPNTLAEFGLNQYEGQDFIDISVIDGFNVPMDFLPADGTTGCPKGGPRCDADITAQ  156
HvTLP8          QYGQAPNTLAEFGLNKYMGQDFFDISLIDGYNVPMSFVPAPGSPGCPKGGPRCPKVITPA  180
OT3098-AsTLP8-D ----APNTLAEFGLNKFNNLDFFDISLIDGFNVPMNFLPAGSGAGCPKGGPRCPKVITPQ  136
Park-AsTLP8-D   QYGQAPNTLAEFGLNKFNNLDFFDISLIDGFNVPMNFLPAGSGAGCPKGGPRCPKVITPQ  156
Park-AsTLP8-C   QYGQAPNTLAEFGLNKFNNLDFFDISLIDGFNVPMNFLPAGSGAGCPKGGPRCPKVITPQ  156
OT3098-AsTLP8-C QYGQAPNTLAEFGLNKFNNLDFFDISLIDGFNVPMNFLPAGSGAGCPKGGPRCPKVITPQ  156
```

Figure 3. 2: Sugar-binding motif variations between *TLP8* amino acid sequences in barley and oat. The sequence in all three subgenomes (A, C, D) of both variety Park and OT3098 are partially shown. The sequence in barley (HvTLP8) is also shown. The yellow highlighted sequences demonstrate the sugar-binding motif described in (Singh et al. 2017). Residues highlighted in red indicate a change in the sugar-binding motif. The sequences of subgenomes A and C in Park and A in OT3098 demonstrate a one residue change in the second position of the sugar-binding motif. The D genome sequence in Park has a 20 amino acid deletion that completely removes the sugar-binding motif. The value in the right column indicates the position of the last amino acid in the row within its respective sequence. Alignment was done using the EMBL-EBI MUltiple Sequence Comparison by Log-Expectation (MUSCLE) tool (https://www.ebi.ac.uk/Tools/msa/muscle/).

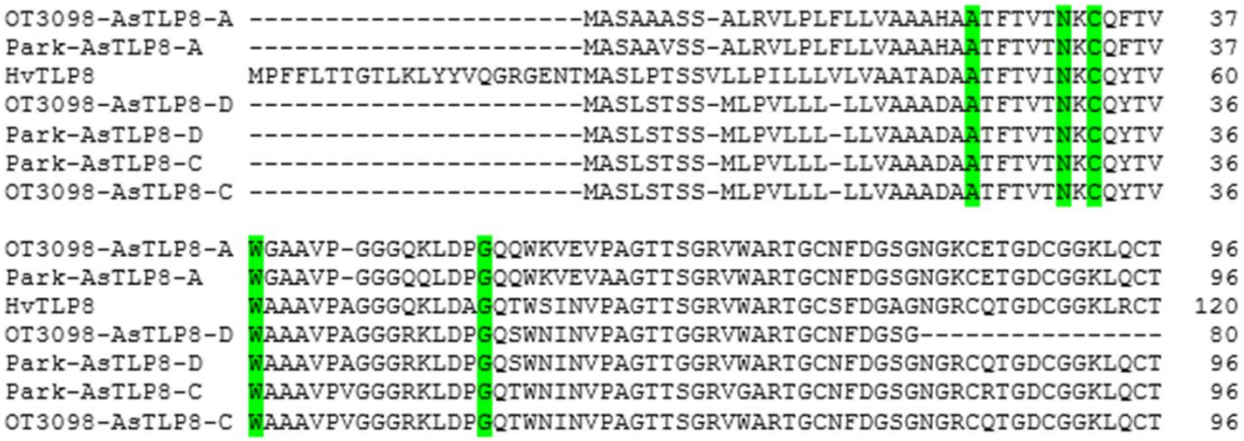

Figure 3. 3: All *TLP8* homoeologs and orthologs contain conserved amino acids in fungal beta-1,3-glucanases. The sequence in all three subgenomes (A, C, D) of both variety Park and OT3098 are partially shown. The sequence in barley (*HvTLP8*) is also shown. The highlighted sequences are residues conserved in Thaumatin-Like Proteins that exhibit endo-beta-1,3-glucanase activity (Grenier et al. 2000). All sequences contain the conserved residues. The value in the right column indicates the position of the last amino acid in the row within its respective sequence Alignment was done using the EMBL-EBI MUltiple Sequence Comparison by Log-Expectation (MUSCLE) tool (https://www.ebi.ac.uk/Tools/msa/muscle/).

3.4.3 Standardizing qRT-PCR-Based Analysis of *AsTLP8* homoeologs

The sequence-based analysis led to interesting inferences into the role of *AsTLP8* homoeologs in beta-glucan regulation. However, we were interested in demonstrating a similar relationship between beta-glucan and *TLP8* expression in oat as observed in barley (Singh et al. 2017). Therefore, primers for qRT-PCR were designed to target each homoeolog separately. Considering the beta-glucan content data available in the literature is typically measured by dry weight of the mature seed (Appendix A8), we looked at the relative expression of *AsTLP8* homoeologs within the mature seed. Although the means of certain varieties varied greatly, namely Terra and Goslin, the standard deviation was high between replicates (Figures 3.4). Further analysis using the Tukey test, a post hoc analysis of the ANOVA one-way test, determined no statistically significant difference between the relative expressions (Keselman and Rogan 1977). Therefore, it is difficult to infer the relationship between *TLP8* expression and beta-glucan content and deserves further attention. Validation of genotypic and phenotypic relations could be discerned by generating and

analysing gene specific mutants. In the next section, efforts have been made to edit each homoeologs of TLP8 in oat.

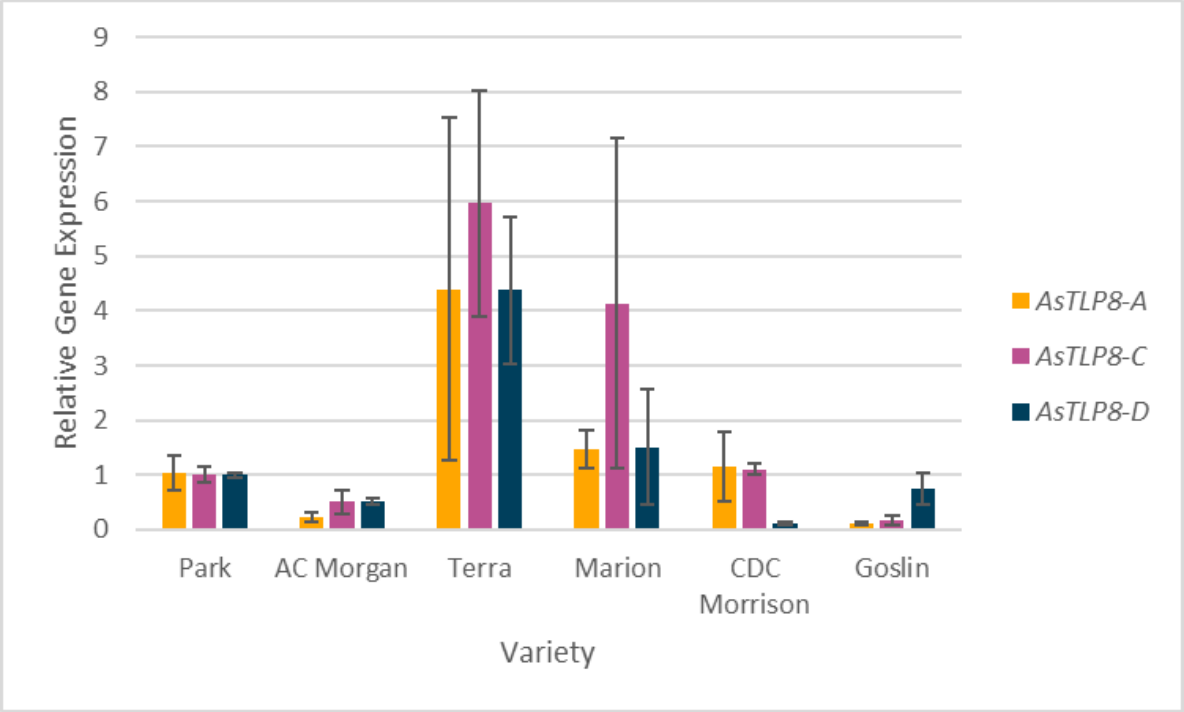

Figure 3. 4: Transcript abundance of *AsTLP8* homoeologs in the mature seed of different varieties. The relative gene expression was measured in the mature seed of each variety through qRT-PCR. The variety park was used as the control for relative gene expression. Error bars were calculated by taking the relative expression's standard deviation of biological and technical replicates. None of the relative gene expressions were significantly different based on the Tukey test with a $p < 0.05$ (Keselman and Rogan 1977).

3.4.4 Designing CRISPR/Cas9 gene-editing constructs

In order to further evidence the role of *TLP8* in the beta-glucan content of oat, CRISPR/Cas9 gene-editing constructs were made. Gene-editing constructs were designed to target the *TLP8* homoeolog of each subgenome. Three guide RNA were designed for each homoeolog. When designing the guide RNA, the position within the gene, the predicted on-target efficiency (Doench et al. 2014), and potential off-targets (Hsu et al. 2013) were considered. For each subgenome, two guide RNA were designed upstream of the sugar-binding motif (position 250bp) and one

downstream of this motif. So, in the occurrence of a deletion, the sugar-binding motif would be removed from the sequence altogether. After position, gRNAs were chosen based on having both high activity and specificity score (Table 3.4). The specificity score of most gRNA was low (<80%) because the OT3098 genome was used as a database and considered the targeted gene itself as an off target. In other words, when designing a gRNA to target the *AsTLP8-A* sequence in variety Park, the program considered the *AsTLP8-A* sequence in OT3098 as an off-target. In each case, the potential off-targets were analyzed to have an off-target score of less than 15% (Hsu et al. 2013).

Table 3. 4: Single-guide RNA designed for gene-editing *AsTLP8* homoeologs

gRNA	*Direction*	*PAM Sequence*	*Target Sequence*	*Doench (2014) Activity Score*	*Specificity (%)*	*Score*	*Cut position (bp)*
AsTLP8-A Guide 1	Forward	TGG	GCAACAGTGGAAGGTCGAGG	0.497	56.4		173
AsTLP8-A Guide 2	Reverse	TGG	CTTGTTGGTGACGGTGAACG	0.623	57.51		80
AsTLP8-A Guide 3	Reverse	TGG	TGAAGTCCTGGCCTTCGTAC	0.361	62.18		338
AsTLP8-C Guide 1	Forward	CGG	CGTGCCCATGAACTTCCTGC	0.709	55		404
AsTLP8-C Guide 2	Forward	CGG	TGGAACATCAACGTGCCGGC	0.752	73.29		180
AsTLP8-C Guide 3	Reverse	CGG	AGCTTCCTGCCCCCGCCGAC	0.376	78.18		130
AsTLP8-D Guide 1	Forward	CGG	TGGAACATCAACGTGCCTGC	0.602	70.12		180
AsTLP8-D Guide 2	Reverse	GGG	GTTGAGCCCGAACTCGGCCA	0.866	68.5		317
AsTLP8-D Guide 3	Forward	CGG	GTGCCTGCCGGCACGACGGG	0.35	71.81		192

The designed sgRNA were inserted into shuttle vectors and then into the destination vector through Golden Gate Cloning. Each construct contains three gRNA targeting the same subgenome (Figure 3.5). The insertion of the intended sequence was checked through digestion (Figure 3.6) and further confirmed through sanger sequencing.

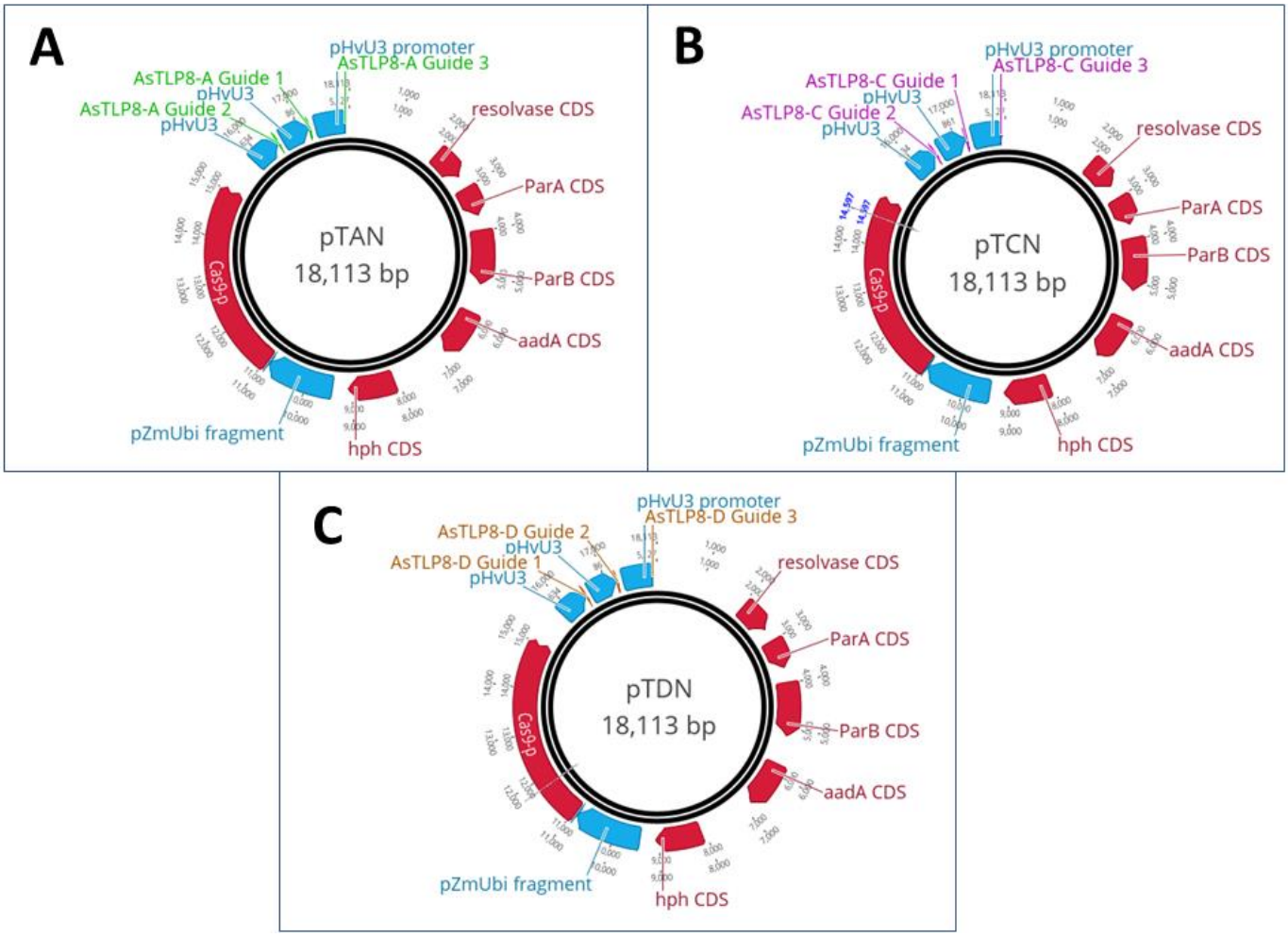

Figure 3. 5: Gene-editing constructs targeting each *AsTLP8* homoeolog. Each construct shares a backbone sharing various features. Rep origin demonstrates the replication origin (PVS1) of the destination vector backbone. ParA CDS and ParB CDS denote the coding sequences of the partitioning proteins ParA and ParB, respectively. The aadA CDS is the coding sequence of streptomycin adenyltransferase, which confers streptomycin resistance. The *hph* CDS produces hygromycin phosphotransferase and provides Hygromycin resistance. pZmUbifragment denotes the *Zea mays* ubiquitin promoter. *Cas9-p* encodes for *Streptococcus pyogenes* Cas9 protein. (**A**) Construct targeting *AsTLP8* in the A subgenome. The designed gRNA are placed in an order (5' → 3') of *AsTLP8-A* Guide 2, *AsTLP8-A* Guide 1, and *AsTLP8-A* Guide 3 (Table SG). Each gRNA is under the control of the *Hordeum vulgare* U3 promoter (Kumar et al. 2018). (**B**) Construct targeting *AsTLP8* in the C subgenome. The designed gRNA are placed in an order (5' → 3') of *AsTLP8-C* Guide 2, *AsTLP8-C* Guide 1, and *AsTLP8-C* Guide 3 (Table SG). Each gRNA is under the control of the *Hordeum vulgare* U3 promoter (Kumar et al. 2018). (**C**) Construct targeting *AsTLP8* in the D subgenome. The designed gRNA are placed in an order (5' → 3') of *AsTLP8-D* Guide 1, *AsTLP8-D* Guide 2, and *AsTLP8-D* Guide 3 (Table SG). Each gRNA is under the control of the *Hordeum vulgare* U3 promoter (Kumar et al. 2018).

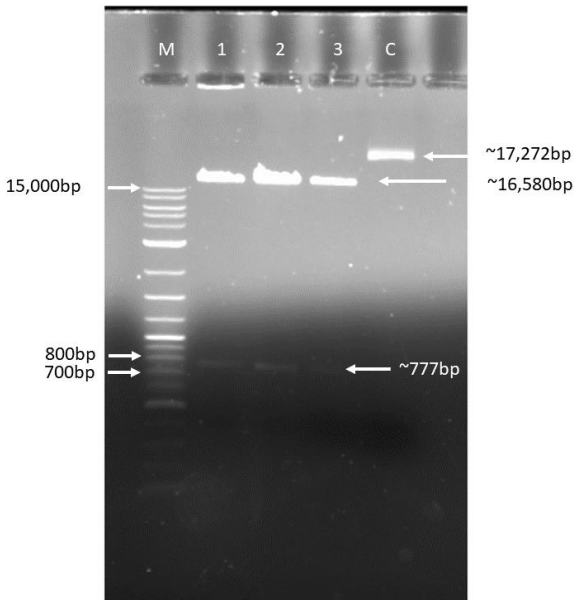

Figure 3. 6: Digestion of *AsTLP8* targeting CRISPR/Cas9 constructs with SacI. Lanes 1, 2, and 3 contain the constructs targeting the A-, C-, and D-genome, respectively. The C lane contains the destination vector without the insertion of gRNAs and *HvU3* promoters. The M lane contains a 1kb+ ladder (NEB). The insertions have three SacI cut sites leading to three segments. The first segment is present in lanes 1-3 at a size of 16,580bp. The two other segments are identical in size (777bp) and are also visible in lanes 1-3. The destination plasmid contains no cut sites and appears as one band in lane C (17,272bp).

3.4.5 Transformation of oats using the *AsTLP8* gene-editing constructs

The three gene-editing constructs were introduced into the common oat (v. Park) via microprojectile bombardment. Considering the presence of Hygromycin phosphotransferase in each construct, Hygromycin was used to select for calli carrying the foreign DNA. A total of 210, 210, and 280 calli were bombarded for the *AsTLP8-A*, *AsTLP8-C*, and *AsTPL8-D* targeting constructs, respectively. The A-genome targeting plasmid (pTAN) demonstrated the highest plantlet regeneration frequency at 87.5% of the calli that survived Hygromycin selection. Meanwhile, the D- and C-genome targeting plasmids correspondingly demonstrated a 65% and 66% plantlet regeneration frequency. Regenerated plantlets were then PCR tested for transformation using gRNA within their respective constructs (Table 3.2).

Table 3. 5: Regeneration frequency of gene-editing constructs.

Construct	Plates Bombarded	Calli pieces	Selection Medium	Calli Passed Selection	Plantlets Regenerated	Regeneration Frequency (%)
pTAN	6	210	Hygromycin	48	42	87.5
pTCN	6	210	Hygromycin	40	26	65
pTDN	8	280	Hygromycin	53	35	66

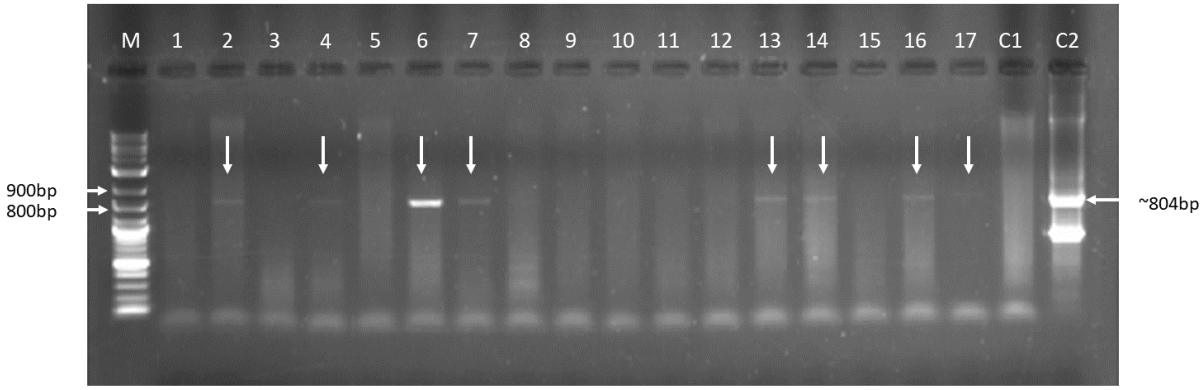

Figure 3. 7: PCR-based analysis of putative pTAN transformed plants. Samples were PCR amplified using the primers ASG1O1 and ASG3O2 (Table P). The M Lane contains a 1kb+ ladder (NEB). Lanes 1-17 denote genomic DNA of plantlets that survived Hygromycin selection and bombardment using the pTAN construct. Lane C1 contains the genomic DNA of the wild-type Park as a negative control, and C2 contains the pTAN construct as a positive control. Samples were run on a 0.8% agarose gel. Lanes 2, 4, 6, 7, 13, 14, 16, 17, and C2 contain a band approximately the size of the expected 804bp.

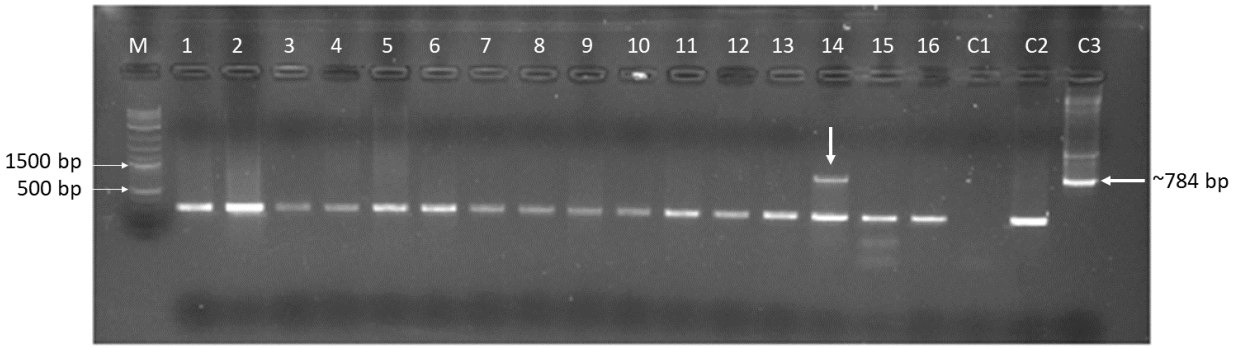

Figure 3. 8: PCR-based analysis of putative pTCN transformed plants. Samples were PCR amplified using the primers CSG2O1 and CSG1O2 (Table P). The M lane contains a 1kb+ ladder (NEB). Lanes 1-17 denote genomic DNA of plantlets that survived Hygromycin selection and bombardment using the pTCN construct. Lane C2 contains the genomic DNA of the wild-type Park, and C1 contains water as negative controls. The C3 lane contains the pTCN plasmid as a positive control Samples were run on a 0.8% agarose gel. Lanes 14 and C3 contain a band approximately the size of the expected 784 bp.

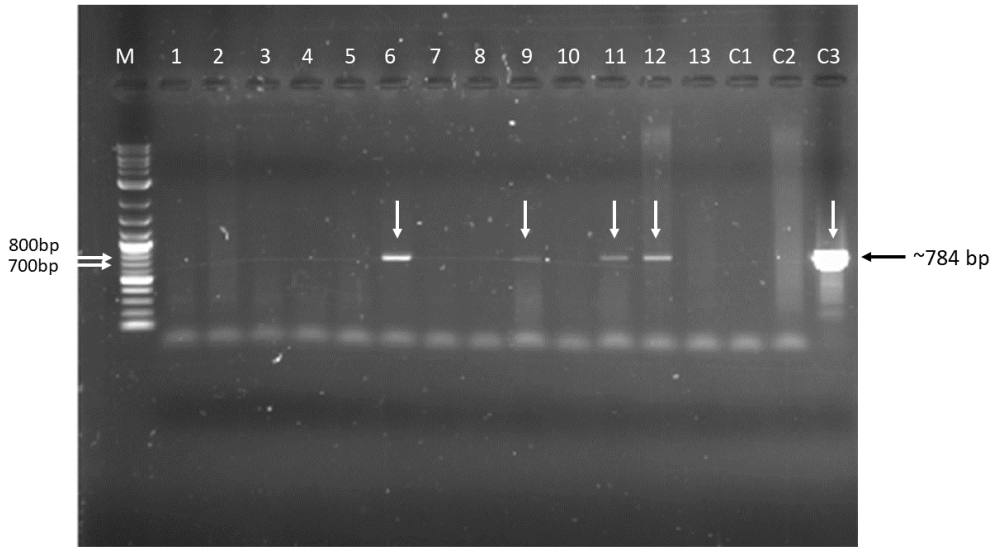

Figure 3. 9: PCR-based analysis of putative pTDN transformed plants. Samples were PCR amplified using the primers DSG1O1 and DSG2O2 (Table P). The M lane contains a 1kb+ ladder (NEB). Lanes 1-13 denote genomic DNA of plantlets that survived Hygromycin selection after bombardment using the pTDN construct. Lane C2 contains the genomic DNA of the wild-type Park, and C1 contains water as negative controls. The C3 lane contains the pTDN plasmid as a positive control. Samples were run on a 0.8% agarose gel. Lanes 6, 9, 11, 12 and C3 contain a band approximately the size of the expected 784 bp.

The PCR-based analysis confirmed transformants in all three constructs in the T0 generation (Figures 3.7-3.9). The pTAN construct also boasted the highest transformation frequency at 5.23% (Table 3.6). The *AsTLP8-D* (pTDN) targeting construct had a transformation frequency of 2.86, while the *AsTLP8-C* (pTCN) targeting construct had a 0.47% frequency.

Table 3. 6: Transformation frequency of gene-editing constructs

Construct	Calli pieces bombarded	Transformants (PCR +)	Transformation Frequency (%)
pTAN	210	11	5.23
pTCN	210	1	0.47
pTDN	280	8	2.86

3.4.6 Analyzing the CRISPR/Cas9 efficiency in transgenic lines

Plants confirmed to be transgenic were continued into the next generation (T1). The T1 generation was then screened for deletions caused by the gRNA and Cas9 targeting *AsTLP8* homoeologs. Those transformed with the pTAN construct demonstrated no visible shift in band size (Figure 3.10). The pTCN transformed T1 generation had a notable size shift in one sample, which potentially indicates a deletion within the C-genome *AsTLP8*. However, this sample contained two bands, suggesting that this suspected mutation is in the heterozygous state (Figure 3.11). Lastly, small size shifts were observed in the T1 generation of confirmed pTAN transformed T0 lines (Figure 3.12)

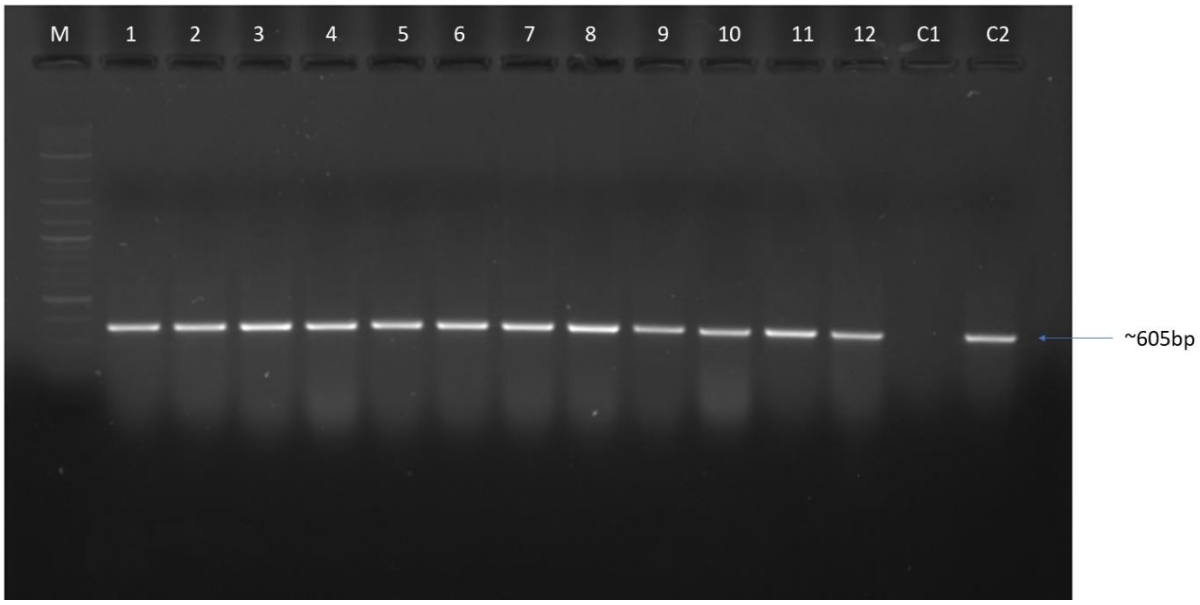

Figure 3. 10: Screening for CRISPR/Cas9 induced deletion within the *AsTLP8-A* gene of T1 transgenic lines. Samples were PCR amplified using the A-genome specific AsTLP8A-In2F and AsTLP8A-In3R primers (Table 3.1). Samples 1-12 indicate genomic DNA of the T1 generation of confirmed T0 transgenic lines. The C1 lane contains a negative water control, and the C2 lane contains the negative wild-type Park control. The M lane contains a 1kb+ marker. Samples were run on a 2% agarose gel. Samples 1-12 and C2 had a band of approximately 605bp with no noticeable shift in size. The water control contained no band.

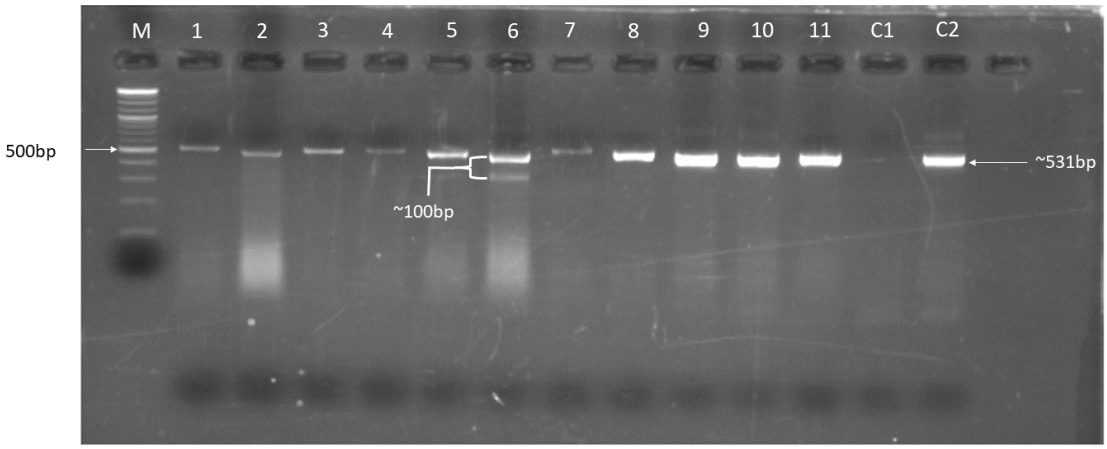

Figure 3. 11: Screening for CRISPR/Cas9 induced deletion within the *AsTLP8-C* gene of T1 transgenic lines. Samples were PCR amplified using the C-genome specific AsTLP8C-In2F and AsTLP8C-In2R primers (Table 3.1). Samples 1-16 indicate the genomic DNA of T1 generation of confirmed T0 transgenic lines. The C1 lane contains a negative water control, and the C2 lane contains the negative wild-type Park control. The M lane contains a 1kb plus (NEB) marker. Samples were run on a 2% agarose gel. Samples 1-12 and C had a band of approximately 531bp.

The water control contained no band. Potential shifts in size can be seen in lanes 2, 5, 9, and 10. A clear shift can be seen in lane 6.

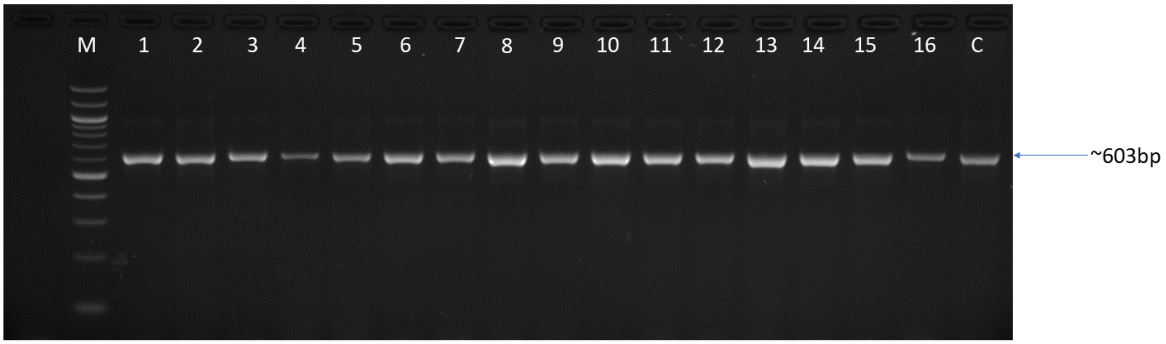

Figure 3. 12: Screening for CRISPR/Cas9 induced deletion within the *AsTLP8-D* gene of T1 transgenic lines. Samples were PCR amplified using the D-genome specific AsTLP8D-In2F and AsTLP8D-In1R primers (Table 3.1). Lanes 1-16 indicate the genomic DNA of the T1 generation of confirmed T0 transgenic lines. The C lane contains the negative wild-type Park control. The M lane contains a 100bp marker (NEB). Samples were run on a 2% agarose gel. Samples 1-12 and C had a band of approximately 603bp. The water control contained no band. Potential variations in size can be seen in lanes 1, 2, 6, 7, 13, and 14.

The T1 plants of the pTDN lines that demonstrated shifts were sent for Sanger sequencing. There were no changes at the site of the second gRNA within any of the sequences (Figure 3.13). At the site of the first gRNA, there were discrepancies between the expected sequence and the sequencing results. Specifically, five of the six shown mutants demonstrated deletions or base pair changes bases three nucleotides upstream from the PAM sequence (CGG) (Figure 3.13). Evidence of gene editing was also visible within the site of the third gRNA. In four of the lines, a four-base deletion is visible three nucleotides upstream of the PAM sequence (CGG). In the same position, the line TD-1C-3 (Figure 3.13) demonstrated a 3-nucleotide deletion. Overall, the *AsTLP8-D* targeting guide 1, 2, and 3 demonstrated a mutation frequency of 70, 0, and 80%, respectively (Table 3.7). These gene-edited lines are being pursued further to develop homozygous lines for downstream analysis for homoeologous specific *TLP8* expression (standardized in section 3.2.3) and beta-glucan content in mature and imbibed seeds.

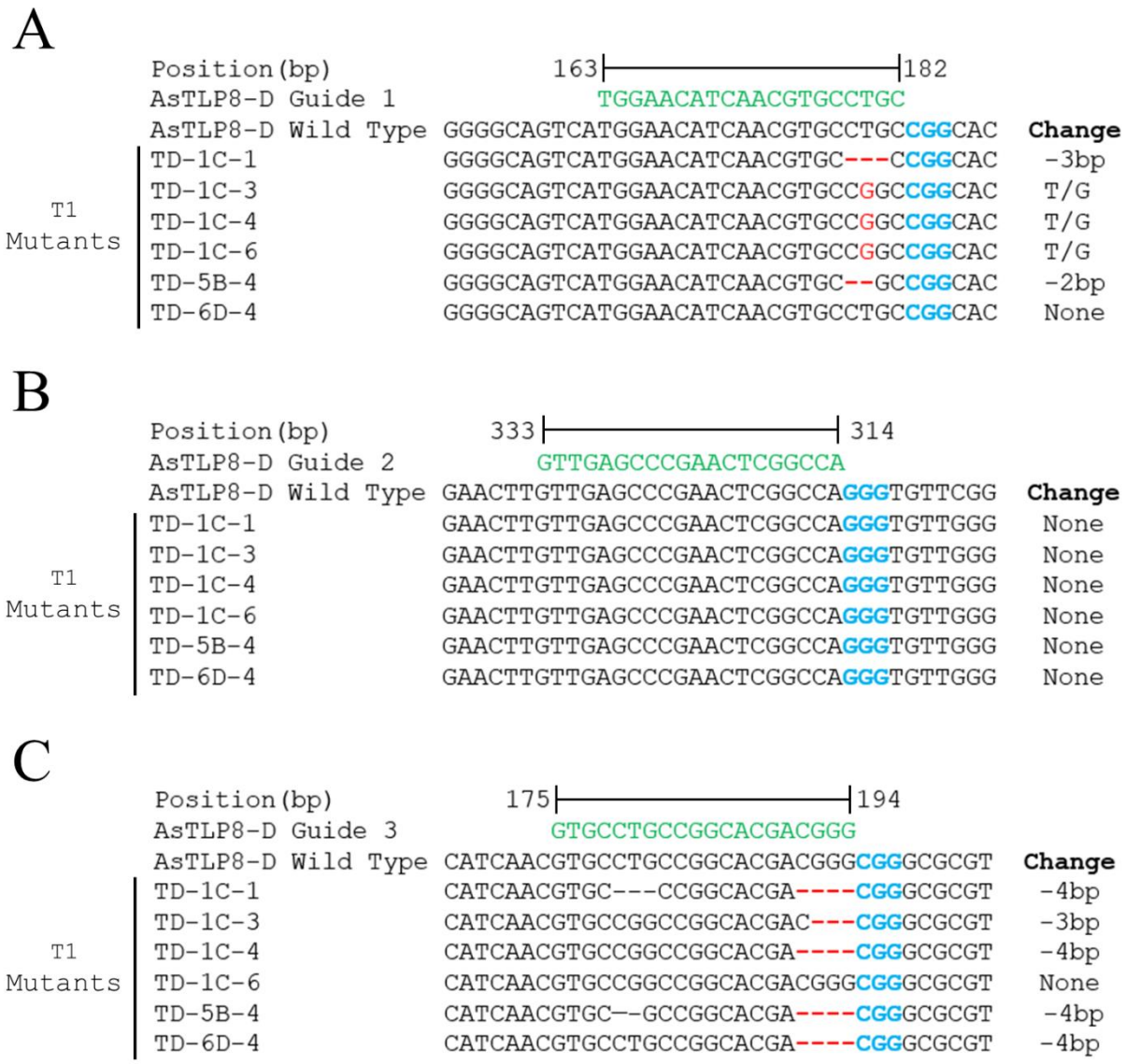

Figure 3. 13: Mutations detected through sanger sequencing of gene-edited T1 plants. Sequences were aligned using the Geneious alignment tool. The position row denotes the position of the respective guide RNA within the *AsTLP8-D* gene. The PAM sequence of each gRNA is denoted in blue type. The gRNA is denoted in green type. **(A)** The site of gRNA 1 within the *AsTLP8-D* sequence (Table 3.4). The D1 and expected have the same sequence based on the Sanger sequencing results. Two mutants demonstrate a deletion ranging from 2bp to 3bp three positions upstream of the PAM sequence (CGG). Likewise, three mutants have a one nucleotide change (T →G). **(B)** The site of gRNA 2 within the *AsTLP8-D* sequence (Table 3.4). All the gene-edited lines have no changes from the wild-type sequence based on the Sanger sequencing results. **(C)** The site of gRNA 3 within the *AsTLP8-D* sequence (Table 3.4). Five of the six gene-edited mutants demonstrated a 3bp to 4bp deletion next to the PAM sequence.

Table 3. 7: Mutation frequency in *AsTLP8-D* of CRISPR/Cas9 by guide RNA.

Guide RNA	Transgenic T1 plants tested	Transgenic T1 plants with CRISPR/Cas9 induced mutation	Mutation frequency	Predicted Activity Score (Doench 2014)
AsTLP8-D Guide 1	10	7	70%	0.62
AsTLP8-D Guide 2	10	0	0%	0.866
AsTLP8-D Guide 3	10	8	80%	0.35

3.5 Discussion

Beta-glucan comes in a plethora of forms across a vast range of species. This polysaccharide plays an essential role in prokaryotes, algae, fungi, and within cereal grains (Zeković et al. 2005). Within cereals, the unique beta-(1,3;1,4)-glucan exists. This soluble fibre plays a crucial role in glucose storage for the plant (Roulin et al. 2002). In terms of human nutrition, beta-(1,3;1,4)-glucan is important in reducing the incidence of cardiovascular heart disease (Cicero et al. 2020), reducing daily consumption (Lumaga et al. 2012), and lowering the rate of bacterial and viral infection (Daou and Zhang 2012). Despite the growing interest in oat consumption due to these health benefits, the body of knowledge surrounding the mechanism of beta-glucan production is deficient. So, the correlation between *HvTLP8* expression and beta-glucan content spikes interest. In this study, we first described the sequences of *AsTLP8* in oat variety Park through PCR-amplifying and sequencing each homoeologue. The sequences of the variety OT3098 were also described, derived from the released OT3098 genome v1. Through comparing these sequences to the barley *TLP8*, significant differences were observed. The A-genome amino acid sequences in Park and OT3098 have a mutation within the second residue of the previously described sugar-binding motif (CQTGDCC) (Singh et al. 2017). This change is significant because Glutamine (Q) is a non-charged amino acid, while the A-genome's glutamic acid (E) is positively charged. Considering the A-genome diploid species of oat have been associated with higher beta-glucan content (Welch

et al. 2000), this change could suggest that this mutation contributes to a reduced sugar-binding interaction.

Interestingly, this same residue was mutated in the C-genome of the Park variety. The second amino acid was changed from the neutral Glutamine (Q) to a positively charged Arginine (R). This result came as a surprise, as the C-genome diploid species are not known to have substantial beta-glucan content. However, there is evidence that certain QTLs for beta-glucan content are not present within the C-genome. Specifically, the *Cellulose synthase-like F6* (*CslF6*) of OT3098's C genome was, unlike the A- and D-genome, considered to have a neutral or negative contribution to the beta-glucan content in a genome-wide association study (GWAS) (Fogarty et al. 2020). In other words, the *AsCslF6-C* was not found within a beta-glucan controlling QTLs, suggesting that this homoeolog of the gene did not contribute to overall beta-glucan content. Another vital aspect to consider is that Glutamine and Arginine are considered flexible side-chains during ligand binding (Najmanovich et al. 2000). In other words, both have a high chance to undergo a conformational change during the binding of a ligand. As a sugar-binding domain, having similar flexibility would minimize the potential for functional changes. Further evidencing the potentially reduced binding of the A-genome homoeologue of *AsTLP8,* glutamic acid has a lower ligand flexibility score than Glutamine. Beyond the ligand flexibility scale, the change in charges cannot be discounted. Beta-glucan is a zwitterionic polysaccharide, meaning it carries both positive and negative charges (Chan et al. 2009). So, depending on the adherence site of the sugar-binding motif, a change in the charge could disrupt the binding of this motif with beta-glucan. Further studies are required to determine the effect of these charge-changing mutations on the beta-glucan binding described by Singh et al. (2017).

The amino acid sequence of all *AsTLP8* homoeologs in both varieties Park and OT3098 contain conserved residues in fungal and TLP beta-1,3-glucanases (Grenier et al. 2000). Many Thaumatin-Like Proteins have been described to be involved in host defence against fungal infection. In spruce trees, certain TLPs were shown to inhibit the mycelial growth of pathogenic fungi through the degradation of beta-1,3-glucan in the cell wall (Liu et al. 2021). These conserved residues allude to the putative role of *AsTLP8* in host defence. Still, the question remains: Could *AsTLP8* also be involved in regulating beta-glucan content within oats itself? To answer this, it is essential to look at where TLPs are expressed and where beta-glucan is produced. In the case of both barley and oat, beta-glucan is found within the aleurone of the endosperm-coating bran (Butardo and Sreenivasulu 2016; Miller and Fulcher 2011). Similarly, during oat and barley seeds development, TLP expression has been shown to switch to the aleurone layer (Skadsen et al. 2000). It is not out of the realm of possibility that the expression of *HvTLP8* began as a host defence mechanism but now has the side effect of lowering beta-glucan content. To further explore this potential relationship, we sought to definitively correlate beta-glucan content to *AsTLP8* homoeologs through CRISPR/Cas9 induced knockout.

The *TLP8* gene in *Hordeum vulgare* was demonstrated to have an inverse correlation with the beta-glucan content. So, this relationship was explored in the common oat. The expression of *AsTLP8* between varieties with varying beta-glucan content was measured using quantitative RT-PCR primers designed to target each homoeolog specifically. Relative gene expression between each variety demonstrated some variance in means (Figure 3.4). Nevertheless, in every homoeolog, the differences were not statistically significant based on the Tukey test (Keselman and Rogan 1977). However, comparing certain groups using an unpaired T-test did demonstrate significance. For example, the difference within the relative expression of *AsTLP8-D* in varieties

Terra and Goslin were determined to be statistically significant using the T-test ($p<0.05$). This result is intriguing, considering there are differences between the beta-glucan content of these two varieties in previous field trials (Appendix A8). Unfortunately, the beta-glucan content of oats is heavily influenced by their environment, and no definitive relationship can be extrapolated with these results. Future studies would benefit from comparing the same plant's beta-glucan content and relative gene expression. The relative expression was also measured in the mature seed. However, the relationship between *HvTLP8* and beta-glucan was determined within the germinating seeds of barley (Singh et al. 2017). This study has standardized the measurement of relative gene expression in all three homoeologs of *AsTLP8*. In further studies, this process can be used to compare the beta-glucan content and gene expression of germinating seeds. In doing so, the relationship described by Singh et al. (2017) can be investigated in the common oat.

The CRISPR/Cas9 system opens the door for precise gene-editing experiments. This system has been used successfully in various plant species for improving biotic stress resistance (Ji et al. 2015; Wang et al. 2014c; Zhou et al. 2015), abiotic stress resistance (Shan et al. 2014; Shi et al. 2017; Wang et al. 2017b), and nutritional traits (Du et al. 2016; Ito et al. 2015). Despite the growing use of precise gene-editing tools, the CRISPR/Cas9 system has yet to be implemented in *Avena sativa*. Therefore, this study aimed to use this technique in oats for the first time. A total of three constructs (Figure 3.5), each targeting a different *AsTLP8* homoeolog, were designed and transformed through microprojectile bombardment. The construct targeting *AsTLP8-A*, *AsTLP8-C*, and *AsTLP8-D* demonstrated a transformation frequency of 5.23, 0.47, and 2.86%, respectively. These transformation frequencies were much lower than previously reported studies of oat, which ranged from 26-35% (Cho et al. 1999; Somers et al. 1992). However, the transformed constructs in these studies (<6kb) were relatively small compared to those used in our study (18.1kb). It has been well

documented that a larger plasmid leads to a lower transformation frequency (Li et al. 2017; Parveez and Majid 2008). Another potential explanation for a low transformation frequency could be the use of the Cauliflower mosaic virus 35S promoter (CaMV35S). Similar studies using this sequence as a promoter for Hygromycin resistance demonstrated a similar transformation frequency (Liang et al. 2021), suggesting that transgenic plants may have been eliminated during selection due to the low expression of *Hygromycin phosphotransferase*. In addition, a recent study from our lab also indicates a much lower transformation (1.9%) frequency when hygromycin was used in selection (Mahmoud et al. 2021). Nonetheless, PCR-confirmed transgenic lines were brought to the T1 generation and further analyzed.

Every T1 plant was analyzed for an approximately 100bp deletion in their respective targeted homoeolog. In all but one plant, no apparent deletion is visible (Figure 3.10-3.12). It is essential to consider that the designed 100bp deletion is only one of the possible outcomes. For a deletion to occur, both ends of the desired deletion must have a double-stranded break (DSB) at the same moment. In this case, the NHEJ repair mechanism will ligate the two blunt ends, thereby removing the desired sequence. However, in the absence of the second DSB, the NHEJ repair mechanism repairs the strand, leading to an indel. To add, even in the case of simultaneous DSBs, inversion and reinsertion are possibilities (Canver et al. 2014). In other words, even when the desired sequence has been excised with CRISPR/Cas9, the NHEJ mechanism may repair the sequence back into its original position (reinsertion) or flip it (inversion). Still, reports have shown that deletions of up to 431bp have demonstrated deletion frequencies of 21% in rice (Wang et al. 2017b). The low deletion frequency may also be explained by the promoter used for each sgRNA. Within the constructs, the inserted sgRNA were under the control of the *Hordeum vulgare U3* promoter (*HvU3*). The study from which the *HvU3* promoter was derived developed this promoter

in response to a similar concern that we faced in our results (Kumar et al. 2018). When using promoters of other cereal species to drive sgRNA expression, such as the *Oryza sativa* U6 (OsU6) promoter and *Triticum aestivum* U6 (TaU6) promoter in CRISPR/Cas9 gene editing, low mutation rates were observed in barley (Gasparis et al. 2018; Kapusi et al. 2017; Lawrenson et al. 2015). Future CRISPR/Cas9 gene-editing experiments in oat would benefit from establishing an efficient endogenous *U3/U6* promoter. The activity score of the sgRNA may have also contributed to the low deletion efficiency of our gene editing constructs. Considering the strong similarities between the three *AsTLP8* homoeologs, the specificity score was prioritized over the activity score (Figure SG). In some cases, the Doench et al. (2016) activity score is below 0.5. In these cases, the mutation frequency is predicted to be low.

The pTDN T1 lines demonstrating a potential shift (Figure 3.12) were sent for further Sanger sequencing analysis. Within the ten sequences sent for analysis, the *AsTLP8-D* targeting guide RNA 1, 2, and 3 had CRISPR/Cas9-induced mutations frequencies of 70%, 0% and 80%, respectively. The mutation frequencies of gRNAs 1 and 3 are higher than previously reported values of 7-48% in maize and wheat (Char et al. 2017; Tang et al. 2021). Interestingly, these frequencies are similar to those of the study by Kumar et al. (2018) in barley (77%), from which the gene-editing constructs were received. As previously mentioned, the gRNA mutation frequency is highly variable and depends on the gRNA sequence, position on the genomic DNA sequence, and promoter used (Doench et al. 2016; Kumar et al. 2018). The Doench (2014) activity score did not reliably predict the mutation frequency of each gRNA (Table 3.7). This prediction model is based on the activity of gRNA within animal cells, which may explain the discrepancy between the predicted and actual mutation frequency. To further evidence this, Naim et al. (2020) compared various gRNA optimizing tools against *In vivo* effectiveness in *Nicotiana benthamiana*.

This study found no statistically significant correlation between predicted and *in vivo* efficiency. So, most gRNA optimizing tools are not a good indicator of *in vivo* gene-editing activity.

Ten lines were screened for CRISPR/Cas9-induced mutations. The detected mutations included deletions and nucleotide substitutions. However, no insertions were demonstrated. Although the NHEJ repair mechanism typically causes both, a study by Song et al. (2021) showed that the gRNA can skew towards a preferred mutation in some cases. This study demonstrated that some targets demonstrated a deletion mutation rate of more than 80%. Considering the number of mutants detected and the tendency of some guide RNA target sites to cause deletions, it is understandable that no insertions were detected. Overall, this is the first instance of successful CRISPR/Cas9-induced gene-editing within the common oat.

3.6 Future studies

The presented study is the foundation for future works in divulging the relationship between *TLP8* and beta-glucan in oat. There are many avenues to explore to truly characterize the role of *AsTLP8* homoeologs in the common oat. Our results demonstrate that certain homoeologs have mutations within the previously described sugar-binding motif (Singh et al. 2017). As discussed, these mutations lead to residue changes that could have significant impacts on the physiochemistry of *TLP8* binding with beta-glucan. Subsequent studies demonstrating both the binding of *AsTLP8* homoeologs with beta-glucan, and the effect of mutations on these putative bindings would be crucial to confirm any potential interaction between the two parties. Preliminary results demonstrate that there was no statistically significant difference between the varieties differing in beta-glucan content and the gene expression of the *AsTLP8* homoeologs (Figure 3.12). However, the expression of these homoeologs was measured within the mature seeds of each variety. On the other hand, the relationship between the beta-(1,3;1,4)-glucan content and *HvTLP8* expression in

barley was determined within germinating seeds (Singh et al. 2017). Future work would benefit from comparing the beta-glucan content of each oat variety with the *AsTLP8* homoeologs in imbibed seeds.

The homoeologs of *AsTLP8* in oat contained conserved residues in *TLPs* demonstrating beta-glucanase activity (Grenier et al. 2000). However, these residues do not prove that *AsTLP8s* contain beta-glucanase activity. Measuring the hydrolyzing capabilities of these proteins would provide further clues to the role of *AsTLP8* homoeologs in *Avena sativa*.

This study demonstrates the first case of CRISPR/Cas9-induced gene editing in the common oat. Although the process yielded success, improvements can be made within the process. Namely, the *HvU3* promoter is used to drive the gRNA. In the study by Kumar et al. (2018), the *HvU3* promoter was characterized and optimized because the *U3* promoter from wheat and rice demonstrated relatively weaker efficiency in barley. Using similar methods, the *U3* promoter within *Avena sativa* should be identified and optimized to improve efficiency in further CRISPR/Cas9 experiments in oat.

The confirmed CRISPR/Cas9 mutated lines will be analyzed further. Primarily, the influence of *AsTLP8-A, -C,* and *-D* knockouts on the beta-glucan content will be measured. Thaumatin-like proteins are involved in host defence, abiotic stress resistance, and cell signalling (Liu et al. 2010; Liu et al. 2021). Specifically, in the naked oat (*Avena nuda*), TLPs have been shown to play a crucial role in resisting fungal pathogens (Liu et al. 2019). Although the primary purpose of this study was to explore the relationship between *AsTLP8* homoeologs and the beta-glucan content, these proteins may also play some role in host defence. Therefore, quantifying any change in the pathogen resistance in *AsTLP8-A, -C* and *-D* knock-out mutants is an essential future perspective to consider.

Chapter IV General Conclusion

The common oat (*Avena sativa*) is a valuable crop in Canada. The importance of oats in Canada is compounded by the growing interest in its health benefits. This cereal contains its own class of strong antioxidants, a high protein content, and soluble dietary fibre (Andersson and Börjesdotter 2011; Hastings and Kenealey 2017; Mäkinen et al. 2017). These soluble fibres, beta-(1,3;1,4)-glucan, are of economic importance because of their various applications, including skin health (Du et al. 2014), antitumour activity (Choromanska et al. 2018), and cholesterol-lowering capabilities (Theuwissen and Mensink 2008; Whitehead et al. 2014). Therefore, one can understand the importance of understanding the synthesis mechanism of these valuable components of cereal grains. Singh et al. (2017) demonstrated an inverse relationship between the beta-glucan content in barley and the expression of *Thaumatin-like protein 8* (*TLP8)*. This study sought to investigate this relationship within the common oat.

Our first objective was to determine whether *TLP8* orthologs were present in oats and whether the same relationship with beta-glucan was observed. First, the sequences of each *TLP8* homoeolog within *Avena sativa* were determined. When compared to the sequence in barley, exciting changes were observed. Within the previously described sugar-binding motif (Singh et al. 2017), the A- and C-genome *AsTLP8* homoeologs of the variety Park demonstrated a mutation in the second residue. Furthermore, residues described as being conserved in TLPs boasting beta-glucanase activity were also present in every *AsTLP8* homoeolog. To further explore the relationship between beta-glucan and the *AsTLP8* genes, the relative gene expression in the mature seed of 6 varieties was measured through qRT-PCR using homoeolog-specific primers. No statistically significant difference was observed within the varieties in any of the *AsTLP8* homoeologs. However, the relationship between *HvTLP8* and dietary fibre was within germinating seeds (Singh et al. 2017).

Therefore, the measurement of *AsTLP8-A*, *-C*, and *-D* gene expression has been standardized to analyze further this relationship within germinating oat seeds.

The second objective was to knockout *AsTLP8* homoeologs in the variety Park using the CRISPR/Cas9 system. Three constructs, each containing three guide RNA, were designed to separately target the different *AsTLP8* sequences. The guide RNAs were designed to create a 100bp deletion detectable through PCR-based analysis. Through microprojectile bombardment, the constructs pTAN, pTCN, and pTDN demonstrated transformation frequencies of 5.23, 0.47, and 2.86%, respectively. The T1 generation of the PCR-confirmed pTDN transformants was sent for Sanger sequencing. The majority of the transformants sequenced demonstrate CRISPR/Cas9-induced mutations at one of the predicted sites. These results show the first-ever successful gene-editing of *Avena sativa* using the CRISPR/Cas9 system. Future research should first and foremost include an analysis of the *AsTLP8* mutations on the overall beta-glucan content.

Appendices

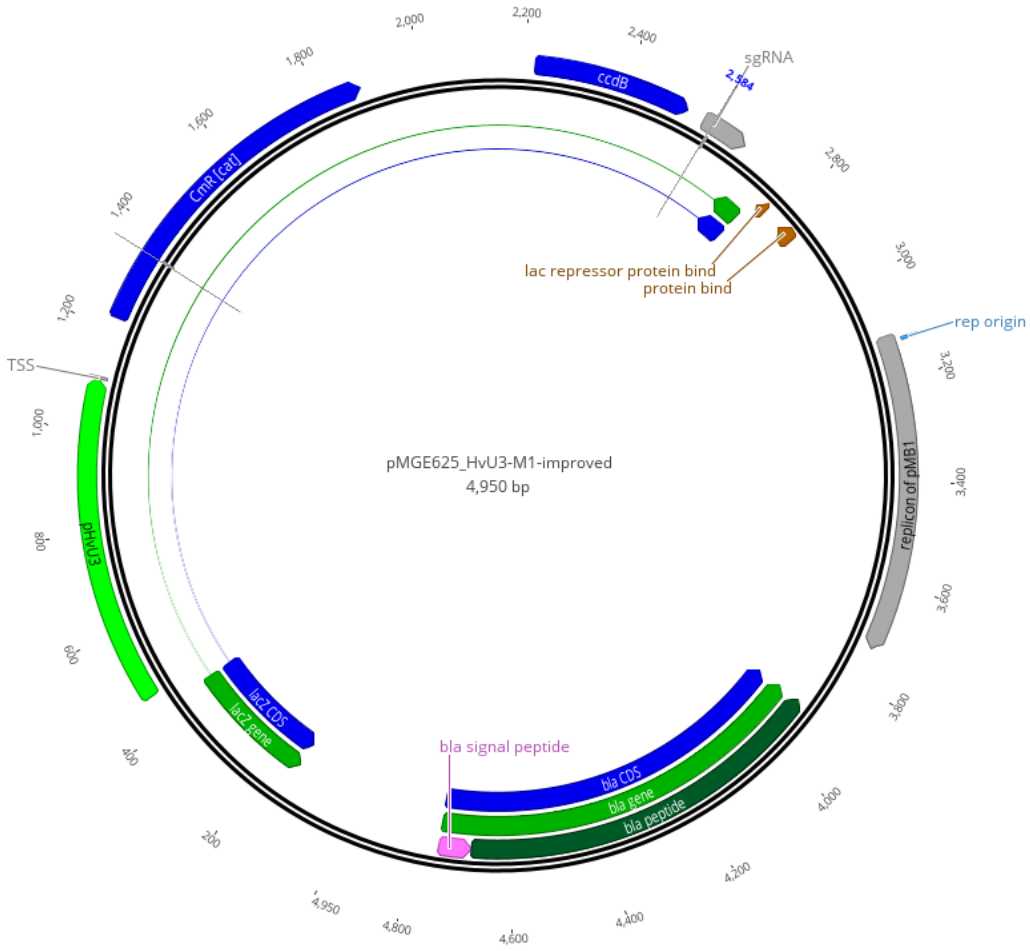

Appendix A 1: Shuttle vector carrying the first sgRNA. Replicon of pMB1 demonstrates the replication origin of the shuttle vector backbone. The *bla* CDS is the coding sequence of beta-lactamase, which confers ampicillin resistance. The lacZ CDS is the coding sequence for beta-galactosidase, which cleaves X-gal to act as a marker for successful plasmid transformation. pHvU3 is the U3 promoter optimized for *Hordeum vulgare* (barley) (Kumar et al. 2018). The CmR sequence gives chloramphenicol resistance. The ccdB sequence produces a post-segregational killing (PSK) toxin. The shuttle vector contains a BpiI (BbsI) cut site before the CmR and after the ccdB CDS. The shuttle vector also contains a BsaI cut site that leads to overhands of ACTA and CGGT.

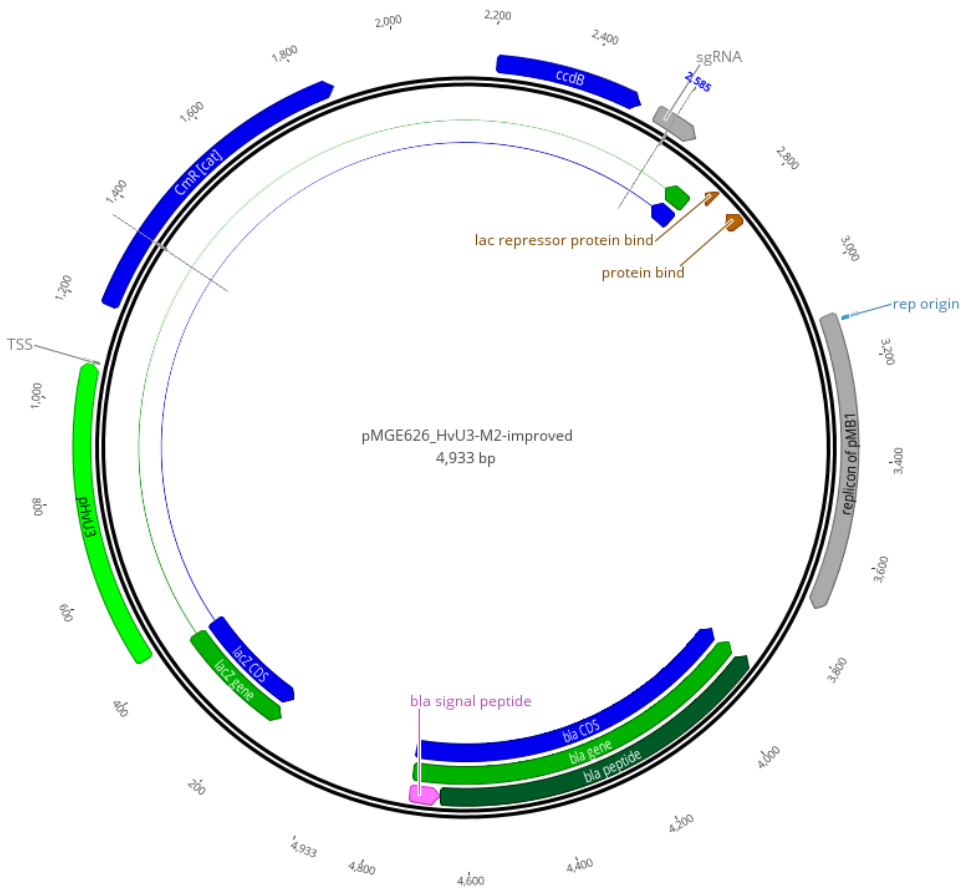

Appendix A 2: Shuttle vector carrying the second sgRNA. Replicon of pMB1 demonstrates the replication origin of the shuttle vector backbone. The bla CDS is the coding sequence of beta-lactamase, which confers ampicillin resistance. The lacZ CDS is the coding sequence for beta-galactosidase, which cleaves X-gal to act as a marker for successful plasmid transformation. pHvU3 is the U3 promoter optimized for *Hordeum vulgare* (barley) (Kumar et al. 2018). The CmR sequence gives chloramphenicol resistance. The ccdB sequence produces a post-segregational killing (PSK) toxin. The shuttle vector contains a BpiI (BbsI) cut site before the CmR and after the ccdB CDS. The shuttle vector also contains a BsaI cut site that leads to overhands of CGGT and GCAC.

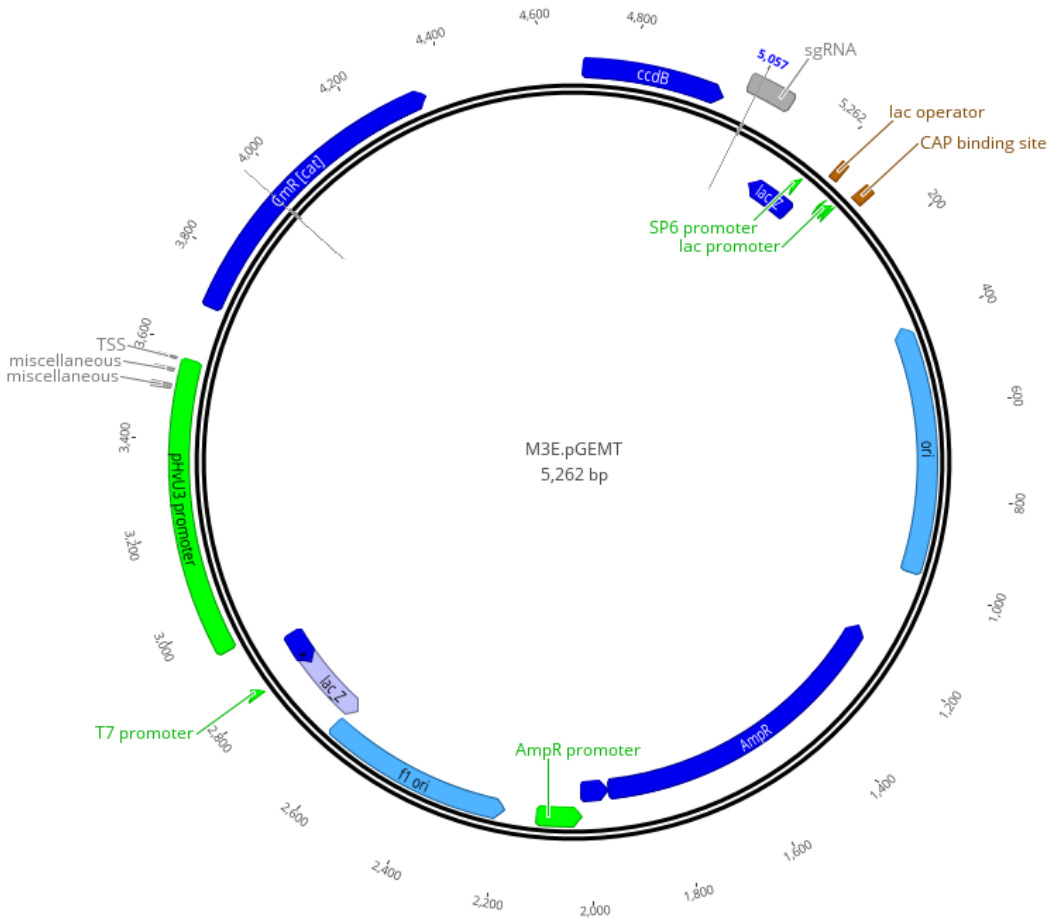

Appendix A 3: Shuttle vector carrying the third sgRNA. Ori demonstrates the replication origin of the shuttle vector backbone. The AmpR is the coding sequence of beta-lactamase, which confers ampicillin resistance. The lacZ CDS is the coding sequence for beta-galactosidase, which cleaves X-gal to act as a marker for successful plasmid transformation. pHvU3 is the U3 promoter optimized for *Hordeum vulgare* (barley) (Kumar et al. 2018). The CmR sequence gives chloramphenicol resistance. The ccdB sequence produces a post-segregational killing (PSK) toxin. The shuttle vector contains a BpiI (BbsI) cut site before the CmR and after the ccdB CDS. The shuttle vector also includes a BsaI cut site that leads to overhands of GCAC and GGGA.

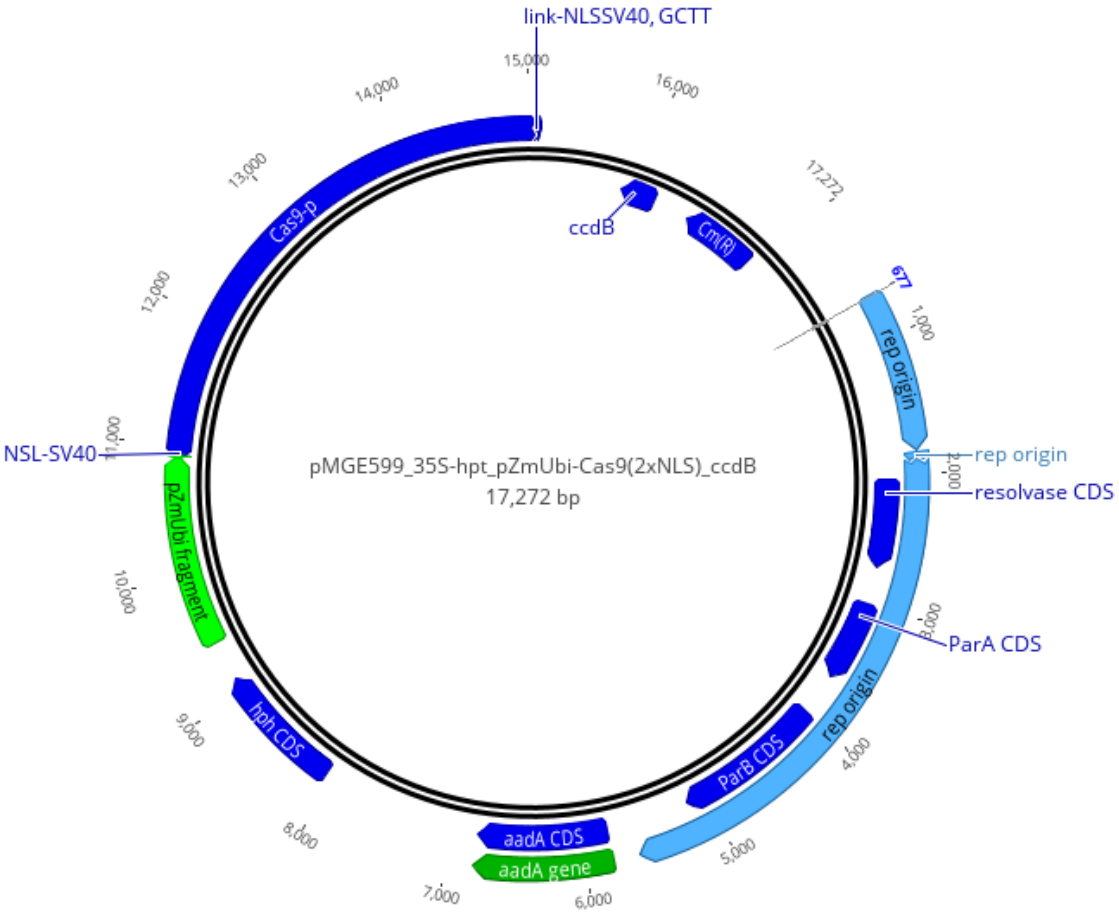

Appendix A 4: Destination vector of the CRISPR/Cas9 gene editing constructs. Rep origin demonstrates the replication origin (PVS1) of the destination vector backbone. ParA CDS and ParB CDS denotes the coding sequences of the partitioning proteins ParA and ParB, respectively. The aadA CDS is the coding sequence of streptomycin adenyltransferase, which confers streptomycin resistance. The *hph* CDS produces hygromycin phosphotransferase and provides Hygromycin resistance. pHvU3 is the U3 promoter optimized for *Hordeum vulgare* (barley) (Kumar et al. 2018). pZmUbifragment denotes the *Zea mays* ubiquitin promoter. *Cas9-p* encodes for *Streptococcus pyogenes* Cas9 protein. The CmR sequence confers chloramphenicol resistance. The ccdB sequence produces a post-segregational killing (PSK) toxin. The shuttle vector contains a BpiI (BbsI) cut site before the CmR and after the ccdB CDS that lead to overhangs of ACTA and GGGA.

Appendix A 5: Sequences of *HvTLP8* orthologs in *Avena sativa* variety Park

Species	Genome	Sequence
Avena sativa v. Park	A	ATGGCGTCGGCAGCCGTCTCCTCCGCCCTGCGCGTCCTGCCTCTGTTCCTC CTCGTCGCCGCCGCCCACGCGGCCACGTTCACCGTCACCAACAAGTGCCA GTTCACCGTGTGGGGTGCGGCCGTGCCCGGCGGTGGCCAGCAGCTCGACC CGGGGCAACAGTGGAAGGTCGAGGTGGCGGCCGGCACGACCAGCGGGCG CGTGTGGGCGCGCACGGGCTGCAACTTCGACGGCAGCGGCAACGGGAAG TGCGAGACGGGCGACTGCGGCGGCAAGCTGCAGTGCACGTAGTACGGGC AGGCGCCCAACACGCTGGCCGAGTTCGGGCTGAACCAGTACGAAGGCCA GGACTTCATCGACATCTCCGTCATCGACGGCTTCAACGTGCCCATGGACT TCCTGCCCGCCGACGGCACCACCGGGTGCCCCAAGGGCGGGCCGCGCTG CGACGCCGACATCACGGCGCAGTGCCCGAACGAGCTCAAGGCCACCGGA GGGTGCAACAACGCGTGCACGGTGTTCAAGGAGGACCAGTACTGCTGTA CCGGCTCGGCGGCGAACAACTGCGGGCCCACCGACTACTCCAGGTTCTTC AAGGGCCTGTGCCCGGACGCCTACAGCTACCCCAAGGACGACGCCACCA GCATCTACACTTGCCCCGGCGGCACCAACTATCAGGTCATCTTCTGCCCG TGA
	C	ATGGCATCCCTCTCCACCTCTTCCATGTTGCCCGTGCTCCTCCTCTTGCTC GTCGCTGCCGCCGACGCGGCGACCTTCACCGTCACCAACAAGTGCCAGTA CACGGTGTGGGCGGCGGCCGTGCCGGTCGGCGGGGGCAGGAAGCTCGAC CCGGGGCAGACATGGAACATCAACGTGCCGGCCGGCACGACAAGCGGGC GCGTGGGGGCGCGCACGGGCTGCAACTTCGACGGCAGCGGCAACGGGCG GTGCCGGACGGGCGACTGCGGCGGCAAGCTGCAGTGCACGCAGTACGGG CAGGCGCCCAACACGCTGGCCGAGTTCGGGCTCAACAAGTTCAACAACCT CGACTTCTTCGACATCTCCCTCATCGACGGCTTCAACGTGCCCATGAACTT CCTGCCGGCCGGCAGCGGCGCCGGGTGCCCCAAGGGCGGGCCGCGGTGC CCGAAGGTGATCACGCCGCAGTGCCCGAACGAGCTCAAGGCCACTGGAG GGTGCAACAACGCCTGCACGGTGTTCAAGCAGGACAAGTACTGCTGCAC CGGCTCGGCGGCGGACAACTGCGGGCCGACCGACTACTCCAGGTTCTTCA AGGGGCAGTGCTCTGACGCCTACAGCTACCCCAAGGACGACGCCACCAG CACCTACACTTGCCCCGGCGGCACCAACTACCAGGTCATCTTCTGCCCAT GA
	D	ATGGCATCCCTCTCCACCTCTTCCATGCTGCCCGTGCTCCTCCTCTTGCTC GTCGCTGCCGCCGACGCGGCGACCTTCACCGTCACCAACAAGTGCCAGTA CACGGTGTGGGCGGCGGCCGTGCCGGCGGGCGGGGGCAGGAAGCTCGAC CCGGGGCAGTCATGGAACATCAACGTGCCTGCCGGCACGACGGGCGGGC GCGTGTGGGCGCGCACGGGCTGCAACTTCGACGGCAGCGGCAACGGGCG GTGCCAGACGGGCGACTGCGGCGGGAAGCTGCAGTGCACGCAGTACGGG CAGGCGCCGAACACCCTGGCCGAGTTCGGGCTCAACAAGTTCAACAACCT CGACTTCTTCGACATCTCCCTTATCGACGGCTTCAATGTGCCCATGAACTT CCTGCCCGCCGGCAGCGGCGCCGGCTGCCCCAAGGGCGGGCCGCGGTGC CCCAAGGTGATCACGCCGCAGTGCCCGAACGAGCTAAAGGCCACCGGAG GGTGCAACAACGCGTGCACGGTGTTCAAGCAGGACAAGTACTGCTGCAC CGGCTCGGCGGCGGACAACTGCGGGCCGACGAACTACTCCAGGTTCTTCA AGGGGCAGTGCTCCGACGCGTACAGCTACCCCAAGGACGACGCCACCAG CACCTACACTTGCCCCGGTGGCACCAACTACCAGGTCATCTTCTGCCCAT GA

Appendix A 6: Sequences of *HvTLP8* orthologs in *Avena sativa* variety OT3098

Species	Genome	Sequence
Avena sativa v. OT3098	A	ATGGCATCGGCAGCTGCCTCCTCCGCCCTGCGCGTCCTCCCTCTGTTCCTC CTCGTCGCCGCCGCCCACGCCGCCACGTTCACCGTCACCAACAAGTGCCA GTTCACCGTGTGGGGCGCGGCCGTGCCCGGCGGGGGCCAGAAGCTCGAC CCGGGGCAGCAGTGGAAGGTCGAGGTGCCGGCCGGCACGACCAGCGGGC GCGTGTGGGCGCGCACGGGCTGCAACTTCGACGGCAGCGGCAACGGGAA GTGCGAGACGGGCGACTGCGGCGGCAAGCTGCAGTGCACGCAGTACGGG CAGGCGCCCAACACGCTGGCCGAGTTCGGGCTCAACCAGTACGAAGGCC AGGACTTCATCGACATCTCCGTCATCGACGGCTTCAACGTGCCCATGGAC TTCCTGCCCGCCGACGGCACCACCGGGTGCCCCAAGGGCGGGCCGCGCTG CGACGCCGACATCACGGCGCAGTGCCCGTCCGAGCTCAAGGCCACCGGA GGGTGCAACAACGCGTGCACGGTGTTCAAGGAGGACCAGTACTGCTGCA CCGGCTCGGCGGCGAACAACTGCGGACCGACCGACTACTCCAAGTTCTTC AAGGGGCTGTGCCCAGACGCCTACAGCTACCCCAAGGACGACGCCACCA GCATCTACACTTGCCCCGGCGGCACCAACTATCAGGTCATCTTCTGCCCG TGA
	C	ATGGCATCCCTCTCCACCTCTTCCATGTTGCCCGTGCTCCTCCTCTTGCTC GTCGCTGCCGCCGACGCGGCGACCTTCACCGTCACCAACAAGTGCCAGTA CACGGTGTGGGCGGCGGCCGTGCCGGTCGGCGGGGGCAGGAAGCTCGAC CCGGGGCAGACATGGAACATCAACGTGCCGGCCGGCACGACAAGCGGGC GCGTGTGGGCGCGCACGGGCTGCAACTTCGACGGCAGCGGCAACGGGCG GTGCCAGACGGGCGACTGCGGCGGCAAGCTGCAGTGCACGCAGTACGGG CAGGCGCCCAACACGCTGGCCGAGTTCGGGCTCAACAAGTTCAACAACCT CGACTTCTTCGACATCTCCCTCATCGACGGCTTCAACGTGCCCATGAACTT CCTGCCGGCCGGCAGCGGCGCCGGGTGCCCCAAGGGCGGGCCGCGGTGC CCGAAGGTGATCACGCCGCAGTGCCCGAACGAGCTCAAGGCCACTGGAG GGTGCAACAACGCCTGCACGGTGTTCAAGCAGGACAAGTACTGCTGCAC CGGCTCGGCGGCGGACAACTGCGGGCCGACCGACTACTCCAGGTTCTTCA AGGGGCAGTGCTCTGACGCCTACAGCTACCCCAAGGACGACGCCACCAG CACCTACACTTGCCCCGGCGGCACCAACTACCAGGTCATCTTCTGCCCAT GA
	D	ATGGCATCCCTCTCCACCTCTTCCATGCTGCCCGTGCTCCTCCTCTTGCTC GTCGCTGCCGCCGACGCGGCGACCTTCACCGTCACCAACAAGTGCCAGTA CACGGTGTGGGCGGCGGCCGTGCCGGCGGGCGGGGGCAGGAAGCTCGAC CCGGGGCAGTCATGGAACATCAACGTGCCTGCCGGCACGACGGGCGGGC GCGTGTGGGCGCGCACGGGCTGCAACTTCGACGGCAGCGGCGCGCCGAA CACCCTGGCCGAGTTCGGGCTCAACAAGTTCAACAACCTCGACTTCTTCG ACATCTCCCTTATCGACGGCTTCAATGTGCCCATGAACTTCCTGCCCGCCG GCAGCGGCGCCGGCTGCCCCAAGGGCGGGCCGCGGTGCCCCAAGGTGAT CACGCCGCAGTGCCCGAACGAGCTAAAGGCCACCGGAGGGTGCAACAAC GCGTGCACGGTGTTCAAGCAGGACAAGTACTGCTGCACCGGCTCGGCGG CGGACAACTGCGGGCCGACGAACTACTCCAGGTTCTTCAAGGGGCAGTG CTCCGACGCGTACAGCTACCCCAAGGACGACGCCACCAGCACCTACACTT GCCCCGGTGGCACCAACTACCAGGTCATCTTCTGCCCATGA

Appendix A 7: Sequences of *HvTLP8* orthologs in *Avena byzantina* (red oat)

Species	Genome	Sequence
Avena byzantina	A	ATGGCATCGGCAGCTGCCTCCTCCGCCCTGCGCGTCCTCCCTCTGTTCCTC CTCGTCGCCGCCGCCCACGCCGCCACGTTCACCGTCACCAACAAGTGCCA GTTCACCGTGTGGGGCGCGGCCGTGCCCGGCGGGGGCCAGAAGCTCGAC CCGGGGCAGCAGTGGAAGGTCGAGGTGCCGGCCGGCACGACCAGCGGGC GCGTGTGGGCGCGCACGGGCTGCAACTTCGACGGCAGCGGCAACGGGAA GTGCGAGACGGGCGACTGCGGCGGCAAGCTGCAGTGCACGCAGTACGGG CAGGCACCCAACACGCTGGCCGAGTTCGGGCTCAACCAGTACGAAGGCC AGGACTTCATCGACATCTCCGTCATCGACGGCTTCAACGTGCCCATGGAC TTCCTGCCCGCCGACGGCACCACCGGGTGCCCCAAGGGCGGGCCGCGCTG CGACGCCGACATCACGGCGCAGTGCCCGTCCGAGCTCAAGGCCACCGGA GGGTGCAACAACGCGTGCACGGTGTTCAAGGAGGACCAGTACTGCTGCA CCGGCTCGGCGGCGAACAACTGCGGACCGACCGACTACTCCAAGTTCTTC AAGGGGCTGTGCCCAGACGCCTACAGCTACCCCAAGGACGACGCCACCA GCATCTACACTTGCCCCGGCGGCACCAACTATCAGGTCATCTTCTGCCCG TGA
	C	ATGGCATCCCTCTCCACCTCTTCCATGTTGCCCGTGCTCCTCCTCTTGCTC GTCGCTGCCGCCGACGCGGCGACCTTCACCGTCACCAACAAGTGCCAGTA CACGGTGTGGGCGGCGGCCGTGCCGGTCGGCGGGGGCAGGAAGCTCGAC CCGGGGCAGACATGGAACATCAACGTGCCGGCCGGCACGACAAGCGGGC GCGTGTGGGCGCGCACGGGCTGCAACTTCGACGGCAGCGGCAACGGGCG GTGCCAGACGGGCGACTGCGGCGGCAAGCTGCAGTGCACGCAGTACGGG CAGGCGCCCAACACGCTGGCCGAGTTCGGGCTCAACAAGTTCAACAACCT CGACTTCTTCGACATCTCCCTCATCGACGGCTTCAACGTGCCCATGAACTT CCTGCCGGCCGGCAGCGGCGCCGGGTGCCCCAAGGGCGGGCCGCGGTGC CCGAAGGTGATCACGCCGCAGTGCCCGAACGAGCTCAAGGCCACTGGAG GGTGCAACAACGCCTGCACGGTGTTCAAGCAGGACAAGTACTGCTGCAC CGGCTCGGCGGCGGACAACTGCGGGCCGACCGACTACTCCAGGTTCTTCA AGGGGCAGTGCTCTGACGCCTACAGCTACCCCAAGGACGACGCCACCAG CACCTACACTTGCCCCGGCGGCACCAACTACCAGGTCATCTTCTGCCCAT GA
	D	ATGGCATCCCTCTCCACCTCTTCCATGCTGCCCGTGCTCCTCCTCTTGCTC GTCGCTGCCGCCGACGCGGCGACCTTCACCGTCACCAACAAGTGCCAGTA CACGGTGTGGGCGGCGGCCGTGCCGGCGGGCGGGGGCAGGAAGCTCGAC CCGGGGCAGTCATGGAACATCAACGTGCCTGCCGGCACGACGGGCGGGC GCGTGTGGGCGCGCACGGGCTGCAACTTCGACGGCAGCGGCAACGGGCG GTGCCAGACGGCCGACTGCGGCGGGAAGCTGCAGTGCACGCAGTACGGG CAGGCGCCGAACACCCTGGCCGAGTTCGGGCTCAACAAGTTCAACAACCT CGACTTCTTCGACATCTCCCTTATCGACGGCTTCAATGTGCCCATGAACTT CCTGCCCGCCGGCAGCGGCGCCGGCTGCCCCAAGGGCGGGCCGCGGTGC CCCAAGGTGATCACGCCGCAGTGCCCGAACGAGCTAAAGGCCACCGGAG GGTGCAACAACGCGTGCACGGTGTTCAAGCAGGACAAGTACTGCTGCAC CGGCTCGGCGGCGGACAACTGCGGGCCGACGAACTACTCCAGGTTCTTCA AGGGGCAGTGCTCCGACGCGTACAGCTACCCCAAGGACGACGCCACCAG CACCTACACTTGCCCCGGTGGCACCAACTACCAGGTCATCTTCTGCCCAT GA

Appendix A 8: Beta-glucan content by dry weight (d.w.) of various *Avena sativa* varieties.

Variety	Beta-glucan content (g/kg d.w.)	Reference
AC Morgan	37.8	POGA (2018)
Terra	57	Havrlentova and Kraic (2006)
Marion	58.7	Lee et al. (1997)
CDC Morrison	47.1	Herrera et al. (2016)
Goslin	47	Blake et al. (2016)
OT3098	60	Beattie and Rossnagel (2017)

References

Adams KL, Wendel JF. 2005. Polyploidy and genome evolution in plants. Current opinion in plant biology. 8(2):135-141.

Ajithkumar A, Andersson R, Åman P. 2005. Content and molecular weight of extractable β-glucan in american and swedish oat samples. Journal of Agricultural and Food Chemistry. 53(4):1205-1209.

Alston JM, Beddow JM, Pardey PG. 2009. Agricultural research, productivity, and food prices in the long run. Science. 325(5945):1209-1210.

Altpeter F, Springer NM, Bartley LE, Blechl AE, Brutnell TP, Citovsky V, Conrad LJ, Gelvin SB, Jackson DP, Kausch AP et al. 2016. Advancing crop transformation in the era of genome editing. The Plant Cell. 28(7):1510-1520.

Andersson AA, Börjesdotter D. 2011. Effects of environment and variety on content and molecular weight of β-glucan in oats. Journal of Cereal Science. 54(1):122-128.

Andersson M, Ellegård L, Andersson H. 2002. Oat bran stimulates bile acid synthesis within 8 h as measured by 7α-hydroxy-4-cholesten-3-one. The American Journal of Clinical Nutrition. 76(5):1111-1116.

Asoro FG, Newell MA, Scott MP, Beavis WD, Jannink J-L. 2013. Genome-wide association study for beta-glucan concentration in elite north american oat. Crop Science. 53(2):542-553.

Babiker EM, Gordon TC, Chao S, Newcomb M, Rouse MN, Jin Y, Wanyera R, Acevedo M, Brown-Guedira G, Williamson S et al. 2015. Mapping resistance to the ug99 race group of the stem rust pathogen in a spring wheat landrace. Theoretical and Applied Genetics. 128(4):605-612.

Bachhawat N, Ouyang Q, Henry SA. 1995. Functional characterization of an inositol-sensitive upstream activation sequence in yeast. A cis-regulatory element responsible for inositol-choline mediated regulation of phospholipid biosynthesis. The Journal of biological chemistry. 270(42):25087-25095.

Baltes NJ, Gil-Humanes J, Voytas DF. 2017. Chapter one - genome engineering and agriculture: Opportunities and challenges. In: Weeks DP, Yang B, editors. Progress in molecular biology and translational science. Academic Press. p. 1-26.

Barrangou R, Fremaux C, Deveau H, Richards M, Boyaval P, Moineau S, Romero DA, Horvath P. 2007. Crispr provides acquired resistance against viruses in prokaryotes. Science. 315(5819):1709-1712.

Baum BR, Baum BR. 1977. Oats: Wild and cultivated: A monograph of the genus avena l.(poaceae). Biosystematics Research Institute.

Baum BR, Rajhathy T, Sampson DR. 1973. An important new diploid avena species discovered on the canary islands. Canadian Journal of Botany. 51(4):759-762.

Beattie A, Rossnagel B. Forthcoming 2017. Request for support for registration of ot3098. University of Saskatchewan

Belhaj K, Chaparro-Garcia A, Kamoun S, Nekrasov V. 2013. Plant genome editing made easy: Targeted mutagenesis in model and crop plants using the crispr/cas system. Plant Methods. 9(1):39.

Belhaj K, Chaparro-Garcia A, Kamoun S, Patron NJ, Nekrasov V. 2015. Editing plant genomes with crispr/cas9. Current Opinion in Biotechnology. 32:76-84.

Blake VC, Birkett C, Matthews DE, Hane DL, Bradbury P, Jannink JL. 2016. The triticeae toolbox: Combining phenotype and genotype data to advance small-grains breeding. The Plant Genome. 9(2):plantgenome2014.2012.0099.
Bortesi L, Fischer R. 2015. The crispr/cas9 system for plant genome editing and beyond. Biotechnology Advances. 33(1):41-52.
Brouns SJ, Jore MM, Lundgren M, Westra ER, Slijkhuis RJ, Snijders AP, Dickman MJ, Makarova KS, Koonin EV, Van Der Oost J. 2008. Small crispr rnas guide antiviral defense in prokaryotes. Science. 321(5891):960-964.
Burton R, Fincher G. 2012. Current challenges in cell wall biology in the cereals and grasses. Frontiers in Plant Science. 3(130).
Burton RA, Collins HM, Kibble NA, Smith JA, Shirley NJ, Jobling SA, Henderson M, Singh RR, Pettolino F, Wilson SM et al. 2011. Over-expression of specific hvcslf cellulose synthase-like genes in transgenic barley increases the levels of cell wall (1,3;1,4)-beta-d-glucans and alters their fine structure. Plant biotechnology journal. 9(2):117-135.
Burton RA, Fincher GB. 2009. (1,3;1,4)-beta-d-glucans in cell walls of the poaceae, lower plants, and fungi: A tale of two linkages. Molecular plant. 2(5):873-882.
Burton RA, Gidley MJ, Fincher GB. 2010. Heterogeneity in the chemistry, structure and function of plant cell walls. Nature chemical biology. 6(10):724-732.
Burton RA, Jobling SA, Harvey AJ, Shirley NJ, Mather DE, Bacic A, Fincher GB. 2008. The genetics and transcriptional profiles of the cellulose synthase-like hvcslf gene family in barley. Plant Physiology. 146(4):1821-1833.
Burton RA, Wilson SM, Hrmova M, Harvey AJ, Shirley NJ, Medhurst A, Stone BA, Newbigin EJ, Bacic A, Fincher GB. 2006. Cellulose synthase-like *cslf* genes mediate the synthesis of cell wall (1,3;1,4)-ß-d-glucans. Science. 311(5769):1940-1942.
Butardo VM, Sreenivasulu N. 2016. Chapter two - tailoring grain storage reserves for a healthier rice diet and its comparative status with other cereals. In: Jeon KW, editor. International review of cell and molecular biology. Academic Press. p. 31-70.
Canada S. 2019. Leading causes of death, total population, by age group. Statistics Canada Ottawa, ON.
Canver MC, Bauer DE, Dass A, Yien YY, Chung J, Masuda T, Maeda T, Paw BH, Orkin SH. 2014. Characterization of genomic deletion efficiency mediated by clustered regularly interspaced short palindromic repeats (crispr)/cas9 nuclease system in mammalian cells. The Journal of biological chemistry. 289(31):21312-21324.
Chan GC-F, Chan WK, Sze DM-Y. 2009. The effects of β-glucan on human immune and cancer cells. Journal of Hematology & Oncology. 2(1):25.
Char SN, Neelakandan AK, Nahampun H, Frame B, Main M, Spalding MH, Becraft PW, Meyers BC, Walbot V, Wang K. 2017. An agrobacterium-delivered crispr/cas9 system for high-frequency targeted mutagenesis in maize. Plant biotechnology journal. 15(2):257-268.
Chen C-Y, Milbury PE, Kwak H-K, Collins FW, Samuel P, Blumberg JB. 2004. Avenanthramides and phenolic acids from oats are bioavailable and act synergistically with vitamin c to enhance hamster and human ldl resistance to oxidation. The Journal of Nutrition. 134(6):1459-1466.
Chen J, Dellaporta S. 1994. Urea-based plant DNA miniprep. In: Freeling M, Walbot V, editors. The maize handbook. New York, NY: Springer New York. p. 526-527.

Chen J, Seviour R. 2007. Medicinal importance of fungal β-(1→3), (1→6)-glucans. Mycological Research. 111(6):635-652.
Cheng M, Fry JE, Pang S, Zhou H, Hironaka CM, Duncan DR, Conner TW, Wan Y. 1997. Genetic transformation of wheat mediated by agrobacterium tumefaciens. Plant Physiology. 115(3):971-980.
Cho M-J, Jiang W, Lemaux PG. 1998. Transformation of recalcitrant barley cultivars through improvement of regenerability and decreased albinism. Plant Science. 138(2):229-244.
Cho M-J, Jiang W, Lemaux PG. 1999. High-frequency transformation of oat via microprojectile bombardment of seed-derived highly regenerative cultures. Plant Science. 148(1):9-17.
Cho SW, Kim S, Kim Y, Kweon J, Kim HS, Bae S, Kim J-S. 2014. Analysis of off-target effects of crispr/cas-derived rna-guided endonucleases and nickases. Genome research. 24(1):132-141.
Choi H-W, G. Lemaux P, Cho M-j. 2000. High frequency of cytogenetic aberration in transgenic oat (avena sativa l.) plants. Plant Science. 156(1):85-94.
Choromanska A, Kulbacka J, Harasym J, Oledzki R, Szewczyk A, Saczko J. 2018. High- and low-molecular weight oat beta-glucan reveals antitumor activity in human epithelial lung cancer. Pathology & Oncology Research. 24(3):583-592.
Cicero AF, Fogacci F, Veronesi M, Strocchi E, Grandi E, Rizzoli E, Poli A, Marangoni F, Borghi C. 2020. A randomized placebo-controlled clinical trial to evaluate the medium-term effects of oat fibers on human health: The beta-glucan effects on lipid profile, glycemia and intestinal health (belt) study. Nutrients. 12(3):686.
Comai L. 2005. The advantages and disadvantages of being polyploid. Nature Reviews Genetics. 6(11):836-846.
Cong L, Ran FA, Cox D, Lin S, Barretto R, Habib N, Hsu PD, Wu X, Jiang W, Marraffini LA. 2013. Multiplex genome engineering using crispr/cas systems. Science. 339(6121):819-823.
Connelly S, Marshallsay C, Leader D, Brown J, Filipowicz W. 1994. Small nuclear rna genes transcribed by either rna polymerase ii or rna polymerase iii in monocot plants share three promoter elements and use a strategy to regulate gene expression different from that used by their dicot plant counterparts. Molecular and cellular biology. 14(9):5910-5919.
Craig IL, Murray BE, Rajhathy T. 1974. Avena canariensis: Morphological and electrophoretic polymorphism and relationship to the a. Magna–a. Murphyi complex and a. Sterilis. Canadian Journal of Genetics and Cytology. 16(3):677-689.
Cristea S, Freyvert Y, Santiago Y, Holmes MC, Urnov FD, Gregory PD, Cost GJ. 2013. In vivo cleavage of transgene donors promotes nuclease-mediated targeted integration. Biotechnology and Bioengineering. 110(3):871-880.
Daou C, Zhang H. 2012. Oat beta-glucan: Its role in health promotion and prevention of diseases. Comprehensive reviews in food science and food safety. 11(4):355-365.
De Koeyer DL, Tinker NA, Wight CP, Deyl J, Burrows VD, O'Donoughue LS, Lybaert A, Molnar SJ, Armstrong KC, Fedak G et al. 2004. A molecular linkage map with associated qtls from a hulless × covered spring oat population. Theoretical and Applied Genetics. 108(7):1285-1298.
Deltcheva E, Chylinski K, Sharma CM, Gonzales K, Chao Y, Pirzada ZA, Eckert MR, Vogel J, Charpentier E. 2011. Crispr rna maturation by trans-encoded small rna and host factor rnase iii. Nature. 471(7340):602-607.

Doblin MS, Pettolino FA, Wilson SM, Campbell R, Burton RA, Fincher GB, Newbigin E, Bacic A. 2009. A barley cellulose synthase-like cslh gene mediates (1,3;1,4)-beta-d-glucan synthesis in transgenic arabidopsis. Proceedings of the National Academy of Sciences of the United States of America. 106(14):5996-6001.
Doench JG, Fusi N, Sullender M, Hegde M, Vaimberg EW, Donovan KF, Smith I, Tothova Z, Wilen C, Orchard R et al. 2016. Optimized sgrna design to maximize activity and minimize off-target effects of crispr-cas9. Nature Biotechnology. 34:184.
Doench JG, Hartenian E, Graham DB, Tothova Z, Hegde M, Smith I, Sullender M, Ebert BL, Xavier RJ, Root DE. 2014. Rational design of highly active sgrnas for crispr-cas9–mediated gene inactivation. Nature Biotechnology. 32:1262.
Dong OX, Yu S, Jain R, Zhang N, Duong PQ, Butler C, Li Y, Lipzen A, Martin JA, Barry KW. 2020. Marker-free carotenoid-enriched rice generated through targeted gene insertion using crispr-cas9. Nature communications. 11(1):1-10.
Du B, Bian Z, Xu B. 2014. Skin health promotion effects of natural beta-glucan derived from cereals and microorganisms: A review. Phytotherapy Research. 28(2):159-166.
Du H, Zeng X, Zhao M, Cui X, Wang Q, Yang H, Cheng H, Yu D. 2016. Efficient targeted mutagenesis in soybean by talens and crispr/cas9. Journal of Biotechnology. 217:90-97.
Eastwood MA, Hamilton D. 1968. Studies on the adsorption of bile salts to non-absorbed components of diet. Biochimica et biophysica acta. 152(1):165-173.
Edney MJ, Mather DE. 2004. Quantitative trait loci affecting germination traits and malt friability in a two-rowed by six-rowed barley cross. Journal of Cereal Science. 39(2):283-290.
Engler C, Marillonnet S. 2014. Golden gate cloning. In: Valla S, Lale R, editors. DNA cloning and assembly methods. Totowa, NJ: Humana Press. p. 119-131.
FAO. 2019. World agricultural production. November 8, 2019 ed. Foreign Agricultural Service.
Feng C, Yuan J, Wang R, Liu Y, Birchler JA, Han F. 2016. Efficient targeted genome modification in maize using crispr/cas9 system. Journal of Genetics and Genomics. 43(1):37-43.
Fincher GB. 2009. Revolutionary times in our understanding of cell wall biosynthesis and remodeling in the grasses. Plant Physiology. 149(1):27-37.
Fincher GB, Stone BA. 2004. Chemistry of nonstarch polysaccharides. Encyclopedia of Grain Science. 1:206-223.
Fogarty MC, Smith SM, Sheridan JL, Hu G, Islamovic E, Reid R, Jackson EW, Maughan PJ, Ames NP, Jellen EN et al. 2020. Identification of mixed linkage β-glucan quantitative trait loci and evaluation of ascslf6 homoeologs in hexaploid oat. Crop Science. 60(2):914-933.
Fominaya A, Vega C, Ferrer E. 1988. Giemsa c-banded karyotypes of avena species. Genome. 30(5):627-632.
Galli M, Martiny E, Imani J, Kumar N, Koch A, Steinbrenner J, Kogel KH. 2021. Crispr/sp cas9-mediated double knockout of barley microrchidia morc1 and morc6a reveals their strong involvement in plant immunity, transcriptional gene silencing and plant growth. Plant biotechnology journal.
Gao H, Wu X, Chai J, Han Z. 2012. Crystal structure of a tale protein reveals an extended n-terminal DNA binding region. Cell Research. 22(12):1716-1720.

Garneau JE, Dupuis M-È, Villion M, Romero DA, Barrangou R, Boyaval P, Fremaux C, Horvath P, Magadán AH, Moineau S. 2010. The crispr/cas bacterial immune system cleaves bacteriophage and plasmid DNA. Nature. 468(7320):67.

Gasiunas G, Barrangou R, Horvath P, Siksnys V. 2012. Cas9–crrna ribonucleoprotein complex mediates specific DNA cleavage for adaptive immunity in bacteria. Proceedings of the National Academy of Sciences. 109(39):E2579-E2586.

Gasparis S, Bregier C, Orczyk W, Nadolska-Orczyk A. 2008. Agrobacterium-mediated transformation of oat (avena sativa l.) cultivars via immature embryo and leaf explants. Plant cell reports. 27(11):1721-1729.

Gasparis S, Kała M, Przyborowski M, Łyżnik LA, Orczyk W, Nadolska-Orczyk A. 2018. A simple and efficient crispr/cas9 platform for induction of single and multiple, heritable mutations in barley (hordeum vulgare l.). Plant Methods. 14(1):111.

Godfray HCJ, Beddington JR, Crute IR, Haddad L, Lawrence D, Muir JF, Pretty J, Robinson S, Thomas SM, Toulmin C. 2010. Food security: The challenge of feeding 9 billion people. science. 327(5967):812-818.

Grenier J, Potvin C, Asselin A. 2000. Some fungi express β-1,3-glucanases similar to thaumatin-like proteins. Mycologia. 92(5):841-848.

Grenier J, Potvin C, Trudel J, Asselin A. 1999. Some thaumatin-like proteins hydrolyse polymeric beta-1,3-glucans. The Plant journal : for cell and molecular biology. 19(4):473-480.

Grundy MML, Quint J, Rieder A, Ballance S, Dreiss CA, Cross KL, Gray R, Bajka BH, Butterworth PJ, Ellis PR et al. 2017. The impact of oat structure and β-glucan on in vitro lipid digestion. J Funct Foods. 38(Pt A):378-388.

Gutierrez-Gonzalez JJ, Wise ML, Garvin DF. 2013. A developmental profile of tocol accumulation in oat seeds. Journal of Cereal Science. 57(1):79-83.

Gutiérrez L, Cuesta-Marcos A, Castro AJ, von Zitzewitz J, Schmitt M, Hayes PM. 2011. Association mapping of malting quality quantitative trait loci in winter barley: Positive signals from small germplasm arrays. The Plant Genome. 4(3):256-272.

Han F, Ullrich S, Chirat S, Menteur S, Jestin L, Sarrafi A, Hayes P, Jones B, Blake T, Wesenberg D. 1995. Mapping of β-glucan content and β-glucanase activity loci in barley grain and malt. Theoretical and Applied Genetics. 91(6-7):921-927.

Hartung F, Schiemann J. 2014. Precise plant breeding using new genome editing techniques: Opportunities, safety and regulation in the eu. The Plant Journal. 78(5):742-752.

Hastings J, Kenealey J. 2017. Chemotherapeutic effects of avenanthramides on breast cancer cells. The FASEB Journal. 31(1_supplement):790.716-790.716.

Havrlentova M, Kraic J. 2006. Content of beta-d-glucan in cereal grains. Journal of Food and Nutrition Research (Slovak Republic).

Hayasaki M, Morikawa T, Tarumoto I. 2000. Intergenomic translocations of polyploid oats (genus avena) revealed by genomic in situ hybridization. Genes & genetic systems. 75(3):167-171.

He L-x, Zhao J, Huang Y-s, Li Y. 2016. The difference between oats and beta-glucan extract intake in the management of hba1c, fasting glucose and insulin sensitivity: A meta-analysis of randomized controlled trials. Food & function. 7(3):1413-1428.

Herrera MP, Gao J, Vasanthan T, Temelli F, Henderson K. 2016. B-glucan content, viscosity, and solubility of canadian grown oat as influenced by cultivar and growing location. Canadian Journal of Plant Science. 96(2):183-196.

Hsu PD, Scott DA, Weinstein JA, Ran FA, Konermann S, Agarwala V, Li Y, Fine EJ, Wu X, Shalem O et al. 2013. DNA targeting specificity of rna-guided cas9 nucleases. Nature Biotechnology. 31(9):827-832.
Igartua E, Hayes P, Thomas W, Meyer R, Mather D. 2002. Genetic control of quantitative grain and malt quality traits in barley. Journal of Crop Production. 5(1-2):131-164.
Iliakis G, Wang H, Perrault AR, Boecker W, Rosidi B, Windhofer F, Wu W, Guan J, Terzoudi G, Pantelias G. 2004. Mechanisms of DNA double strand break repair and chromosome aberration formation. Cytogenet Genome Res. 104(1-4):14-20.
Ishino Y, Shinagawa H, Makino K, Amemura M, Nakata A. 1987. Nucleotide sequence of the iap gene, responsible for alkaline phosphatase isozyme conversion in escherichia coli, and identification of the gene product. Journal of Bacteriology. 169(12):5429-5433.
Islamovic E, Obert DE, Oliver RE, Harrison SA, Ibrahim A, Marshall JM, Miclaus KJ, Hu G, Jackson EW. 2013. Genetic dissection of grain beta-glucan and amylose content in barley (hordeum vulgare l.). Molecular Breeding. 31(1):15-25.
Ismagul A, Yang N, Maltseva E, Iskakova G, Mazonka I, Skiba Y, Bi H, Eliby S, Jatayev S, Shavrukov Y et al. 2018. A biolistic method for high-throughput production of transgenic wheat plants with single gene insertions. BMC Plant Biology. 18(1):135.
Ito Y, Nishizawa-Yokoi A, Endo M, Mikami M, Toki S. 2015. Crispr/cas9-mediated mutagenesis of the rin locus that regulates tomato fruit ripening. Biochemical and Biophysical Research Communications. 467(1):76-82.
Jansen R, Embden JDAv, Gaastra W, Schouls LM. 2002. Identification of genes that are associated with DNA repeats in prokaryotes. Molecular Microbiology. 43(6):1565-1575.
Jellen E, Gill B. 1996. C-banding variation in the moroccan oat species avena agadiriana (2n= 4x= 28). Theoretical and applied genetics. 92(6):726-732.
Jellen EN, Gill BS, Cox TS. 1994. Genomic in situ hybridization differentiates between a/d- and c-genome chromatin and detects intergenomic translocations in polyploid oat species (genus avena). Genome. 37(4):613-618.
Ji X, Zhang H, Zhang Y, Wang Y, Gao C. 2015. Establishing a crispr–cas-like immune system conferring DNA virus resistance in plants. Nature Plants. 1(10):15144.
Jinek M, Chylinski K, Fonfara I, Hauer M, Doudna JA, Charpentier E. 2012. A programmable dual-rna–guided DNA endonuclease in adaptive bacterial immunity. Science. 337(6096):816-821.
Kang C, Shin WS, Yeo D, Lim W, Zhang T, Ji LL. 2018. Anti-inflammatory effect of avenanthramides via nf-κb pathways in c2c12 skeletal muscle cells. Free Radical Biology and Medicine. 117:30-36.
Kapusi E, Corcuera-Gómez M, Melnik S, Stoger E. 2017. Heritable genomic fragment deletions and small indels in the putative engase gene induced by crispr/cas9 in barley. Frontiers in Plant Science. 8(540).
Kaur M, Singh S. 2017. Physical characteristics of different oat cultivars: Influence on pasting, functional and antioxidant properties. Quality Assurance and Safety of Crops & Foods. 9(3):285-293.
Kaur S, Dhugga KS, Beech R, Singh J. 2017. Genome-wide analysis of the cellulose synthase-like (csl) gene family in bread wheat (triticum aestivum l.). BMC Plant Biology. 17(1):193.

Kemppainen TA, Heikkinen MT, Ristikankare MK, Kosma VM, Julkunen RJ. 2010. Nutrient intakes during diets including unkilned and large amounts of oats in celiac disease. European Journal of Clinical Nutrition. 64(1):62-67.
Keneni G, Bekele E, Imtiaz M, Dagne K. 2012. Genetic vulnerability of modern crop cultivars: Causes, mechanism and remedies. Int J Plant Res. 2(3):69-79.
Keselman H, Rogan JC. 1977. The tukey multiple comparison test: 1953–1976. Psychological Bulletin. 84(5):1050.
Keshavareddy G, Kumar A, Ramu VS. 2018. Methods of plant transformation-a review. Int J Curr Microbiol App Sci. 7(7):2656-2668.
Khan SH. 2019. Genome-editing technologies: Concept, pros, and cons of various genome-editing techniques and bioethical concerns for clinical application. Molecular Therapy - Nucleic Acids. 16:326-334.
Kim H-S, Park K-G, Baek S-B, Kim J-G. 2011. Inheritance of (1–3)(1–4)-beta-d-glucan content in barley (hordeum vulgare l.). Journal of Crop Science and Biotechnology. 14(4):239-245.
King J, Stimart D. 1998. Genetic analysis of variation for auxin-induced adventitious root formation among eighteen ecotypes of arabidopsis thaliana l. Heynh. Journal of Heredity. 89(6):481-487.
Kritchevsky D, Story JA. 1974. Binding of bile salts in vitro by nonnutritive fiber. The Journal of Nutrition. 104(4):458-462.
Kumar N, Galli M, Ordon J, Stuttmann J, Kogel KH, Imani J. 2018. Further analysis of barley morc1 using a highly efficient rna-guided cas9 gene-editing system. Plant biotechnology journal. 16(11):1892-1903.
Ladizinsky G. 1998. A new species of avena from sicily, possibly the tetraploid progenitor of hexaploid oats. Genetic Resources and Crop Evolution. 45(3):263-269.
Lawrenson T, Shorinola O, Stacey N, Li C, Østergaard L, Patron N, Uauy C, Harwood W. 2015. Induction of targeted, heritable mutations in barley and brassica oleracea using rna-guided cas9 nuclease. Genome Biology. 16(1):258.
Lee CJ, Horsley R, Manthey F, Schwarz P. 1997. Comparisons of β-glucan content of barley and oat. Cereal Chemistry. 74(5):571-575.
Leggett JM, Thomas H. 1995. Oat evolution and cytogenetics. In: Welch RW, editor. The oat crop: Production and utilization. Dordrecht: Springer Netherlands. p. 120-149.
Li D, Tang Y, Lin J, Cai W. 2017. Methods for genetic transformation of filamentous fungi. Microbial Cell Factories. 16(1):168.
Li J, Båga M, Rossnagel BG, Legge WG, Chibbar RN. 2008. Identification of quantitative trait loci for β-glucan concentration in barley grain. Journal of Cereal Science. 48(3):647-655.
Liang X-D, Shalapy M, Zhao S-F, Liu J-H, Wang J-Y. 2021. A stress-responsive transcription factor penac1 regulating beta-d-glucan biosynthetic genes enhances salt tolerance in oat. Planta. 254(6):130.
Liang Z, Chen K, Li T, Zhang Y, Wang Y, Zhao Q, Liu J, Zhang H, Liu C, Ran Y. 2017. Efficient DNA-free genome editing of bread wheat using crispr/cas9 ribonucleoprotein complexes. Nature communications. 8(1):1-5.
Liang Z, Chen K, Zhang Y, Liu J, Yin K, Qiu J-L, Gao C. 2018. Genome editing of bread wheat using biolistic delivery of crispr/cas9 in vitro transcripts or ribonucleoproteins. Nat Protoc. 13(3):413-430.

Liang Z, Zhang K, Chen K, Gao C. 2014. Targeted mutagenesis in zea mays using talens and the crispr/cas system. Journal of Genetics and Genomics. 41(2):63-68.
Liepman AH, Wilkerson CG, Keegstra K. 2005. Expression of cellulose synthase-like (csl) genes in insect cells reveals that csla family members encode mannan synthases. Proceedings of the National Academy of Sciences of the United States of America. 102(6):2221-2226.
Lim WL, Collins HM, Byrt CS, Lahnstein J, Shirley NJ, Aubert MK, Tucker MR, Peukert M, Matros A, Burton RA. 2019. Overexpression of hvcslf6 in barley grain alters carbohydrate partitioning plus transfer tissue and endosperm development. Journal of Experimental Botany.
Linares C, Ferrer E, Fominaya A. 1998. Discrimination of the closely related a and d genomes of the hexaploid oat avena sativa l. Proceedings of the National Academy of Sciences. 95(21):12450-12455.
Liu H-J, Jian L, Xu J, Zhang Q, Zhang M, Jin M, Peng Y, Yan J, Han B, Liu J et al. 2020. High-throughput crispr/cas9 mutagenesis streamlines trait gene identification in maize[open]. The Plant Cell. 32(5):1397-1413.
Liu J-J, Sturrock R, Ekramoddoullah AKM. 2010. The superfamily of thaumatin-like proteins: Its origin, evolution, and expression towards biological function. Plant Cell Reports. 29(5):419-436.
Liu J, Han D, Shi Y. 2019. Gene cloning, expression, and antifungal activities of permatin from naked oat (avena nuda). Probiotics and Antimicrobial Proteins. 11(1):299-309.
Liu Y, Liu L, Asiegbu FO, Yang C, Han S, Yang S, Zeng Q, Liu Y. 2021. Molecular identification and antifungal properties of four thaumatin-like proteins in spruce (picea likiangensis). Forests. 12(9):1268.
Livak KJ, Schmittgen TD. 2001. Analysis of relative gene expression data using real-time quantitative pcr and the 2(-delta delta c(t)) method. Methods (San Diego, Calif). 25(4):402-408.
Loskutov IG. 2008. On evolutionary pathways of avena species. Genetic Resources and Crop Evolution. 55(2):211-220.
Lumaga RB, Azzali D, Fogliano V, Scalfi L, Vitaglione P. 2012. Sugar and dietary fibre composition influence, by different hormonal response, the satiating capacity of a fruit-based and a β-glucan-enriched beverage. Food & function. 3(1):67-75.
Maeder ML, Gersbach CA. 2016. Genome-editing technologies for gene and cell therapy. Molecular Therapy. 24(3):430-446.
Mahmoud M. 2019. A first successful effort of heterologous transposons movement in oat genome. McGill University (Canada).
Mahmoud M, Zhou Z, Kaur R, Bekele W, Tinker N, Singh J. 2021. Toward the development of ac/ds transposon-mediated gene tagging system for functional genomics in oat (avena sativa l.). . Functional Integrative Genomics (submitted).
Mäkinen OE, Sozer N, Ercili-Cura D, Poutanen K. 2017. Protein from oat: Structure, processes, functionality, and nutrition. Sustainable protein sources. Elsevier. p. 105-119.
Marcotuli I, Houston K, Schwerdt JG, Waugh R, Fincher GB, Burton RA, Blanco A, Gadaleta A. 2016. Genetic diversity and genome wide association study of β-glucan content in tetraploid wheat grains. PLoS One. 11(4):e0152590.

Maughan PJ, Lee R, Walstead R, Vickerstaff RJ, Fogarty MC, Brouwer CR, Reid RR, Jay JJ, Bekele WA, Jackson EW et al. 2019. Genomic insights from the first chromosome-scale assemblies of oat (avena spp.) diploid species. BMC Biology. 17(1):92.
McMullen M, Doehlert D, Miller J. 2005. Registration of 'hifi' oat. Crop Science - CROP SCI. 45.
Meikle PJ, Hoogenraad NJ, Bonig I, Clarke AE, Stone BA. 1994. A (1-->3,1-->4)-beta-glucan-specific monoclonal antibody and its use in the quantitation and immunocytochemical location of (1-->3,1-->4)-beta-glucans. The Plant journal : for cell and molecular biology. 5(1):1-9.
Miao J, Guo D, Zhang J, Huang Q, Qin G, Zhang X, Wan J, Gu H, Qu L-J. 2013. Targeted mutagenesis in rice using crispr-cas system. Cell Research. 23(10):1233-1236.
Miller SS, Fulcher RG. 2011. Chapter 5 - microstructure and chemistry of the oat kernel11s. S. Miller is an employee of the department of agriculture and agri-food, government of canada. ©her majesty the queen in right of canada, as represented by the minister of agriculture and agri-food canada. In: Webster FH, Wood PJ, editors. Oats (second edition). AACC International Press. p. 77-94.
Mojica F, Ferrer C, Juez G, Rodriguez-Valera F. 1995. Long stretches of short tandem repeats are present in the largest replicons of the archaea haloferax mediterranei and haloferax volcanii and could be involved in replicon partitioning. Molecular microbiology. 17(1):85-93.
Mojica FJ, Díez-Villaseñor C, García-Martínez J, Almendros C. 2009. Short motif sequences determine the targets of the prokaryotic crispr defence system. Microbiology. 155(3):733-740.
Molina-Cano JL, Moralejo M, Elía M, Muñoz P, Russell JR, Pérez-Vendrell AM, Ciudad F, Swanston JS. 2007. Qtl analysis of a cross between european and north american malting barleys reveals a putative candidate gene for β-glucan content on chromosome 1h. Molecular Breeding. 19(3):275-284.
Mozaffarian D, Benjamin EJ, Go AS, Arnett DK, Blaha MJ, Cushman M, Das SR, De Ferranti S, Després J-P, Fullerton HJ. 2016. Executive summary: Heart disease and stroke statistics—2016 update: A report from the american heart association. Circulation. 133(4):447-454.
Naim F, Shand K, Hayashi S, O'Brien M, McGree J, Johnson AAT, Dugdale B, Waterhouse PM. 2020. Are the current grna ranking prediction algorithms useful for genome editing in plants? PLOS ONE. 15(1):e0227994.
Najmanovich R, Kuttner J, Sobolev V, Edelman M. 2000. Side-chain flexibility in proteins upon ligand binding. Proteins: Structure, Function, and Bioinformatics. 39(3):261-268.
Nemeth C, Freeman J, Jones HD, Sparks C, Pellny TK, Wilkinson MD, Dunwell J, Andersson AA, Åman P, Guillon F. 2010. Down-regulation of the cslf6 gene results in decreased (1, 3; 1, 4)-β-d-glucan in endosperm of wheat. Plant physiology. 152(3):1209-1218.
Newell MA, Asoro FG, Scott MP, White PJ, Beavis WD, Jannink J-L. 2012. Genome-wide association study for oat (avena sativa l.) beta-glucan concentration using germplasm of worldwide origin. Theoretical and Applied Genetics. 125(8):1687-1696.
Obert DE, Hang A, Hu G, Burton C, Satterfield K, Evans CP, Jackson EW, Marshall JM. 2011. Registration of 'transit' high β-glucan spring barley. Journal of Plant Registrations. 5(3):270-272.

Olhoft PM, Flagel LE, Donovan CM, Somers DA. 2003. Efficient soybean transformation using hygromycin b selection in the cotyledonary-node method. Planta. 216(5):723-735.
Oliver RE, Jellen EN, Ladizinsky G, Korol AB, Kilian A, Beard JL, Dumlupinar Z, Wisniewski-Morehead NH, Svedin E, Coon M et al. 2011a. New diversity arrays technology (dart) markers for tetraploid oat (avena magna murphy et terrell) provide the first complete oat linkage map and markers linked to domestication genes from hexaploid a. Sativa l. Theoretical and Applied Genetics. 123(7):1159.
Oliver RE, Lazo GR, Lutz JD, Rubenfield MJ, Tinker NA, Anderson JM, Wisniewski Morehead NH, Adhikary D, Jellen EN, Maughan PJ et al. 2011b. Model snp development for complex genomes based on hexaploid oat using high-throughput 454 sequencing technology. BMC Genomics. 12(1):77.
Orr W, Molnar SJ. 2008. Development of pcr-based scar and caps markers linked to β-glucan and protein content qtl regions in oat. Genome. 51(6):421-425.
Parveez GKA, Majid NiA. 2008. Factors affecting green fluorescence protein (gfp) gene expression in oil palm after microprojectile bombardment. J Oil Palm Res. 20:495-507.
Paszkowski J, Shillito RD, Saul M, Mandak V, Hohn T, Hohn B, Potrykus I. 1984. Direct gene transfer to plants. The EMBO journal. 3(12):2717-2722.
Pavletich N, Pabo C. 1991. Zinc finger-DNA recognition: Crystal structure of a zif268-DNA complex at 2.1 a. Science. 252(5007):809-817.
Pereira MA, O'Reilly E, Augustsson K, Fraser GE, Goldbourt U, Heitmann BL, Hallmans G, Knekt P, Liu S, Pietinen P. 2004. Dietary fiber and risk of coronary heart disease: A pooled analysis of cohort studies. Archives of internal medicine. 164(4):370-376.
Phillips GO, Cui SW. 2011. An introduction: Evolution and finalisation of the regulatory definition of dietary fibre. Food Hydrocolloids. 25(2):139-143.
POGA. 2018. Increase the oat acres in alberta by finding a high yielding oat variety that maximizes producer income and meets the demands of the millers. In: Association POG, editor.
Prince VE, Pickett FB. 2002. Splitting pairs: The diverging fates of duplicated genes. Nature Reviews Genetics. 3(11):827-837.
Puchta H. 2004. The repair of double-strand breaks in plants: Mechanisms and consequences for genome evolution. Journal of Experimental Botany. 56(409):1-14.
Ratanasut K, Rod-In W, Sujipuli K. 2017. In planta agrobacterium-mediated transformation of rice. Rice Science. 24(3):181-186.
Repellin A, Båga M, Jauhar PP, Chibbar RN. 2001. Genetic enrichment of cereal crops via alien gene transfer: New challenges. Plant cell, tissue and organ culture. 64(2-3):159-183.
Roulin S, Buchala AJ, Fincher GB. 2002. Induction of (1→3,1→4)-β-d-glucan hydrolases in leaves of dark-incubated barley seedlings. Planta. 215(1):51-59.
Sánchez-León S, Gil-Humanes J, Ozuna CV, Giménez MJ, Sousa C, Voytas DF, Barro F. 2018. Low-gluten, nontransgenic wheat engineered with crispr/cas9. Plant biotechnology journal. 16(4):902-910.
Sanford JC. 1988. The biolistic process. Trends in Biotechnology. 6(12):299-302.
Schubert M, Marcussen T, Meseguer AS, Fjellheim S. 2019. The grass subfamily pooideae: Cretaceous–palaeocene origin and climate-driven cenozoic diversification. Global Ecology and Biogeography. 28(8):1168-1182.
Shan Q, Wang Y, Li J, Gao C. 2014. Genome editing in rice and wheat using the crispr/cas system. Nat Protoc. 9(10):2395.

Shi J, Gao H, Wang H, Lafitte HR, Archibald RL, Yang M, Hakimi SM, Mo H, Habben JE. 2017. Argos 8 variants generated by crispr-cas9 improve maize grain yield under field drought stress conditions. Plant biotechnology journal. 15(2):207-216.
Shrawat AK, Lörz H. 2006. Agrobacterium-mediated transformation of cereals: A promising approach crossing barriers. Plant biotechnology journal. 4(6):575-603.
Singh S, Tan HQ, Singh J. 2012. Mutagenesis of barley malting quality qtls with ds transposons. Funct Integr Genomics. 12(1):131-141.
Singh S, Tripathi RK, Lemaux PG, Buchanan BB, Singh J. 2017. Redox-dependent interaction between thaumatin-like protein and β-glucan influences malting quality of b(Song et al. 2021)arley. Proceedings of the National Academy of Sciences. 114(29):7725-7730.
Skadsen R, Sathish P, Kaeppler H. 2000. Expression of thaumatin-like permatin pr-5 genes switches from the ovary wall to the aleurone in developing barley and oat seeds. Plant Science. 156(1):11-22.
Somers DA, Rines HW, Gu W, Kaeppler HF, Bushnell WR. 1992. Fertile, transgenic oat plants. Bio/technology. 10(12):1589-1594.
Song B, Yang S, Hwang G-H, Yu J, Bae S. 2021. Analysis of nhej-based DNA repair after crispr-mediated DNA cleavage. International Journal of Molecular Sciences. 22(12):6397.
Supartana P, Shimizu T, Shioiri H, Nogawa M, Nozue M, Kojima M. 2005. Development of simple and efficient in planta transformation method for rice (oryza sativa l.) using agrobacterium tumefaciens. Journal of Bioscience and Bioengineering. 100(4):391-397.
Svitashev S, Young JK, Schwartz C, Gao H, Falco SC, Cigan AM. 2015. Targeted mutagenesis, precise gene editing, and site-specific gene insertion in maize using cas9 and guide rna. Plant physiology. 169(2):931-945.
Taketa S, Yuo T, Tonooka T, Tsumuraya Y, Inagaki Y, Haruyama N, Larroque O, Jobling SA. 2012. Functional characterization of barley betaglucanless mutants demonstrates a unique role for cslf6 in (1,3;1,4)-beta-d-glucan biosynthesis. J Exp Bot. 63(1):381-392.
Tang H, Liu H, Zhou Y, Liu H, Du L, Wang K, Ye X. 2021. Fertility recovery of wheat male sterility controlled by ms2 using crispr/cas9. Plant biotechnology journal. 19(2):224-226.
Tester M, Langridge P. 2010. Breeding technologies to increase crop production in a changing world. Science. 327(5967):818-822.
Theuwissen E, Mensink RP. 2008. Water-soluble dietary fibers and cardiovascular disease. Physiology & Behavior. 94(2):285-292.
Thomas H. 1992. Cytogenetics of avena. Oat science and technology.473-507.
Tian L, Canli FA, Wang X, Sibbald S. 2009. Genetic transformation of prunus domestica l. Using the hpt gene coding for hygromycin resistance as the selectable marker. Scientia Horticulturae. 119(3):339-343.
Tilman D, Balzer C, Hill J, Befort BL. 2011. Global food demand and the sustainable intensification of agriculture. Proceedings of the National Academy of Sciences. 108(50):20260-20264.
Tingay S, McElroy D, Kalla R, Fieg S, Wang M, Thornton S, Brettell R. 1997. Agrobacterium tumefaciens-mediated barley transformation. The Plant Journal. 11(6):1369-1376.
Tiwari U, Cummins E. 2009. Nutritional importance and effect of processing on tocols in cereals. Trends in food science & technology. 20(11-12):511-520.

Tiwari U, Cummins E. 2011. Meta-analysis of the effect of β-glucan intake on blood cholesterol and glucose levels. Nutrition. 27(10):1008-1016.
Trafford K, Fincher G. 2014. Barley grain carbohydrates: Starch and cell walls. p. 71-95.
USDA. 2019. Grain: World markets and trade Monthly. November 8, 2019 ed. Foreign Agricultural Service.
USDA. 2021. World agricultural production. Monthly. December 2021 ed. Foreign Agricultural Service.
Van Den Elzen PJ, Townsend J, Lee KY, Bedbrook JR. 1985. A chimaeric hygromycin resistance gene as a selectable marker in plant cells. Plant Molecular Biology. 5(5):299-302.
Vis RB, Lorenz K. 1998. Malting and brewing with a high β-glucan barley. LWT - Food Science and Technology. 31(1):20-26.
Wang B, Zhong Z, Wang X, Han X, Yu D, Wang C, Song W, Zheng X, Chen C, Zhang Y. 2020. Knockout of the osnac006 transcription factor causes drought and heat sensitivity in rice. Int J Mol Sci. 21(7).
Wang F, Wang C, Liu P, Lei C, Hao W, Gao Y, Liu Y-G, Zhao K. 2016. Enhanced rice blast resistance by crispr/cas9-targeted mutagenesis of the erf transcription factor gene oserf922. PLOS ONE. 11(4):e0154027.
Wang L, Chen L, Li R, Zhao R, Yang M, Sheng J, Shen L. 2017a. Reduced drought tolerance by crispr/cas9-mediated slmapk3 mutagenesis in tomato plants. Journal of Agricultural and Food Chemistry. 65(39):8674-8682.
Wang T, Wei JJ, Sabatini DM, Lander ES. 2014a. Genetic screens in human cells using the crispr-cas9 system. Science. 343(6166):80-84.
Wang Y, Cheng X, Shan Q, Zhang Y, Liu J, Gao C, Qiu J-L. 2014b. Simultaneous editing of three homoeoalleles in hexaploid bread wheat confers heritable resistance to powdery mildew. Nature biotechnology. 32(9):947.
Wang Y, Cheng X, Shan Q, Zhang Y, Liu J, Gao C, Qiu J-L. 2014c. Simultaneous editing of three homoeoalleles in hexaploid bread wheat confers heritable resistance to powdery mildew. Nature Biotechnology. 32:947.
Wang Y, Geng L, Yuan M, Wei J, Jin C, Li M, Yu K, Zhang Y, Jin H, Wang E et al. 2017b. Deletion of a target gene in indica rice via crispr/cas9. Plant Cell Reports. 36(8):1333-1343.
Welch R, Brown J, Leggett J. 2000. Interspecific and intraspecific variation in grain and groat characteristics of wild oat (avena) species: Very high groat (1→ 3),(1→ 4)-β-d-glucan in an avena atlantica genotype. Journal of Cereal Science. 31(3):273-279.
Whitehead A, Beck EJ, Tosh S, Wolever TM. 2014. Cholesterol-lowering effects of oat β-glucan: A meta-analysis of randomized controlled trials. The American Journal of Clinical Nutrition. 100(6):1413-1421.
Woodward AW, Bartel B. 2005. Auxin: Regulation, action, and interaction. Annals of Botany. 95(5):707-735.
Woodward JR, Fincher GB, Stone BA. 1983. Water-soluble (1→3), (1→4)-β-d-glucans from barley (hordeum vulgare) endosperm. Ii. Fine structure. Carbohydrate Polymers. 3(3):207-225.
Xie K, Yang Y. 2013. Rna-guided genome editing in plants using a crispr–cas system. Molecular plant. 6(6):1975-1983.

Yan H, Bekele WA, Wight CP, Peng Y, Langdon T, Latta RG, Fu Y-B, Diederichsen A, Howarth CJ, Jellen EN et al. 2016a. High-density marker profiling confirms ancestral genomes of avena species and identifies d-genome chromosomes of hexaploid oat. Theoretical and Applied Genetics. 129(11):2133-2149.

Yan H, Martin SL, Bekele WA, Latta RG, Diederichsen A, Peng Y, Tinker NA. 2016b. Genome size variation in the genus avena. Genome. 59(3):209-220.

Yang Z, Wang K, Aziz U, Zhao C, Zhang M. 2020. Evaluation of duplicated reference genes for quantitative real-time pcr analysis in genome unknown hexaploid oat (avena sativa l.). Plant Methods. 16(1):138.

Young J, Zastrow-Hayes G, Deschamps S, Svitashev S, Zaremba M, Acharya A, Paulraj S, Peterson-Burch B, Schwartz C, Djukanovic V. 2019. Crispr-cas9 editing in maize: Systematic evaluation of off-target activity and its relevance in crop improvement. Scientific reports. 9(1):1-11.

Yu Z, Chen M, Nie L, Lu H, Ming X, Zheng H, Qu L-J, Chen Z. 1999. Recovery of transgenic orchid plants with hygromycin selection by particle bombardment to protocorms. Plant cell, tissue and organ culture. 58(2):87-92.

Zeković DB, Kwiatkowski S, Vrvić MM, Jakovljević D, Moran CA. 2005. Natural and modified (1→3)-β-d-glucans in health promotion and disease alleviation. Critical Reviews in Biotechnology. 25(4):205-230.

Zerai DB, Glenn EP, Chatervedi R, Lu Z, Mamood AN, Nelson SG, Ray DT. 2010. Potential for the improvement of salicornia bigelovii through selective breeding. Ecological Engineering. 36(5):730-739.

Zhang Y, Liang Z, Zong Y, Wang Y, Liu J, Chen K, Qiu J-L, Gao C. 2016. Efficient and transgene-free genome editing in wheat through transient expression of crispr/cas9 DNA or rna. Nature Communications. 7(1):12617.

Zhou J, Peng Z, Long J, Sosso D, Liu B, Eom J-S, Huang S, Liu S, Vera Cruz C, Frommer WB et al. 2015. Gene targeting by the tal effector pthxo2 reveals cryptic resistance gene for bacterial blight of rice. The Plant Journal. 82(4):632-643.

Zolman BK, Yoder A, Bartel B. 2000. Genetic analysis of indole-3-butyric acid responses in arabidopsis thaliana reveals four mutant classes. Genetics. 156(3):1323-1337.